ALMA MATER STUDIORUM – UNIVERSITÀ DI BOLOGNA

PhD Program in Cellular Molecular and Industrial Biology

Program n. 2: Functional Biology of Cellular and Molecular systems

XXV Cycle

Settore Concorsuale: 05/E2

Settore Scientifico disciplinare: BIO/11

TRANSCRIPTIONAL RESPONSES OF THE

Helicobacter pylori cag PATHOGENICITY

ISLAND

PhD candidate: Andrea Vannini

PhD Program Coordinator:
Prof. **Vincenzo Scarlato**

Tutors:
Prof. **Vincenzo Scarlato**
Dott. **Alberto Danielli**

FINAL EXAM 2013

In my PhD studies I was co-author of the following papers:

Vannini, A., et al., *A convenient and robust in vivo reporter system to monitor gene expression in the human pathogen Helicobacter pylori.* Appl Environ Microbiol, 2012. **78**(18): p. 6524-33.

Vannini, A., et al., *In depth analysis of the Helicobacter pylori cag pathogenicity island transcriptional responses.* In preparation

Vannini, A., et al., *Study of a putative small non-coding RNA (sRNA) in the Helicobacter pylori pathogenicity island.* Experimental work to be finalized for publication

ABSTRACT

The severity of *Helicobacter pylori* infections largely depends on the genetic diversity of the infecting strain, and particularly on the presence of the *cag* pathogenicity island (*cag*-PAI). This virulence locus encodes a type-IV secretion system able to translocate in the host cell at least the *cag*-encoded toxin CagA and peptidoglycan fragments, that together are responsible for the pathogenic phenotype in the host. Little is known about the bacterial regulators that underlie the coordinated expression of *cag* gene products, needed to assemble a functional secretion system apparatus. To fill this gap, a comprehensive analysis of the transcriptional regulation of the *cag*-PAI operons was undertaken.

To pursue this goal, a robust tool for the analysis of gene expression in *H. pylori* was first implemented. A bioluminescent reporter system based on the *P. luminescens luxCDABE* operon was constructed and validated by comparisons with transcriptional analyses, then it was systematically used for the comprehensive study and mapping of the *cag* promoters.

The identification of bona fide *cag* promoters had permitted to pinpoint the set of *cag* transcriptional units of the PAI. The responses of these *cag* transcriptional units to metabolic stress signals were analyzed in detail, and integrated with transcription studies in deletion mutants of important *H. pylori* virulence regulators and protein-DNA interaction analyses to map the binding sites of the regulators.

Finally, a small regulatory RNA *cncR1* encoded by the *cag*-PAI was identified, and the 5'- and 3'-ends of the molecule were mapped by primer extension analyses, northern blot and studies with *lux* reporter constructs. To identify regulatory effects exerted by *cncR1* on the *H. pylori* gene expression, the Δ*cncR1* strain was derived and compared to the parental wild type strain by a macroarray approach. Results suggest a negative effect exerted by *cncR1* on the regulome of the alternative sigma factor σ^{54}.

CONTENTS

INTRODUCTION

1.1 *Helicobacter pylori*

1.1.1 Epidemiology and infection

Helicobacter pylori is a gram-negative, spiral shaped, microaerophilic bacterial pathogen (Fig. 1), which colonizes the mucosal layer overlying the gastric epithelium of the human stomach. Isolated in 1982 by Robin Warren and Barry Marshall, it is recognized as the principal causative agent of chronic active gastritis (Blaser, 1990), as well as gastric and peptic ulcer diseases (Nomura et al., 1994), and is associated with the development of B-cell mucosa-associated lymphoid tissue lymphoma and gastric adenocarcinoma (Du and Isaccson, 2002; Parsonnet et al., 1994; Peek and Blaser, 2002).

Fig. 1 Electron micrograph of *Helicobacter pylori*. *H. pylori* in vivo and under optimum in vitro conditions is an S-shaped bacterium with 1 to 3 turns, 0.5×5 μm in length, with a tuft of 5 to 7 polar sheathed flagella. Field emission SEM, bar = 0.5 μm (Mobley et al., 2001).

While the infection is chronic and often asymptomatic, this bacterium infects over 50% of the world's population (Dunn et al., 1997). The sheer number of infected individuals leads to a significant number of *H. pylori*-associated diseases cases each year, worldwide. Moreover, since colonization usually occurs early in childhood and remains throughout the person's life if the infection is not treated with

antibiotics (Blaser, 1990; de Reuse and Bereswill, 2007), the chronicity increases the likelihood of disease. For these reasons *H. pylori* is considered an important public health problem with serious economic consequences and the World Health Organization has classified the organism as a class 1 carcinogen in 1994 (Bouvard et al., 2009).

After initial infection, *H. pylori* rapidly reaches to the gastric mucosa layer in close contact with epithelial cells (Josenhans et al., 2007). Here, the bacterium faces with harsh physiological conditions such as mild to strong acidity, fluctuating nutrient, availability and osmolarity, oxygen tension and a vigorous host immune response. Therefore, *H. pylori* produces a number of factors to cope with changes in the micro-environment and the host response (van Vliet et al., 2001a). Several factors that facilitate its survival, such as flagellins (Suerbaum et al., 1993) and urease (Cussac et al., 1992), and that are associated with pathogenesis, like the *cag* pathogenicity island (Covacci et al., 1993) and the vacuolating toxin (Cover et al., 1994; Telford et al., 1994), have been extensively studied, and significant advances regarding the regulation of these factors have been made (Akada et al., 2000; Joyce et al., 2001).

H. pylori infections can be successfully cured with antibiotic treatment, associated with a proton pump inhibitor (Megraud and Lamouliatte, 2003). Unfortunately, the available antimicrobial therapies are beginning to lose efficacy principally because of insurgence of antibiotic resistance, which frequently emerges de novo in *H. pylori*. Altered expression of gene products sensitive to antibiotic treatment seems to be especially important for resistance to penicillins and especially nitrimidazoles, the most common form of resistance encountered in *H. pylori* (Gerrits et al., 2006). However, because it would be unrealistic to use antimicrobial therapies to eradicate an infection that affects 50% of the world population, it remains necessary to explore and identify both bacterial and host markers to diagnose individuals at high risk for the most severe infection outcomes, as well as to develop new effective therapeutic strategies. For these reasons, *H. pylori* remains a bacterial pathogen of major medical importance. This was acknowledged by the Nobel Price for Medicine in 2005 to Warren and Marshal who first discovered the bacterium (Marshall and Warren, 1984).

1.1.2 Genome and regulatory functions

The complete genomic sequence of many *H. pylori* strains derived from unrelated clinical isolates are currently available, as Hp26695 (Tomb et al., 1997), HpJ99 (Alm et al., 1999), HpAG1, (Oh et al., 2006) and HpG27 (Baltrus et al., 2009) strains. Although *H. pylori* was believed to exhibit a large degree of genomic and allelic diversity, the overall genomic organization, gene order and predicted gene products of these strains were found to be remarkably similar (Alm et al., 1999).

The *H. pylori* genome is 1600 kb long and contains approximately 1500 open reading frames (ORFs) of which 60% were similar to genes of known function and could, therefore, be designated a putative identification, 18% showed similarity to genes that are conserved throughout other bacteria but do not have a known function and 23% were specific to *H. pylori* (Alm et al., 1999; Scarlato et al., 2001).

One of the most striking features of the *H. pylori* genome is the singular paucity of transcription factor and regulatory protein predicted (Scarlato et al., 2001; Tomb et al., 1997). Analysis of genome led to the identification of only 32 gene products classified as having a possible regulatory function of which only 17 are predicted to have a role in the regulation of transcription (Fig. 2). This is approximately half the number of those reported for *H. influenzae*, which has a genome of comparable size to *H. pylori* and less than a quarter to those predicted for *E. coli*. In addition, only one-third of the number of two-component regulatory systems of *E. coli* are present in *H. pylori* which possesses only four sensor proteins and seven response regulators (Tomb et al., 1997).

The low abundance of regulators is consistent with a small genome, where transcription factors have been lost due the absence of selective pressure (Madan Babu et al., 2006), reflecting the reductive evolution of this pathogen, which has been attributed to a constrained gastric habitat and the absence of other competitive microorganisms in this hostile environment (de Reuse and Bereswill, 2007).
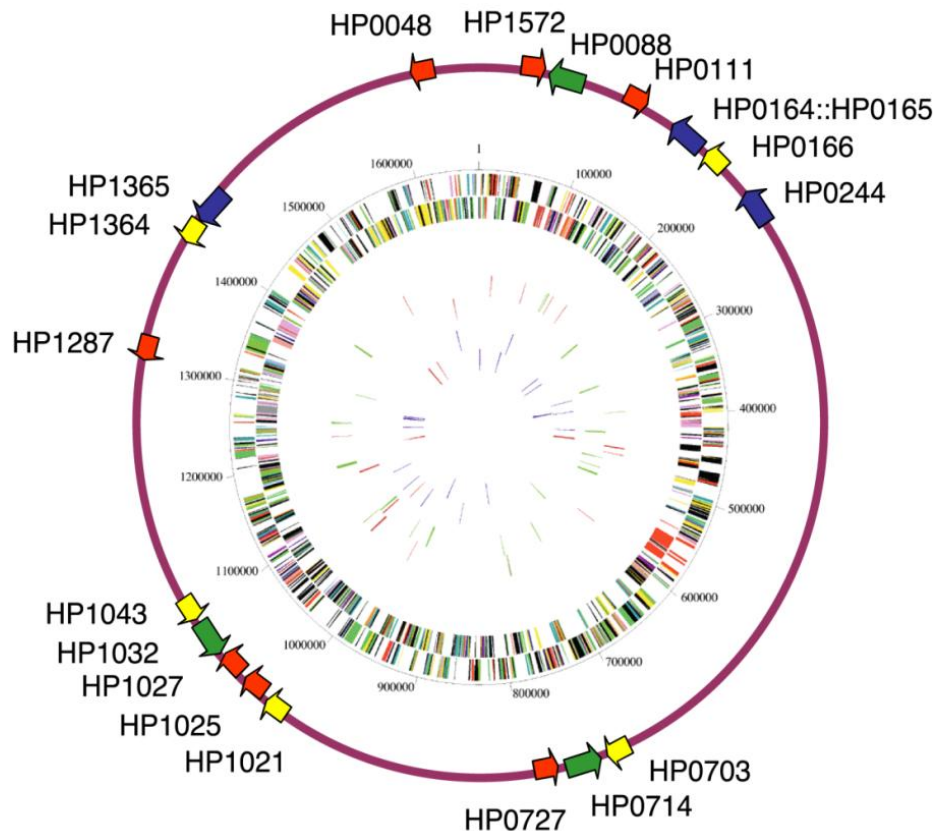
Fig. 2   Schematic representation of *H. pylori* genome and map position of regulatory genes (Scarlato et al., 2001; Tomb et al., 1997). Outer concentric circle: predicted coding regions on the plus strand; second concentric circle: predicted coding regions on the minus strand. Symbols: green arrow boxes, sigma factors (3); blue arrow boxes, sensor kinase (3); yellow arrow boxes, response regulator (5); red arrow boxes, transcriptional regulator (7).

There is, however, evidence that *H. pylori* uses other mechanisms of regulation. These include slipped-strand mispairing within genes (Josenhans et al., 2007) and in putative promoter regions (Alm et al., 1999), and methylation by its nine type II methyltransferases (Marais et al., 1999). Moreover, mechanisms of post-transcriptional regulation have been described in *H. pylori*, through antisense transcription and the expression of at least 60 small RNAs (Sharma et al., 2010), as well as through RNA-binding proteins that modulate mRNA stability and translation efficiency (Douillard et al., 2009).

Finally, the *H. pylori* genome does not have extensive operon structure. For example, the flagellar regulon is not contained in operons in this organism, which further confounds the apparent lack of regulation.

Thus, despite the limited number of proteins putatively involved in regulation of transcription functions (as deduced from genome), *H. pylori* seems to use complex and fascinating mechanisms to control transcription. The key issue is how the few regulatory factors of *H. pylori* can exploit their functions in order to regulate different sets of genes in a coordinate manner.

1.2   Regulatory modules

Globally, the coordinated expression of the genetic repertoire is controlled by the transcriptional regulatory network (TRN), which controls the decision making of the bacterium in response to changes in the environment (Balazsi and Oltvai, 2005). Recent evidence points to a very shallow of *H. pylori* TNR in which the few regulators are encompassed in four main modules which process the physiological responses needed to colonize the gastric niche: respectively, motility and chemotaxis, heat and stress response, acid acclimation and metal ion homeostasis (Danielli et al., 2010).

1.2.1 Motility and chemotaxis

Flagellar, chemotaxis, and motor protein encoding genes are key virulence factors in *H. pylori*. Their deletion leads to strains with an attenuated or completely defective ability to establish colonization in animal models (Eaton et al., 1996; Foynes et al., 2000; Josenhans and Suerbaum, 2002), possibly because of a failure to move in response to favorable or noxious gradients. The ~40 motility genes of *H. pylori* are unclustered, frequently scattered within multicistronic gene operons (Alm et al., 1999; Niehus et al., 2004; Tomb et al., 1997). Along with other pleiotropic regulatory effects, such as polarity and DNA supercoiling (Ye et al., 2007), their transcription is hierarchically regulated, employing a remarkable fraction of

dedicated transcriptional factors. This regulated mechanism of gene expression allows flagellar proteins to be produced in stages, facilitating their ordered secretion and proper interactions so that flagellar biosynthesis occurs correctly, and it is accomplished by linking transcription of classes of flagellar genes to structural steps in flagellar biosynthesis.

Flagellar genes are typically positively regulated and hierarchically organized in three main classes according to their activating sigma factor (Macnab, 2003; Niehus et al., 2004). Class I encompasses gene targets transcribed by the vegetative RNA polymerase containing σ^{80} factor (HP0088-RpoD), and comprises mostly flagellar regulatory genes (*rpoN*-σ^{54}, *flgR*, *flgS* and *flhA*) and genes encoding for proteins that form the flagellar base structures, as the MS ring (FliF), the flagellar type III secretion system-T3SS (FlhA, FlhB, FliO, FliP, FliQ and FliR), the cytoplasmic C ring or switch complex (FliG, FliM, and FliN or FliY), and the motor (MotA and MotB) (Kavermann et al., 2003). Class II includes specific targets of the alternative σ^{54} factor (HP0714-RpoN), and encodes for the components of the flagellar basal body (FlgB, FlgC, FlgD and FliE), of the hook (FlgE, FlgL and FlgK) and their corresponding regulators (FliW and FliK). Class III genes encode late both flagellar structures (FlaG, FliD, FliS and FliT) and regulators (HP1032-FliA), and they are transcribed by σ^{28}-(FliA)-containing RNA polymerase.

The flagellar regulatory module adopts a short σ regulatory cascade ($\sigma^{80}>\sigma^{54}>\sigma^{28}$) initiated by the housekeeping σ^{80} factor, where each σ factor activates its dedicated target gene class. Moreover, σ^{80} is also responsible for the transcription of σ^{54}, establishing a hierarchical regulation on the subset of σ^{54}-dependent genes. σ^{54} is proposed to activate its own subset of genes and σ^{28}, but the latter gene seems co-transcribed in a single multicistronic operon with the upstream genes from the σ^{80}-dependent P_{1034} promoter (Sharma et al., 2010). Other factors intersect this regulatory network, obtaining a tightly regulated response of the flagellar origon. In particular, FlgRS two-component systems (HP0703, HP0244) (Brahmachary et al., 2004; Niehus et al., 2004; Spohn and Scarlato, 1999b; Wen et al., 2009), FlhA (HP1041) (Niehus et al., 2004), FlhF (HP1035) (Niehus et al., 2004) and FlgZ (HP0958) (Pereira and Hoover, 2005; Pereira et al., 2011), positively regulate the transcriptional activity of σ^{54}. This regulation likely occurs through the activation of

the σ^{54}-RNA polymerase, by interaction with specific sequences on the promoters, or though the promotion of a stable accumulation of σ^{54}. In contrast, FliK (HP0906) (Douillard et al., 2009; Ryan et al., 2005) and FlgM (HP1122) (Niehus et al., 2004) repress σ^{54} and σ^{28}, respectively, likely establishing a feed-back regulation of the different class of flagellar genes.

1.2.2 Heat shock

The heat shock origon is amongst the best-understood regulatory modules in *H. pylori*. Whereas most Gram-negatives employ specialized sigma factors (σ^{32}) to positively regulate the transcriptional responses to heat shock, *H. pylori* has evolved an opposite strategy, commonly found in Gram-positive bacteria, that implements two repressors with homology to *Bacillus subtilis* HrcA (Narberhaus, 1999; Schulz and Schumann, 1996) and *Streptomyces spp.* HspR (Servant and Mazodier, 2001). Specifically, the heat shock origon of *H. pylori* is composed of HspR and HrcA directly repressing three main target operons, including the *groESL* chaperone genes. All three operons are responsive to heat shock and are activated by the presence of misfolded proteins or stress signals (Homuth et al., 2000; Spohn et al., 2002). HspR alone represses transcription of the *cbpA* operon, thereby negatively autoregulating its own synthesis (Spohn and Scarlato, 1999a). On the contrary, both HspR and HrcA are required for dual repression of the *groESL* and *hrcA* operons (Spohn et al., 2004). The DNA-binding activity of both repressors is enhanced by the product of the *groESL* target gene (Roncarati et al., 2007), suggesting that HrcA and HspR are involved with the GroE chaperonin system in a feedback regulatory loop, complying with the *B. subtilis* "titration model" (Mogk et al., 1997). This model postulates that upon heat shock, GroESL is titrated away by misfolded polypeptides, thereby relieving HspR/HrcA repression, and triggering the stress response.

1.2.3 Acid Origon

The capacity to grow under the harsh acidic conditions encountered in the stomach is a distinctive feature of *H. pylori* and is associated with virulence (Sachs et al., 2003; Scott et al., 2007). Accordingly, the regulated expression of a dedicated set

of so-called acid acclimation genes (the *ure* urease operon, aliphatic amidases *amiE* and *amiF*, arginase *roc*, etc.) allows *H. pylori* to keep acidity of the bacterial periplasm close to neutrality, and to maintain physiologic pH levels in the cytoplasm in the presence of urea and urease activity (Scott et al., 2002; Tsuda et al., 1994; Weeks et al., 2004). Transcription of acid acclimation operons is under control of the housekeeping σ^{80} factor and is regulated principally by the essential acid response regulator ArsR (Pflock et al., 2006b). ArsR is autoregulated and is encoded by an operon that also encompasses the cognate transmembrane ArsS histidine kinase (Dietz et al., 2002). It has been proposed that the signal sensed by ArsS is acidification of the periplasm, transduced through changes in protonation of its histidine residue 94 (pKa ~6.0) in the extracytosolic sensory domain (Pflock et al., 2004). This stimulus triggers phosphorylation of ArsR, thereby promoting its DNA-binding activity towards a specific set of promoters (Pflock et al., 2005; Wen et al., 2006). However, there are three distinct group of targets, which are controlled according to the phosphorylation status of ArsR:

- A first cluster of genes encompasses P~ArsR-dependent target operons regulated by ArsR in a phosphorylation-dependent manner, upon mild acidification of the periplasm through ArsS signaling (*omp11*, *carbonic anhydrase*, *hypA*, *ureAB*).

- A second cluster of genes contains target operons that are regulated by more harsh acidic conditions, promoting acidification of the cytoplasm. Their regulation is P~ArsR-dependent and phosphorylation of the regulator similarly promotes high affinity DNA binding to their promoters. However, they are not deregulated in *arsS* deletion mutants, and may therefore rely on a different (cytoplasmic) acid signal transducer to promote the phosphotransfer needed to activate ArsR. This group includes other genes central to the acid acclimation process such as *amiE*, *amiF*, and others.

- Finally, a third group of genes includes targets of unphosphorylated ArsR (including the *arsRS* operon) and whose regulation is not necessarily pH dependent. The latter group contains genes of unknown function that appear to be essential for viability.

Very interestingly, a recent work identified FlgS, the aforementioned cytosolic NtrB-like histidine kinase belonging to the flagellar biosynthesis module, as being also essential for survival of *H. pylori* at low pH (Wen et al., 2009). Although it is not known whether FlgS is able to trigger ArsR phosphorylation upon acidification of the cytoplasm, it may represent a good candidate as a cytosolic acid sensor feeding into the ArsR regulon. Finally, the pleiotropic metal-dependent transcriptional regulators Fur and NikR are involved in the acidic shock response and in the mechanisms of acid adaptation and tolerance (Valenzuela et al., 2011; van Vliet et al., 2004).

1.2.4 Metals

In many bacterial pathogens, including *H. pylori*, metal starvation triggers the expression of virulence factors, which enables them to compete with the host for these essential nutrients. On the other hand, metal ions are toxic if present intracellularly in high amounts. Therefore, their homeostasis must be tightly controlled (Giedroc and Arunkumar, 2007). Three systems are dedicated to this fundamental task in *H. pylori*: the CrdRS two-component system, the ferric uptake regulator (Fur) involved in iron homeostasis (Bereswill et al., 1998), and a homolog of the Ni-responsive NikR regulator of *E. coli* (van Vliet et al., 2002a). Whilst the only identified genes targets of the CrdRS system appear to be involved in copper resistance (Waidner et al., 2005), Fur and NikR have been described as pleiotropic regulators.

Fur regulates genes involved in both Fe^{2+} uptake (Danielli et al., 2009; Delany et al., 2001a; van Vliet et al., 2002b) and detoxification (Bereswill et al., 2000; Ernst et al., 2005b). Distinctively, the metal ion cofactor can act as co-repressor (*holo*-Fur repressed genes) or as inducer (*apo*-Fur repressed genes) (Carpenter et al., 2009; Delany et al., 2001b). In accordance with its pleiotropic role, exemplified by the observed competitive colonization defects of *fur* mutants (Gancz et al., 2006), Fur is an abundant protein and binds to ~200 target loci *in vivo*, including genes coding for other regulators (*rpoN*, *flgR*, *flgS*, *cheA*, *nikR*) (Danielli et al., 2006). Consequently, hundreds of genes deregulated by *fur* deletion have been reported, although not all appear to be direct targets of the regulator (Danielli et al.,

2006; Ernst et al., 2005a). Moreover, fur deletion mutants are impaired in their acid tolerance (Bijlsma et al., 2002; van Vliet et al., 2003), and Fur in vivo targeting of ArsR has been reported in ChIP-chip experiments (Danielli et al., 2006), substantiating a direct (and hierarchically important) role of Fur in the regulation of acid acclimation. The same study also revealed that protein levels of Fur increase in stationary phase, suggesting that this regulator is involved in the reported growth phase–dependent regulation of genes encoding metallo-proteins and iron-trafficking factors (Choi et al., 2008; Danielli et al., 2009; Merrell et al., 2003).

On the other hand, NikR mediates regulation of Ni^{2+} homeostasis in the cell, central to the activity of the nickel-enzyme urease. In contrast to Fur, *apo*-NikR is unable to bind DNA, and Ni^{2+} coordination at high-affinity metal binding sites drives allosteric changes promoting the DNA binding activity of *holo*-NikR (Abraham et al., 2006; Benanti and Chivers, 2007; Zambelli et al., 2008). According to the position of the operator elements, NikR can act as a positive or negative regulator of transcription (Contreras et al., 2003; Ernst et al., 2005c). NikR might be also involved in the regulation of several acid acclimation genes, including the urease operon (van Vliet et al., 2004; van Vliet et al., 2002a), possibly through increased bioavailability of the Ni^{2+} ion under low pH conditions, or through pH-responsive DNA binding activity, which has recently been reported (Li and Zamble, 2009).

1.3   Antisense transcription and sRNAs

The primary transcriptome analysis of *H. pylori* strain 26695, revealed a massive antisense transcription as well as an high number of more than 60 small RNAs (sRNAs) including potential regulators of *cis*- and *trans*-encoded mRNA targets, indicating that *H. pylori* uses riboregulation for its gene expression control (Sharma et al., 2010). Small RNAs interact with the target mRNAs by base-pairing and can influence their expression by different mechanisms, as translation inhibition, transcription interference and attenuation, transcript stabilization or degradation (Thomason and Storz, 2010).

1.3.1 *Cis*-encoded sRNAs

Cis-encoded antisense RNAs (asRNAs) can overlap the 5′- or 3′-end, the middle, or entire genes that are transcribed oppositely the corresponding *cis*-sRNAs, and the interaction with the target occurs through a perfect extended base-pairing. More than 900 *cis*-encoded asRNAs have been identified in *H. pylori*, including at least one antisense transcriptional start site for almost half of all ORFs (Sharma et al., 2010). Whether all of them are functional or rather represent spurious transcription still need to be clarified. However, the characterization of a naturally occurring 292-nt long *cis*-encoded antisense sRNA from the opposite strand of the urease operon in *H. pylori* strain 43504 further demonstrates the functionality of asRNAs in *H. pylori* (Wen et al., 2011). One of the mechanism of *cis*-RNA mediated regulation is through antisense-induced processing of the dsRNAs, likely performed by the double-strand specific ribonuclease RNase III, as was suggested for *Staphylococcus aureus* (Lasa et al., 2011).

Besides sRNAs, several new small hydrophobic proteins (<50 aa) are encoded by *H. pylori*, some of which are associated with *cis*-encoded asRNAs (Sharma et al., 2010). For example, six structurally related ∼80 nt sRNAs, IsoA1−6 (RNA-inhibitor of small-ORF family A), are expressed antisense to the small ORFs, AapA1−6 (antisense-RNA-associated peptide family A), representing homologous 22–30 aa long peptides. Some of these small ORFs resemble antimicrobial peptides or small toxic peptides from bacteria and functional studies suggested that the *aapA–isoA* loci might represent the first examples of class I toxin–antitoxin systems in *H. pylori*, in which an unstable RNA antitoxin represses expression of a stable peptide toxin (Sharma et al., 2010).

1.3.2 *Trans*-encoded sRNAs

Trans-encoded sRNAs are synthesized as discrete transcripts with dedicated promoter and terminator sequences and share only limited complementarity with their target mRNAs. These sRNAs regulate the translation and/or stability of target mRNAs and are, in many respects, functionally analogous to eukaryotic miRNAs (Aiba, 2007; Gottesman, 2005). The majority of the regulation by the known *trans*-

encoded sRNAs is negative (Aiba, 2007; Gottesman, 2005). Base-pairing between the sRNA and its target mRNA usually leads to repression of protein levels through translational inhibition, mRNA degradation, or both. For the few characterized sRNA-mRNA interactions, the inhibition of ribosome binding is the main contributor to reduced protein levels, while the subsequent degradation of the sRNA-mRNA duplex by RNase E is thought to increase the robustness of the repression and make the regulation irreversible (Morita et al., 2006). However, sRNAs can also activate expression of their target mRNAs through an anti-antisense mechanism whereby base-pairing of the sRNA disrupts an inhibitory secondary structure which sequesters the ribosome binding site (Gottesman, 2005; Prevost et al., 2007).

In many cases, the RNA chaperone Hfq is required for trans-encoded sRNA-mediated regulation, presumably to facilitate RNA-RNA interactions due to limited complementarity between the sRNA and target mRNA (Aiba, 2007; Brennan and Link, 2007; Valentin-Hansen et al., 2004).

Several of the newly identified sRNAs in *H. pylori* are potential candidates for *trans*-encoded antisense RNAs. For example, the abundant 87-nt long HPnc5490 sRNA, was predicted to interact by a C/U rich stretch with a G-repeat in the 5′ UTR of *tlpB* mRNA encoding for one of the four chemotaxis receptors in *H. pylori*. Comparison of *tlpB* expression in the wild-type and a HPnc5490 deletion strain confirmed down-regulation of the *tlpB* mRNA as well as TlpB protein levels by HPnc5490. It has been suggested that TlpB senses protons and diverse studies have demonstrated its potential role in pH-taxis, quorum sensing as well as colonization, and inflammation of the gastric mucosa (Croxen et al., 2006; McGee et al., 2005; Rader et al., 2011; Williams et al., 2007). Therefore, HPnc5490, and probably additional *H. pylori* sRNAs, could play important roles during stress responses or infection, as described for other bacterial pathogens (Papenfort and Vogel, 2010).

Another *H. pylori trans*-encoded sRNA is the homolog of *E. coli* 6S RNA, a ubiquitous riboregulator, which mimics an open promoter complex and thereby sequesters RNA polymerase (Barrick et al., 2005; Sharma et al., 2010; Wassarman and Storz, 2000). Despite only little sequence conservation to *E. coli* 6S RNA, the 180-nt long RNA from *H. pylori* can fold into the characteristic long hairpin structure of 6S RNA (Trotochaud and Wassarman, 2005). Deletion of 6S RNA

results in no obvious phenotype during exponential growth but altered cell survival during stationary phase and under extreme stress conditions in *E. coli* (Wassarman, 2007). Whether 6S RNA has a role during stress response or stationary phase growth in *H. pylori* or, like in *Legionella* (Faucher et al., 2010), impacts on its virulence still needs to be investigated.

1.3.3 Proteins involved in sRNA- and asRNA-mediated regulation

The Sm-like RNA chaperone Hfq is required for the stabilization of sRNAs and facilitates the base-pairing of *trans*-encoded sRNA with their target mRNAs in different bacteria (Vogel and Luisi, 2011). Deletion of *hfq* leads to pleiotropic phenotypes including reduced fitness and virulence in several bacterial pathogens (Chao and Vogel, 2010). However, as is the case for 50% of all bacterial genomes, *hfq* appears to be absent in Epsilonproteobacteria. Whether a different RNA binding protein replaces the function of Hfq or whether sRNAs act without a chaperone in these bacteria is still an open question.

Although the exact mechanism of repression is still unclear, both functionally characterized antisense RNAs in *H. pylori* cause reduced protein levels as well as reduced target-mRNA levels, most likely through transcript destabilization or active recruitment of RNases. In enterobacteria, sRNA-mediated target-mRNA decay mainly depends on the RNA degradosome, a protein complex composed of the endoribonuclease RNase E, polynucleotide phosphorylase PNPase, and the RNA helicase RhlB (Caron et al., 2010; Morita et al., 2005). In *H. pylori*, several RNases are annotated (RNase H, RNase H-II, RNase J, RNase N, RNase P, RNase R, and RNase III) but like all Epsilonproteobacteria it appears to lack a homolog of RNase E. Nevertheless, recent studies have shown that *H. pylori* RNase J and RNase III could be potential RNases participating in sRNA-mediated transcript destabilization (Boisset et al., 2007; Chevalier et al., 2008; Huntzinger et al., 2005; Mathy et al., 2010; Roux et al., 2011). Moreover, the 3′–5′ exoribonuclease RNase R has been shown to post-transcriptionally down-regulate six virulence related genes (Tsao et al., 2009), but its potential role in sRNA-mediated regulation still needs to be investigated.

1.4 Type IV secretion system

T4SS are macromolecular devices that bacteria use to transport various macromolecules, including protein, DNA or nucleic acid/protein complexes, across the cell envelope (Alvarez-Martinez and Christie, 2009; Fronzes et al., 2009). These systems are remarkably versatile and have been classified into three different groups according to their function (Alvarez-Martinez and Christie, 2009).

- T4SS of the first group can mediate the conjugative transfer of plasmid DNA or transposons from one cell to another by a contact-dependent process (Dreiseikelmann, 1994), promoting bacterial genome plasticity and the adaptive response of bacteria to changes in the environment. Typical acceptors are bacterial cells of the same species or of different species (Grohmann et al., 2003; Lawley et al., 2003; Trieu-Cuot et al., 1985), while at least the two Gram-negative *Escherichia coli* and *Agrobacterium tumefaciens* can deliver DNA substrates into fungal, plant or human cells (Bundock et al., 1995; Waters, 2001).

- The second group of T4SS is used for DNA uptake and release from and to the extracellular milieu, promoting the genetic exchange. Examples are the ComB system of *H. pylori* (Smeets and Kusters, 2002) and the GGI system of *Neisseria gonorrhoeae*, (Hamilton et al., 2005).

- The third group consists of T4SSs that transfer protein effectors and function as molecular pumping devices that facilitate host–pathogen interaction and/or inject toxins into the host cell (Wallden et al., 2010). This type of T4SS are exploited by numerous pathogenic bacteria, including *Bordetella pertusis*, *Legionella pneumophila*, *Brucella* species and *Bartonella* species (Backert and Meyer, 2006; Corbel, 1997; Ninio and Roy, 2007), as well as *H. pylori* (Akopyants et al., 1998).

Despite the wide diversity of their substrates and functions, all T4SSs are evolutionarily related (Lessl and Lanka, 1994; Lessl et al., 1992), sharing several components and probably function in a similar manner. The genes encoding the

T4SS components are usually arranged in a single or a few operons. Although variations exist, many of the T4SSs found in Gram-negative bacteria are similar to the *A. tumefaciens* VirB/D T4SS machinery, the best characterized T4SS that is regarded as the prototype among that family members .

1.4.1 Archetypal Agrobacterium tumefaciens T4SS

The *A. tumefaciens* T-DNA (transfer DNA) transfer machinery delivers oncogenic nucleoprotein particles into plant cells, resulting in the development of crown-gall tumors (Cascales and Christie, 2003; Christie, 1997; Schroder et al., 2002). The T4SS proteins mediating T-DNA transfer are the 11 VirB proteins encoded by *virB1–virB11*, as well as the so-called coupling protein VirD4, a nucleoside triphosphatase (Cascales and Christie, 2003; Christie, 1997). They assemble to form three interlinked subparts (Fig. 3): a cytoplasmic/inner membrane complex, a double membrane-spanning channel and an external pilus (Alvarez-Martinez and Christie, 2009). The cytoplasmic/inner membrane complex is composed of four inner membrane scaffold proteins VirB3, VirB6, VirB8, and VirB10, that contribute in various ways to channel formation and activity. The trans-membranes pore complex, also termed "the core complex", is composed by VirB7, VirB9 and VirB10 proteins and it forms a ~1 MDa channel spanning from the inner to the outer membrane. Lastly, VirB2 and VirB5 proteins constitute the external pilus. Other essential non-structural components for the formation of the T4SS complex is VirB1 transglycosylase and the three NTPases VirB4, VirB11 and VirD4. VirB1 protein harbors a muraminidase activity and, delivered across the cytoplasm, it causes the localized degradation of the peptidoglycan, allowing for the insertion of the system in the periplasm (Cascales and Christie, 2003). The NTPases VirB4, VirB11 and VirD4 are the energetic components of the T4SS and they are employed to energize the early steps of machine biogenesis and the substrate recruiting and transfer. In particular, the VirD4 coupling protein (CP) together with VirB11, recruits the T-DNA transfer intermediate complex to the secretion apparatus and promotes its translocation through the secretion channel (Lai and Kado, 2000).
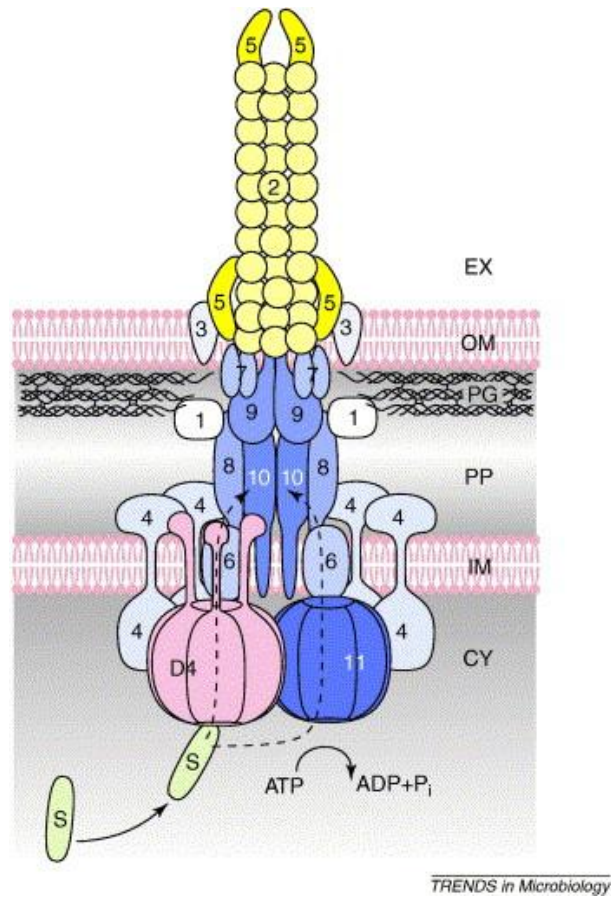
Fig. 3 Model of the VirB/VirD4 type IV secretion system (T4SS) machinery of *Agrobaterium tumefaciens*. Colour code: yellow, pilus-associated extracellular components of the T4SS machinery; blue, all other components of the T4SS machinery (pore complex and energizers); pink, T4CP; green, T4SS substrates. Abbreviations: CY, cytoplasm; EX, extracellular milieu; IM, inner membrane; OM, outer membrane; PG, peptidoglycan layer; PP, periplasm (Schroder and Dehio, 2005).

Although T4SS core complexes are able to form autonomously, they are unlikely to do so constitutively and without a positional preference. In the *A. tumefaciens* Vir system, spatial targeting of the secretion apparatus has been suggested to be determined by VirB8 as a nucleating factor (Judd et al., 2005), possibly together with the peptidoglycan-degrading lytic transglycosylase VirB1 (Alvarez-Martinez and Christie, 2009).

It is important to note that most, but not all, of the T4SSs have homologues of each of these proteins, but a conserved core VirB4, VirB7, VirB9, VirB10 and VirB11 proteins is present in all of them.

1.4.2 *H. pylori cag* encoded T4SS

The *H. pylori cag* pathogenicity island (*cag*-PAI) is a 38 kb multi-operon locus encompassing 28 putative ORFs, encoding functional components of a type IV secretion system (T4SS), homologues of the basic T4SS represented by the *Agrobacterium tumefaciens* virB/D operons (Bourzac and Guillemin, 2005). *H. pylori* T4SS represents a needle-like structure (also called T4SS pilus) protruding from the bacterial surface (Fig. 4) and is induced by host cell contact to inject virulence CagA effector into host cells (Kwok et al., 2007), as well as to stimulate a CagA-independent interleukin-8 secretion, via the host AP-1 and NF-κB signaling pathway (Backert and Selbach, 2005).

Fig. 4   *H. pylori cag*-encoded pilum (Molloy, 2007). *H. pylori* strain 26695 co-cultured with AGS cells and visualized by scanning electron microscopy. Three pili are visible at the interface between the bacteria and the host cell.

In its most common gene arrangement, the *cag*-PAI is inserted between the genes encoding a Sel1 repeat-containing protein (HP0519) and glutamate racemase (HP0549), respectively, and it is flanked by a 31 bp sequence duplication of the latter gene. The amount of sequence diversity among these genes in isolates from different geographic groups has recently been taken as an indication that the *cag*-PAI was acquired only once in the history of *H. pylori* (Olbermann et al., 2010).

By contrast to other T4SS found in *H. pylori*, the Cag-T4SS is only distantly related to T4SS found in other species (Fischer et al., 2010), and only a few *cag* genes encode for proteins with clear sequence similarities to known T4SS proteins. Obvious similarities exist only for CagE (to VirB4), CagX (to VirB9), CagY (to

VirB10), Cagα (to VirB11) and Cagβ (to VirD4), although even these proteins, particularly CagX and CagY, are remarkably different from their counterparts in prototypical systems. Nevertheless, protein topology predictions and determinations, localization studies and functional studies suggested that Cagγ (VirB1), CagC (VirB2), CagL (VirB5), CagW (VirB6), CagT (VirB7) and CagV (VirB8) are further VirB homologues (Andrzejewska et al., 2006; Backert et al., 2008; Buhrdorf et al., 2003; Kutter et al., 2008; Zahrl et al., 2005).

Early systematic studies with isogenic mutants in each *cag* gene (Fischer et al., 2001; Selbach et al., 2002) identified 15 genes that are essential for inducing IL-8 secretion and for CagA translocation, suggesting that these genes encode for components of the secretion apparatus (Table 1). These essential components include all the aforementioned VirB-like proteins and several further components that are unique to the Cag system: Cagδ, CagU, CagM and CagH. Three further gene products (CagN, CagG, CagD) are not absolutely necessary, although their absence results in a reduced efficiency of both phenotypes, and these proteins (supporting components) thus appear to be involved in assembling the secretion apparatus as well. An additional group of genes was shown to be required for CagA translocation but not for IL-8 induction (Fischer et al., 2001), and the encoded gene products (CagZ, CagI, CagF and the toxin CagA) are accordingly termed CagA translocation factors.

Finally, several *cag*-PAI gene products (Cagζ, Cagε, CagS, CagQ, CagP, CagB) do not appear to have a function for the type IV secretion-related phenotypes examined. They might have other as yet unknown functions or even be further effector proteins, or they might simply be unrelated to the T4SS. However, one of these genes (*cagζ*) was found to be among the most highly transcribed among all *cag* genes *in vitro* and *in vivo*, and transcripts of *cagε*, *cagS*, *cagQ*, *cagP* and *cagB* were also found, probably together with a small RNA upstream of *cagP* (Boonjakuakul et al., 2005; Sharma et al., 2010). These observations suggest that all non-essential genes are expressed, and their organization in operons indicates a functional relationship with the T4SS (Cendron, 2011).

Table 1: Overview of characteristics and functions of *cag*PAI-encoded proteins

Gene	Protein	Homologues	(Putative) function(s)	CagA	IL-8
HP0520	Cagζ			-	-
HP0521	Cagε			-	-
HP0522	Cagδ			Essential	Essential
HP0523	Cagγ	VirB1	Peptidoglycan hydrolase	Essential	Essential
HP0524	Cagβ	VirD4	Coupling Protein	Essential	-
HP0525	Cagα	VirB11	ATPase	Essential	Essential
HP0526	CagZ		Cagβ stabilization	Essential	-
HP0527	CagY	VirB10	Core complex	Essential	Essential
HP0528	CagX	VirB9	Core complex	Essential	Essential
HP0529	CagW	VirB6	Inner membrane channel	Essential	Essential
HP0530	CagV	VirB8	Core complex-IMP	Essential	Essential
HP0531	CagU			Essential	Essential
HP0532	CagT	VirB7	Core complex-OMP	Essential	Essential
HP0534	CagS			-	-
HP0535	CagQ			-	-
HP0536	CagP			-	-
HP0537	CagM		Outer Membrane Complex	Essential	Essential
HP0538	CagN			Supportive	Supportive
HP0539	CagL	VirB5	Adhesin - Integrin binding	Essential	Essential
HP0540	CagI			Essential	-
HP0541	CagH			Essential	Essential
HP0542	CagG			Essential	Supportive
HP0543	CagF		Chaperone of CagA	Essential	-
HP0544	CagE	VirB3/B4	ATPase	Essential	Essential
HP0545	CagD			Essential	Supportive
HP0546	CagC	VirB2	Pilus subunit	Essential	Essential
cagB	CagB			Unknown	Unknown
HP0547	CagA		Toxin	Essential	-

1.4.3 Architecture of *H. pylori* type 4 secretion system

The architecture of the *H. pylori* type 4 secretion system is modeled on the homologue *A. Tumefaciens* VirB/D T4SS. However, the *cag* proteins are considerably different from their Vir counterparts, both in size and in amino acidic sequences, suggesting different and/or additional functions. The *H. pylori* T4SS is composed by the cytoplasmic/inner membrane complex, the double membrane-

spanning channel and the external pilus, plus other ancillary components (Fischer, 2011) (Fig. 5).

The *H. pylori cag* core complex is composed by the CagT, CagX and CagY proteins, homologues to VirB7, VirB9 and VirB10. By contrast to other T4SS, this subcomplex appears to harbor two additional components, CagM and Cagδ, that interacting with CagT and CagX, stabilize the scaffold proteins and mediate to oligomerization of the outer membrane subcomplex (Fischer et al., 2001; Kutter et al., 2008). The most divergent core protein is CagY, a huge protein with a peculiar middle region containing extensive sequence repeats. CagY is shown to interact with subcomplex CagX-CagM-CagT-Cagδ, by direct binding of CagX (Kutter et al., 2008). Moreover, CagY is also detected on type IV secretion pilus-like surface appendages (Rohde et al., 2003) and is identified as one of several bacterial interaction partners of β1 integrins, which represent the secretion apparatus receptors on target cells (Jimenez-Soto et al., 2009).

The Cag system contains three essential proteins that might constitute a cytoplasmic membrane pore. CagW is a polytopic inner membrane protein with features that are common among VirB6-like proteins (Kutter et al., 2008), CagU is a second polytopic inner membrane protein with three predicted transmembrane helices that has no counterpart in other systems, and CagH is an essential bitopic inner membrane protein, also without counterparts in other systems. Functional studies with all these components are lacking so far.

The Cag-T4SS elaborates sheathed surface appendages that are dissimilar to the pili commonly found in DNA-transporting T4SS. Nevertheless, these appendages are considered to be composed of the VirB2-like pilin subunit CagC (Andrzejewska et al., 2006) but, in addition, they can be stained with immunogold labels directed against CagY, CagT, CagX and CagL (Kwok et al., 2007; Rohde et al., 2003; Tanaka et al., 2003). It is shown that purified CagL binds via its RGD motif to β1 integrin subunits, suggesting a VirB5-like adhesin function for CagL (Kwok et al., 2007), although conflicting results were obtained with respect to the requirement of this motif during CagA translocation (Jimenez-Soto et al., 2009; Kwok et al., 2007). On the other hand, CagY, CagA and CagI are also identified as Cag proteins binding to β1 integrins (Jimenez-Soto et al., 2009).
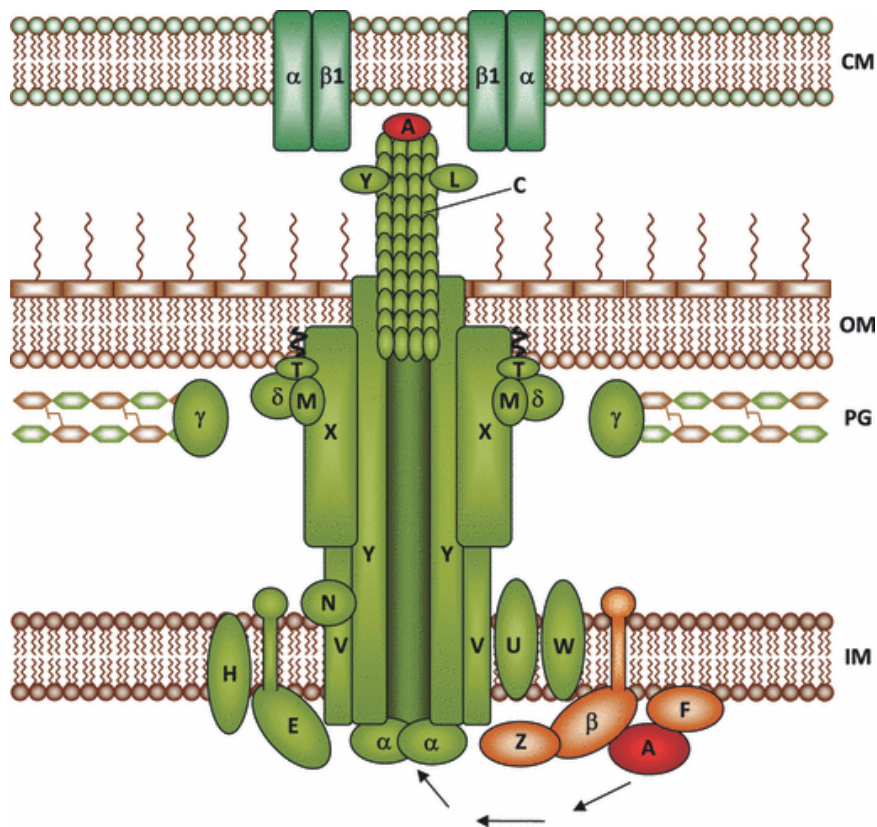
Fig. 5 Assembly and interaction model of the *H. pylori* Cag type IV secretion apparatus (Fischer, 2011). Cag proteins are depicted in their most likely localizations according to sequence prediction or experimental data and designated by their last letters (e.g. 'A' for CagA). Overlapping boxes indicate probable protein–protein interactions. Integrin heterodimers are indicated as receptors on the target cell surface (α, β1). IM, inner (bacterial) membrane; PG, peptidoglycan layer; OM, outer (bacterial) membrane; CM, cytoplasmic membrane of a eukaryotic target cell.

Similarly to *A. tumefaciens* T4SS, the assembly of the T4SS machinery likely relies on both the lytic transglycosylase Cagγ (VirB1 homologue) responsible for the local degradation of peptidoglycan (Zahrl et al., 2005), and CagV, a bitopic inner membrane protein with features similar to the nucleating factor VirB8 (Buhrdorf et al., 2003), capable to interact with Cagδ, CagM and CagT proteins of the core complex. Moreover, on the cytoplasmic face of the secretion apparatus, the ATPases CagE (VirB3-VirB4 fusion homologue) (Kutter et al., 2008) and Cagα (VirB11 homologue) provide the energy for secretion apparatus assembly and/or substrate transport (Kutter et al., 2008).

1.4.4 Mechanisms of CagA translocation

The translocation of the toxin CagA through the T4SS channel has been showed occurring through two consecutive events: the recruitment of CagA to the T4SS complex and the energetic-dependent secretion of the protein through the channel. CagF, CagZ and Cagβ play a central role in the recruitment process, interacting with different motifs on the C-terminal region of CagA. In particular, CagF likely recruits CagA protein interacting with ~100 amino acids in the C-terminal region of CagA (Couturier et al., 2006; Pattis et al., 2007), similarly to the secretion chaperones in type III secretion systems. The ATPase Cagβ forms a stable complex with CagZ at the bacterial cytoplasmic membrane that might recognize the C-terminal secretion signal of CagA (~20 amino acids) (Hohlfeld et al., 2006) and promote the secretion of the protein. The other ATPases CagE (VirB4) and Cagα (VirB11), together with Cagβ (Backert et al., 2008), furnish the energetic power for the translocation of CagA through the T4SS channel (Hohlfeld et al., 2006). The molecular mechanisms of CagA translocation through the secretion apparatus are only poorly understood. Several studies have shown that CagA is located at the bacterial surface, particularly at the pilus tip (Jimenez-Soto et al., 2009; Kwok et al., 2007; Murata-Kamiya et al., 2010), although it has not been examined whether surface- or pilus-associated CagA represents a translocation intermediate. It has also been established that translocation of CagA depends on the presence of β1 integrins as receptors for the Cag secretion apparatus at the target cell surface (Jimenez-Soto et al., 2009; Kwok et al., 2007), as well as CagA itself binds strongly to β1 integrin (Kwok et al., 2007), suggesting that pilus-associated CagA has an important function for translocation. The uptake process into the host cell cytoplasm is not understood, and it is unclear whether CagA uptake involves pore formation in the host cell cytoplasmic membrane or other cellular processes.

1.5   Effects of the *H. pylori* T4SS on the host cells

In *H. pylori cag*-PAI encoded T4SS is identified to translocate the cagA protein into human gastric epithelial cells after bacterial attachment. Injected CagA interferes with physiological signal transduction and causes pathological cellular responses such as increased cell proliferation, motility, apoptosis and morphological change through different mechanisms. In addition, *H. pylori* induces a pronounced pro-inflammatory phenotype in infected gastric epithelial cells by multiple signaling activities that stimulate the transcription factors NF-κB and/or AP-1, in CagA-independent mechanism.

1.5.1 Phosphorylated CagA

The *H. pylori* toxin CagA is considered a paradigm for bacterial carcinogenesis (Hatakeyama and Higashi, 2005). After translocation into gastric epithelial cells, CagA is tyrosine-phosphorylated by host cell kinases of the Src family (SFKs), such as Src, Abl and others (Handa et al., 2007; Wessler and Backert, 2008). CagA harbors numerous phosphorylation sites at the repeated Glu-Pro-Ile-Tyr-Ala (EPIYA)-motifs (Backert et al., 2010; Hatakeyama and Higashi, 2005). Phosphorylated CagA (CagA^{PY}) interacts with Src homology 2 (SH2) domains of more than 20 different human proteins involved in signal transduction, interfering with the signaling cascades at multiple levels, thus affecting host cell gene expression (Backert et al., 2010; Peek, 2005). As a consequence of CagA^{PY} action, epithelial cells will have some of their major functions disturbed, such as cell cycle, cytoskeletal structure, cell-cell adhesion, signaling, adherence and proliferation (Hatakeyama and Higashi, 2005). Gastric epithelial cells infected with *H. pylori in vitro* start to migrate and acquire a morphology that has been originally described as the "hummingbird phenotype" (Al-Ghoul et al., 2004; Backert et al., 2001). This phenotype results from two successive events: the induction of cell scattering and cell elongation. While induction of early cell motility mainly depends on a CagA-independent T4SS factor (Churin et al., 2003), cell elongation is clearly triggered by CagA^{PY} (Backert and Selbach, 2008; Hatakeyama, 2008), through the recruitment of

the tyrosine phosphatase SHP-2 and the activation its phosphatase activity. The activated SHP-2 directly dephosphorylate and inactivate the focal adhesion kinase (FAK), and activate the Rap1→B-Raf→Erk signaling cascade. CagA^{PY}-induced cell elongation phenotype also involves tyrosine dephosphorylation of cortactin, vinculin and ezrin, three well-known actin-binding proteins (Backert and Selbach, 2008), through unknown host phosphatases. CagA^{PY} can also induce the production of reactive oxygen species (ROS) in gastric epithelial cell. Excessive ROS production in eukaryotic cells can cause DNA damage and thus might involve in gastric carcinogenesis (Naito and Yoshikawa, 2002). Interestingly, phosphorylated CagA inhibits the activity of Src kinase in a negative feedback loop, which results in dephosphorylation of many host cell proteins, including the actin-binding protein cortacin (Selbach et al., 2003). This mechanism may enable *cagA*-positive *H. pylori* to establish a chronic infection, avoiding excessive CagA toxicity to the host.

1.5.2 Un-phosphorylated CagA

Injected *H. pylori* CagA affects the host cell also in a non-phosphorylated form, interacting with, at least, 12 cellular partners (Backert et al., 2010). These interactions have been reported to induce the disruption of cell-to-cell junctions, loss of cell polarity and induction of mitogenic responses. In polarized epithelial cells, non-phosphorylated CagA disrupts the cell-to-cell junctions, which are essential components for the integrity of the gastric epithelium (Wessler and Backert, 2008). These effects are achieved via several pathways, as interfering in the E-cadherin pathway, as well as associating with the epithelial tight-junction scaffolding protein ZO-1 and the transmembrane protein JAM, causing an ectopic assembly of tight-junction components at sites of bacterial attachment (Amieva and El-Omar, 2008). Moreover, CagA binds directly and inactivates the central regulator of cell polarity Par1b (Hatakeyama, 2008), inducing the loss of cell polarity. Together, these effects contribute to the *H. pylori*-induced elongation phenotype of AGS cells. Non-phosphorylated CagA forms CagA/Grb2/Sos complexes that promote Ras-GTP formation, which in turn stimulates the Raf→Mek→Erk signaling cascade. The activation of these factors leads to cell scattering as well as to the activation of nuclear transcription factors, involved in cell proliferation and in the expression of

the anti-apoptotic myeloid cell leukaemia sequence-1 (MCL-1) protein (Mimuro et al., 2007). Finally, CagA can also induce the ubiquitination and degradation of RUNX3, a tumor suppressor which is frequently inactivated in gastric cancer (Tsang et al., 2010). In certain *H. pylori* strains, non-phosphorylated CagA can induce IL-8 expression via NF-κB activation (see below) (Brandt et al., 2005; Kim et al., 2006; Lamb et al., 2009), however this mechanism is not universal across all *cag* PAI-positive strains (Keates et al., 1999; Keates et al., 2001; Meyer-ter-Vehn et al., 2000; Naumann et al., 1999).

1.5.3 Bacterial Peptidoglycan

During infection, fragments of the *H. pylori* peptidoglycan (PGN) are transferred to and internalized into the gastric epithelial cells via the *cag* type IV secretion system and outer membrane vesicles (OMV) (Kaparakis et al., 2010). However, it is not clear if the secretion of peptidoglycan muropeptides occurs by a syringe-like mechanism, analogous to CagA, or whether the only intimate contact of the T4SS assemblies with the host cell surface could induce a facilitated internalization of the PGN. The muropeptides are sensed by the nucleotide-binding oligomerization domain 1 (NOD1), an intracytoplasmic pathogen pattern-recognition molecule (Boughan et al., 2006; Viala et al., 2004), that activates host cells signaling molecules, as nuclear factor κB (NF-κB), p38 and Erk (Allison et al., 2009; Viala et al., 2004). These factors stimulate the production of proinflammatory cytokines MIP-2, β-defensin, and IL-8. Moreover, NF-κB induces the expression of AID (a DNA-editing enzyme) in host target cells, which results in the accumulation of mutations in the tumor suppressor protein TP53 (Matsumoto et al., 2007). Thus, induction of AID might be a mechanism whereby gene mutations could emerge during *H. pylori*-associated gastric carcinogenesis. Furthermore, NOD1 activation by *H. pylori* peptidoglycan also regulates the production of type I interferon (IFN), which likely affects Th1 cell differentiation (Watanabe et al., 2010).

1.5.4 Intact T4SS components

During *H. pylori* infection, several host responses rely on an intact T4SS, but are independent from CagA or peptidoglycan delivery. Hence, these responses are likely triggered by the interaction of the T4SS structure with the host cell, or are induced by still unknown secreted factors. Infections of gastric epithelial cells with *H. pylori* are reported to profoundly activate numerous receptor tyrosine kinases (RTKs) in a T4SS-dependent but *cagA*-independent fashion, including the epidermal growth factor receptor EGFR (Churin et al., 2003; Keates et al., 2001), hepatocyte growth factor receptor c-Met and Her2/Neu (Churin et al., 2003). Studies on the downstream signaling indicate that activation of EGFR induces pro-inflammatory responses, leading to the secretion of IL-8 (Keates et al., 2001), while the activation of c-Met (but not EGFR or Her2/Neu) is involved in cell scattering and motogenic responses of infected gastric epithelial cells (Churin et al., 2003). The small Rho GTPases Rac1 and Cdc42 are also activated by a T4SS-dependent but CagA-independent mechanism and play a role in triggering the scattering and motility of infected gastric epithelial cells (Churin et al., 2001). However, the actual T4SS factor involved is unclear. Moreover, *H. pylori* is reported to disrupt the normal cell cycle progression by changing histone H3 phosphorylation levels both at serine residue 10 and threonine residue 3, hence inducing a transient pre-mitotic arrest (Fehri et al., 2009). The *cag*–encoded CagL protein is shown to be involved in the activation of EGFR, Her3/ErbB3, Src and Fak kinases in an RGD-dependent manner (Jimenez-Soto et al., 2009). In facts, CagL mimics some important functions of human fibronectin (Tegtmeyer et al., 2010) and it can directly trigger intracellular signaling pathways upon contact with mammalian cells, both exploiting the natural fibronectin-mediated pathways but also activating fibronectin-independent signaling events. In particular, the interaction of the CagL RGD domain with the integrin member α5β1 triggers the dissociation of the metalloprotease ADAM17, that in turn activate EGFR. Lastly, *H. pylori* expresses a yet unknown T4SS factor exhibiting antiphagocytic activity, which can actively block the uptake of the bacteria by professional phagocytes, playing an essential role in the immune escape processes (Ramarao et al., 2000).

AIMS OF THE PROJECT

The severity of *Helicobacter pylori* infections largely depends on the genetic diversity of the infecting strain, and particularly on specific genotypes of virulence-associated genes, such as the *cag* pathogenicity island (*cag*-PAI). The effects of the *cag*-T4SS on host cell signaling pathways have been extensively described in literature. On the contrary, little is known about the bacterial regulators that underlie the coordinated expression of *cag* gene products, needed to assemble a functional secretion system apparatus. To begin to fill this gap, a comprehensive analysis of the transcriptional regulation of the *cag*-PAI operons was undertaken.

To pursue this goal, a robust tool for the analysis of gene expression in *H. pylori* was first implemented. We constructed a bioluminescent reporter system based on the *P. luminescens luxCDABE* operon, constituted by a promoterless G27 *lux* acceptor strain and a transforming vector pVCC, in which promoters of interest can be conveniently cloned. The reporter system was validated by comparisons with transcriptional analyses and systematically used for the comprehensive study and mapping of the *cag* promoters.

The identification of bona fide *cag* promoters had eventually permitted to pinpoint the set of *cag* transcriptional units of the PAI. The responses of these *cag* transcriptional units to metabolic stress signals were analyzed in detail, and integrated with a) transcription studies in deletion mutants of important *H. pylori* virulence regulators, and b) protein-DNA interaction analyses to map the binding sites of the regulators.

Finally, a small regulatory RNA (sRNA) *cncR1* encoded by *cag*-PAI island was identified upstream of the *cagP* gene (HP0536). In order to validate *cncR1* , which could participate to post-transcriptional *cag*-PAI regulation, northern blot analyses and studies with *lux* reporter constructs have been performed to map the 3' end of the molecule. To identify regulatory effects exerted by *cncR1* on the *H. pylori* gene expression, the

Δ*cncR1* knock out mutant strain was derived and compared to the parental wild type strain by a macroarray approach.

In synthesis, the aims of this thesis is:

1. Implementation of *a robust* reporter system in *H. pylori* allowing for a comprehensive transcriptional analysis of *cag* promoters in vivo;

2. Identification of the *H. pylori cag* pathogenicity island transcriptional units and analysis of their regulatory responses;

3. Functional study of the *cncR1* sRNA encoded by the *H. pylori cag*-pathogenicity island.

PART 1:

Implementation of the *lux* reporter system in
H. pylori

3.1 SPECIFIC INTRODUCTION

Despite its importance as a human pathogen and the enduring interest of the scientific community in its fundamental biology, the study of *Helicobacter pylori* gene expression has been somewhat hindered by the lack of suitable genetic tools (Boneca et al., 2008), in particular by the limited effectiveness of available reporter systems (Carpenter et al., 2007).

An ultimate reporter gene ideally would be expressed without perturbing the physiology of the recipient organism, and it would be readily detectable and quantifiable using standard laboratory instrumentation without the need to disrupt the living cell. In addition, the reporter should be highly sensitive, with low background noise, in order to permit analyte detection at low molar concentrations and, at the same time, to prove rapid enough to enable monitoring of quick response kinetics (Hakkila et al., 2002; van der Meer and Belkin, 2010). Finally, the signal should not perdure or stably accumulate in the cell, as this may lead to significant biases in the estimation of gene expression over time.

Of the many reporter systems tested in Gram-negative bacteria, the bioluminescent systems based on paralogues of the bacterial *luxCDABE* luciferase operons appear to best fulfill these criteria (Hakkila et al., 2002; Meighen, 1993). The luciferase activity is provided by two enzyme subunits, LuxA and LuxB, encoded by the *luxAB* cistrons, which together catalyze the oxidation of a reduced riboflavin phosphate and a long-chain fatty aldehyde, coupling the reaction with bioluminescence, e.g., emission of light in the visible range with a maximum at 490 nm (Meighen and Dunlap, 1993). An enzymatic reductase complex, encoded by paralogues of the *luxCDE* cistrons, is responsible for shunting fatty acid metabolites from the central metabolism to convert them into the aldehyde substrate used by the LuxAB complex to catalyze the bioluminescence reaction *in vivo*.

In *H. pylori*, previous comparisons of reporter fusions to a *cat* cassette (providing chloramphenicol resistance), GFP (encoding green fluorescent protein), and a *Vibrio harveyi luxAB* operon proved the superiority of the luciferase-based system in faithfully reflecting the dynamic changes detected at the mRNA level at

different time points throughout growth (Niehus et al., 2002). In the latter system, fusion of the sole *luxAB* operon as a reporter imposed the external supply of the aldehyde substrate in order to catalyze the emission of bioluminescence, limiting to some extent its usefulness *in vivo* and leaving open the question of whether fusions with the whole *luxCDABE* operon would be functional in *H. pylori* as well. In addition, the *V. harveyi* luciferase has a temperature optimum below 37°C (Meighen, 1991), which may give rise to inconsistent measures at continuous culture at 37°C or prove restrictive if expression has to be analyzed after heat shock or under conditions of metabolic stresses.

Unlike those of the marine *V. harveyi* enzyme, the *luxCDABE* gene products of the soil bacterium *Photorhabdus luminescens* retain mesophilic luciferase activity, operating at temperatures as elevated as 45°C (Meighen and Dunlap, 1993). Accordingly, the *P. luminescens luxCDABE* operon has been successfully employed as a reporter system in *Campylobacter jejuni*, both to image the bacterium (Kassem et al., 2010; Kelana and Griffiths, 2003) and to quantify sigma 28 promoter activity (Allen and Griffiths, 2001; Ding et al., 2005).

The implementation in *H. pylori* of such a bioluminescent reporter system based on the *P. luminescens luxCDABE* cassette is reported. The robustness of this new *lux* reporter system is validated in noninvasive *in vivo* monitoring of dynamic transcriptional responses of inducible as well as repressible promoters and it is demonstrated the suitability of *lux* reporter for the implementation of genetic screens in *H. pylori*.

3.2 RESULTS

3.2.1 Construction of the *H. pylori lux* reporter system

Two separate elements have been used to generate an *H. pylori lux* reporter system: a G27 *lux* acceptor strain and the transforming vector pVCC, both schematically represented in Fig. 6.

The first element is the G27 *lux* acceptor strain (Table 3), a G27 derivative carrying a kanamycin resistance cassette upstream of a divergent, promoterless *luxCDABE* operon derived from *Photorhabdus luminescens*, all engineered in the *vacA* locus (Fig. 6A). The products of the *luxAB* genes retain a mesophilic luciferase activity (Meighen, 1991), while the remaining *luxCDE* cistrons code for the reductase complex responsible for the biosynthesis of the aldehyde substrate, which is used by the luciferase complex to catalyze the bioluminescence reaction. By default, the G27 *lux* acceptor strain lacks bioluminescent activity due to the absence of a functional promoter upstream of the *luxCDABE* operon.

The second element of the system is the pVCC suicide transformation vector, a 5,155-bp plasmid designed to conveniently introduce promoters of interest upstream of the *lux* operon by double homologous recombination in the G27 *lux* acceptor strain. It carries flanking regions with homology to the 3′ end of the *cysS* and the (promoterless) 5′ end of the *luxC* cistrons, respectively. Between these flanking regions, pVCC encompasses a *Campylobacter coli cat* cassette, conferring selectable chloramphenicol resistance, and unique BamHI, KpnI, and SacI restriction sites in which promoters, DNA sequences, or transcriptional fusions of interest can be cloned (Fig. 6B).

Following *H. pylori* G27 *lux* transformation with pVCC and a successful (double) homologous recombination event of the *cysS* and *luxC* regions, the kanamycin resistance will be lost while the new derivatives of G27 *lux* will gain the ability to grow on medium supplemented with chloramphenicol as a selectable marker. Consequently, promoters cloned in pVCC upstream of *luxC* in the correct orientation accordingly will drive the expression of the *luxCDABE* operon *in vivo* to emit bioluminescence. The following can be monitored in a noninvasive and

quantitative manner with a luminometer, a multiplate reader, or even with chemiluminescence imagers.
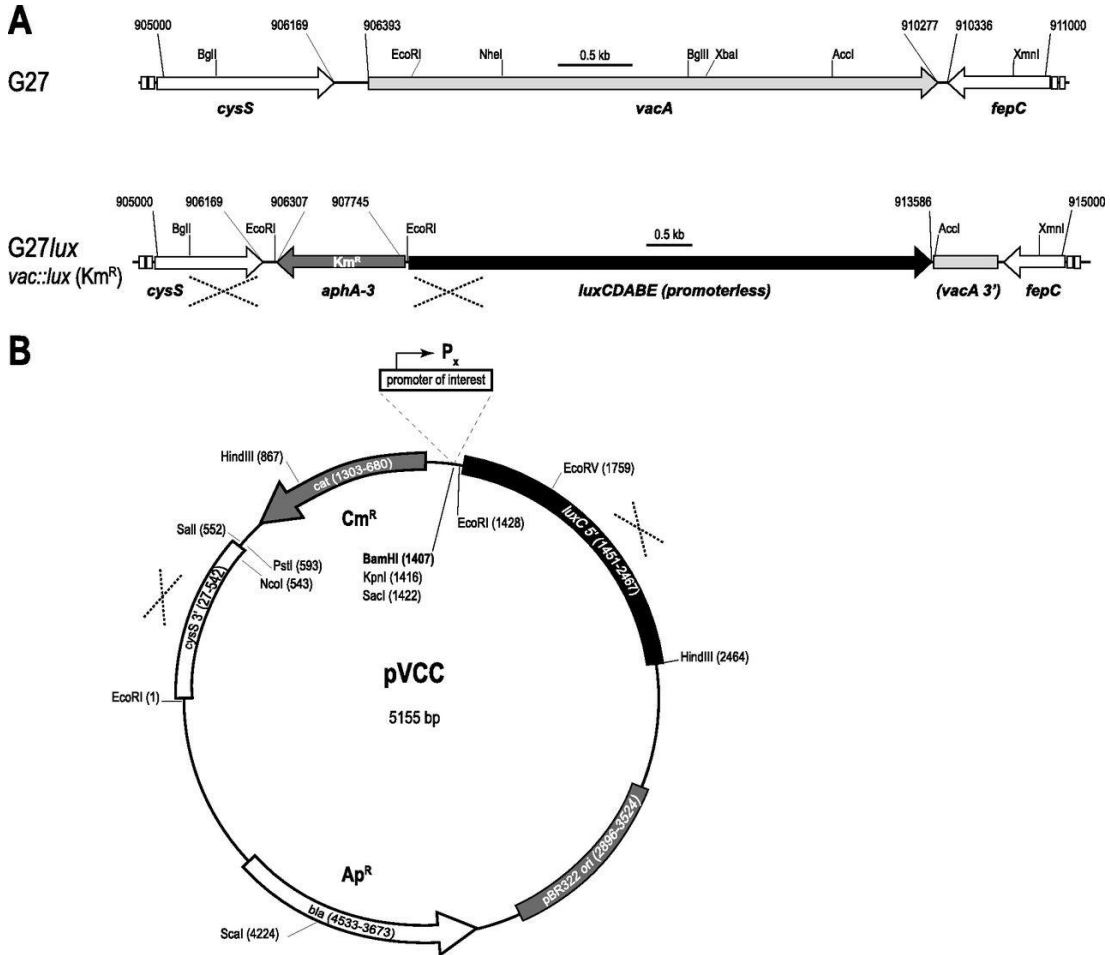
Fig. 6 (A) Genomic organization of *H. pylori* G27 and the derivative G27 *lux* acceptor strain. (B) Detailed map of the pVCC transformation vector. Numeration starts from the EcoRI site upstream of the *cysS* 3′ region. Flanking regions for double homologous recombination in G27 *lux* are indicated by dashed crossed lines. Unique BamHI, KpnI, SacI, and SnaBI restriction sites can be used to clone fragments of interest upstream of the *luxC* 5′ region. The *cat* promoter maps upstream of the promoter cloning site and in divergent orientation with respect to the *lux* operon to avoid bias deriving from antisense transcription.

3.2.2 Linear response of the *lux* reporter system

The expected codon adaptation index (eCAI; 0.754) and the absence of long stretches of rare codons suggested that codon utilization of the *P. luminescens* *luxCDABE* cassette should not represent a problem in *H. pylori*. Thus, to first verify

41

the response of the *lux* system in reporting promoter strength or the abundance of native transcripts in *H. pylori*, transcriptional fusions of the *luxCDABE* operon with P*cagU* and P*cagP* promoters were generated. These two *cag* promoters were chosen because the abundance of their respective transcripts changes according to the growth phase (see next sections). The transcript levels at the P*cagU* promoter remained constant throughout growth (Fig. 7A), while the levels at the P*cagP* promoter decreased markedly toward the late-exponential phase (Fig. 7B). Amplicons encompassing *cagU* and *cagP* promoter regions and parts of their 5' untranslated regions (5'UTRs) were cloned in pVCC leading to the PVCC::P*cagU*-5'UTRtr and PVCC::P*cagP*-5'UTRtr constructs, respectively (Materials and Methods). After transformation, the *cat* selected clones G27 P*cagU*-5'UTRtr-*lux* (hereafter referred as P*cagU-lux*) and G27 P*cagP*-5'UTRtr-*lux* (hereafter referred as P*cagP-lux*) carried the P*cagU*-5'UTRtr and P*cagP*-5'UTRtr regions cloned upstream the *luxCDABE* operon in the same orientation with respect to the reporter. The luminescence emitted by these two mutant strains was assayed with a Victor multiplate reader, normalized according to the OD_{600} of the cultures and compared to the mRNA levels at the native P*cagU* and P*cagP* promoters, measured through quantification of primer extension analyses at different points of the growth curve (Fig. 7). For unvarying (P*cagU*; Fig. 7A) as well as for decreasing transcript levels (P*cagP*; Fig. 7B), the bioluminescence emitted by the respective reporter strains faithfully reflected the trend of the transcript abundance, suggesting a linear response of the *lux* reporter system in the mid- and late-exponential phases. At later time points, when the cultures entered the advanced stationary phase, the emitted luminescence decreased (data not shown). This repeatedly observed phenomenon is likely attributable to the high metabolic burden associated with the expression of the *luxCDABE* reporter operon. On the other hand, no significant retardation of growth rates was observed between the parental G27 wild-type strain and the G27 P*cagU-lux* and G27 P*cagP-lux* derivatives (Fig 7C), suggesting that the expression of the *lux* operon has a modest biological cost in the exponential phase of liquid cultures.
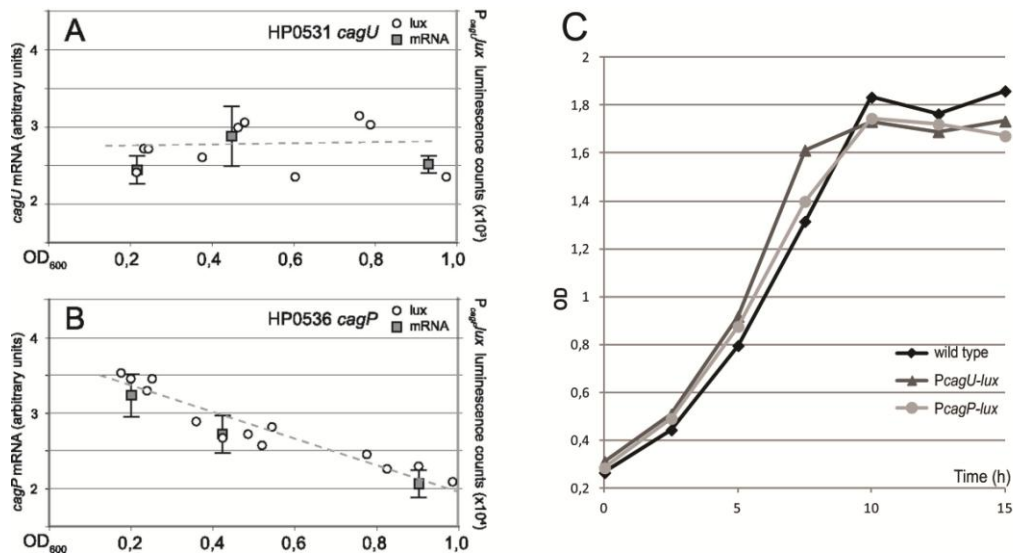
Fig. 7 Linear response of the *lux* reporter system in mid-and late-exponential phase cultures. Transcript levels at the native *cagU* (A) and *cagP* (B) promoters were assayed in triplicate by primer extension analysis. The values are reported as arbitrary units of ^{32}P counts measured in a PhosphorImager (gray squares). Error bars indicate the standard deviations. Values of emitted luminescence of G27 P*cagU-lux* and G27 P*cagP-lux* reporter strains, measured in a multiplate reader and normalized according to the optical density (OD$_{600}$) of the culture, are depicted by white circles. The different trend of *cagU* and *cagP* *lux* fusion expression was confirmed by linear regression analysis fitted using the least-square approach (dotted line). (C) Growth rates of the parental G27 wild-type strain and the P*cagU-lux* and G27 P*cagP-lux* derivatives over a 15 h time-course experiment.

3.2.3 Reporter assays with an inducible promoter

To better characterize the reporter system upon (faster) dynamic transcriptional changes, I set out to assay the response kinetics of the *pfr* promoter, driving the expression of the Pfr bacterioferritin using the *lux* reporter system. This promoter has been extensively studied in *H. pylori* and used to validate a GFP reporter system implemented on a modified endogenous low-copy-number plasmid (Carpenter et al., 2007). It is repressed in iron-depleted conditions by the ferric uptake regulator Fur and promptly induced in response to iron (Carpenter et al., 2009; Delany et al., 2001b). An amplicon of 180 bp containing the regulatory elements upstream of the *pfr* transcriptional start site was cloned in pVCC, obtaining the PVCC::P*pfr* and PVCC::oppP*pfr* constructs (Table 4 and Materials and Methods). After transformation of the G27 *lux* acceptor strain, the *cat* selected G27 P*pfr-lux* and oppP*pfr-lux* strains were obtained, carrying the *pfr* promoter in either direct (P*pfr*) or opposite (oppP*pfr*) orientation with respect to the *luxCDABE* operon.
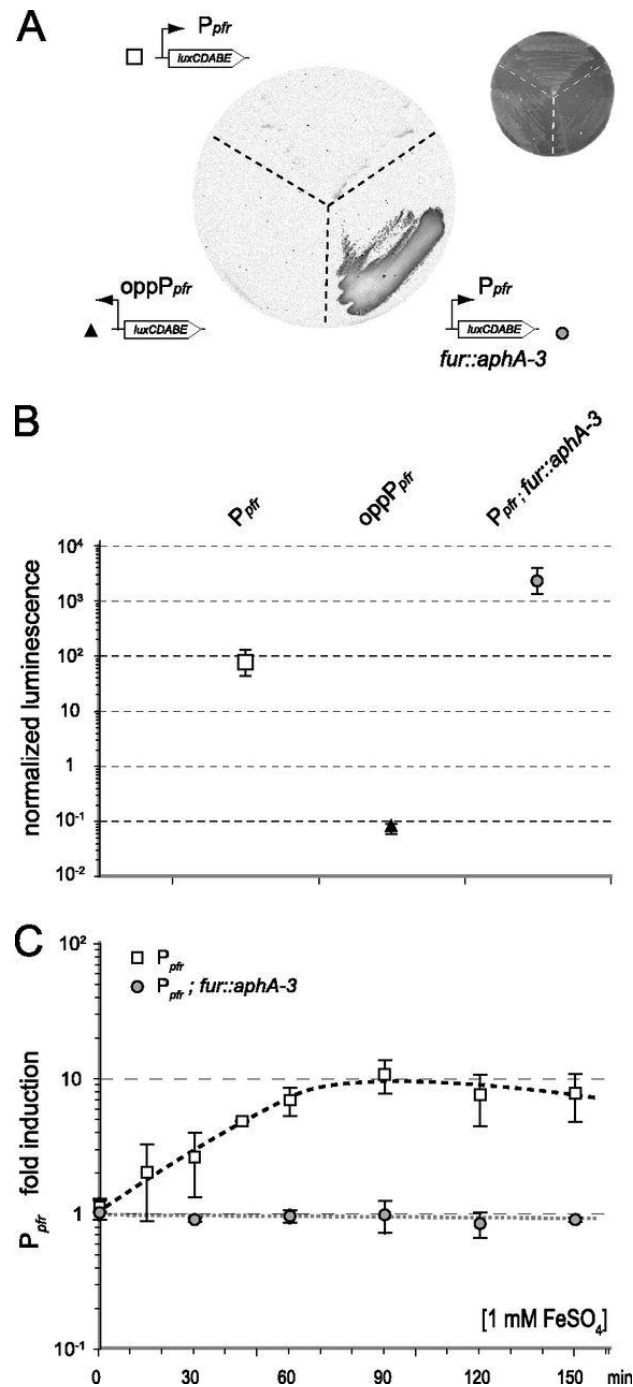
Fig. 8 Reporter assays with the inducible P*pfr* promoter. (A) Inverted dark-field image of luminescence emitted on plates by *H. pylori* reporter strains carrying the P*pfr* promoter in either codirectional (G27 P*pfr-lux*; white squares) or opposite (G27 oppP*pfr-lux*; black triangles) direction with respect to the *luxCDABE* operon and in a wild-type or Δ*fur* (*fur::aphA-3*; gray circles) genetic background. Images were acquired through the CCD camera of a laboratory gel imager. The miniature shows the bright-field image of the plate. (B) Quantification of emitted luminescence (symbols are as described for panel A) measured through a luminometer and normalized according to the optical density (OD$_{600}$) of the cultures. (C) Iron inducibility of the P*pfr* promoter verified through the reporter system in wild-type (white squares) and Δ*fur* (gray circles) genetic background.

44

Moreover, from G27 P*pfr-lux* strain, the mutant G27 P*pfr-lux* Δ*fur* was derived, carrying the P*pfr-lux* transcript fusion in a *fur* knockout background (*fur::aphA-3*). The G27 P*pfr-lux*, oppP*pfr-lux* and P*pfr-lux* Δ*fur* strains were streaked on Columbia agar plates and the bioluminescence emitted on the plates was recorded with the charge-coupled device (CCD) camera of a gel imager (Fig. 8A).

No luminescence was evident in negative controls carrying the *pfr* promoter in the opposite orientation (oppP*pfr*) with respect to *luxCDABE* (oppP*pfr-lux* strain), while a dim light emission could be detected on G27 *lux* derivatives carrying P*pfr* in direct orientation (P*pfr-lux* strain). This luminescence was significantly stronger in the Δ*fur* strain under conditions in which the P*pfr* promoter is constitutively derepressed (Delany et al., 2001b), permitting the identification of even single colonies on the plate. This desirable feature indicates that genetic screenings can be easily implemented using the *lux* reporter system in association with a strong promoter.

In parallel, a luminometer was used to quantify the luminescence of exponentially growing liquid cultures, normalized according to the optical density of the culture (Fig. 8B). The analysis reported a difference of more than four orders of magnitude between derivatives carrying P*pfr* in direct orientation with respect to *luxCDABE* operon, against negative controls carrying P*pfr* in opposite orientation. These results demonstrate that in *H. pylori*, the *lux* reporter system has an intrinsically low background and is therefore suited for sensitive applications. Moreover, the reporter system readily detected the derepression of P*pfr* promoter in the Δ*fur* background, with normalized luminescence increased about another order of magnitude over that of the G27 P*pfr-lux* strain, mirroring published data on *pfr* transcript abundance in wild-type and Δ*fur* strains (Delany et al., 2001b).

Subsequently, the time-response kinetics of the G27 P*pfr-lux* reporter in wild-type and Δ*fur* (G27 P*pfr-lux* Δ*fur*) backgrounds was monitored by using a luminometry, after the addition of 1 mM $(NH_4)_2Fe(SO_4)_2$ to exponentially growing cultures (Fig. 8C). In a wild-type background (G27 P*pfr-lux*), the prompt induction of P*pfr* is reflected in a 10-fold increase of luminescence, reaching a maximum at 60 min after iron treatment. On the contrary, in a *fur* knockout background (G27 P*pfr-lux* Δ*fur*), no induction of luminescence is detected. This is expected for the P*pfr*

promoter, as its iron-dependent regulation is directly mediated by Fur. The observed response curves accurately parallel the kinetics of the *pfr* transcript levels after iron treatment (Delany et al., 2001b), indicating a consistent response of the reporter system.

Finally, the time-response kinetics of the iron-responsive G27 P*pfr-lux* strain, treated with 1 mM $(NH_4)_2Fe(SO_4)_2$ for 120 min and then treated with 1.1 mM 2,2-dipyridyl to sequester stoichiometrically the iron ions was assayed (Fig. 9). After the addition of the chelator, it has been observed a 10-fold reduction of the luminescence (black line - triangles) to values similar to the non-induced samples (dark grey line - diamond) over 90 min, followed by a further 10-fold reduction of luminescence over the subsequent 120 min. In contrast, samples induced with iron, but not treated with 2,2-dipyridyl (light grey line - squares), maintained the aforementioned high levels of luminescence. Likely, the slight excess of the 2,2-dipyridyl sequestered the iron ions either added with the initial treatment and those normally present in the growing medium, prompting the Fur-mediated repression of the P*pfr* promoter below the physiological values of expression.
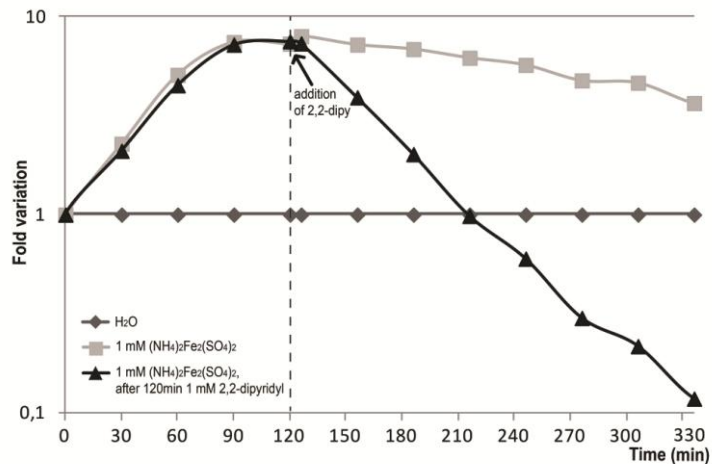
Fig. 9   Iron-dependent response of the *pfr* promoter in presence of divalent Fe ions and iron chelator. Exponential growing cultures of G27 P*pfr-lux* strain were treated with 1 mM $(NH_4)_2Fe(SO_4)_2$ (black line with triangles and light grey line with squares) or sterile water (dark grey line with diamonds). The emitted luminescence was recorded at regular intervals over 120 min and normalized according to the optical density of the cultures. Subsequently, to the iron-enriched samples were treated with 1.1 mM 2,2-dipyridyl (light grey line with squares) or left untreated, and the luminescence was measured at regular intervals over further 210 min. Mean values from two independent experiments were used to determine the n-fold variation of the treated samples with respect to the untreated sample.

Thence, the observed Fe^{2+}-dependent induction of the P*pfr-lux* reporter strain is reversible and the time-response kinetic of repression is similar to the induction.

Together, the results validate the use of the *P. luminescens luxCDABE* operon as a robust tool to monitor the dynamic responses of inducible promoters in *H. pylori*.

3.2.4 Reporter assays with a repressible promoter

To test whether the *lux* reporter could also be valuable to monitor the regulation of other repressible promoters, the system was assayed on the promoter of the *fecA3* gene, encoding a putative outer membrane ferric dicitrate transporter. This promoter is repressed in a nickel-dependent manner by binding of the NikR regulator to two adjacent operators, OPI and OPII, overlapping the transcriptional start site and the extended −10 box, respectively, with OPI being necessary and sufficient for the nickel-dependent repression (Danielli et al., 2009; Ernst et al., 2006; Romagnoli et al., 2011). To this aim, several G27 *lux*–derived reporter strains were created (Fig. 10A and Table 3): the G27 P*fecA3-lux,* carrying the full-length *fecA3* promoter, encompassing the −10 box, the RBS and the start codon of *fecA3* cloned in direct orientation upstream the *luxCDABE* operon; the G27 oppP*fecA3-lux* control strain carrying the full-length *fecA3* promoter in opposite orientation with respect to *luxCDABE*; the G27 P*fecA3*SD*lux-lux* strain, carrying a 3′-shortened sequence missing the native *fecA3* RBS and start codon, in which translation starts on the heterologous *luxC* initiation sequence; and the G27 P*fecA3*SD*lux-lux*ΔOPI*NikR* strain, a P*fecA3*SD*lux-lux* derivative mutant, with the *fecA3* promoter lacking the OPI NikR operator responsible for Ni^{2+}-dependent repression of the promoter. The bioluminescence of these reporter strains was then analyzed as described for the P*pfr* reporter strains, and results are shown in Fig. 10B.

Streaked on plates, the G27 oppP*fecA3-lux* negative-control strain, carrying P*fecA3* in opposite orientation with respect to *luxCDABE*, was unable to emit detectable luminescence. On the contrary, both G27 P*fecA3-lux* and P*fecA3*SD*lux-lux* reporter strains showed a readily detectable signal, which is indicative of robust expression of the *lux* reporter in the absence of Ni^{2+} treatment (Fig. 10B), while an

even stronger luminescence was recorded in the P*fecA3*SD*~lux~*-ΔOPI*~NikR~*-*lux* reporter strain.

These qualitative results were further quantified with a luminometer on exponentially growing liquid cultures. The normalized quantitative luminescence measures paralleled the qualitative observations made on plates, with more than four orders of magnitude stronger signal of strains carrying the codirectional P*fecA3* promoter (G27 P*fecA3-lux*) above levels for strains carrying it in divergent orientation (G27 oppP*fecA3-lux*) with respect to the *lux* operon (Fig. 10C). Interestingly, G27 P*fecA3-lux* and P*fecA3*SD*~lux~*-*lux* strains showed similar luminescence values, suggesting that the absence of the native *fecA3* RBS and ATG initiation codon had no significant influence on the measured levels of *lux* expression. Likely, the Shine-Dalgarno sequence (SD) of *P. luminescens* is well recognized and supported in *H. pylori*. This feature may be convenient if the activity of different promoters or transcriptional fusions has to be compared, as it filters out the bias of dissimilar translation rates that may arise from various ribosome binding sites and/or 5′ untranslated regions (5'UTRs).

In addition, a 3-fold increase of luminescence in the P*fecA3*SD*~lux~*-ΔOPI*~NikR~*-*lux* strain, that carries the *fecA3-lux* fusion deleted of the OPI*~NikR~* regulatory element, was recorded. The observed behavior reflects the constitutive derepression induced by the lack of NikR repressor binding to the promoter. Accordingly, the addition of 1 mM Ni^{2+} to the culture medium resulted in a progressive repression of the luminescence signal only in G27 P*fecA3-lux* and P*fecA3*SD*~lux~*-*lux*, carrying the intact nickel-responsive OPI*~NikR~* element, while in its absence the *lux* reporter strain was completely insensitive to nickel (Fig. 10D). These results demonstrate that the *lux* reporter system can be used to monitor the time-response kinetics of repressible promoters, making it a very versatile instrument in the *H. pylori* molecular toolbox.
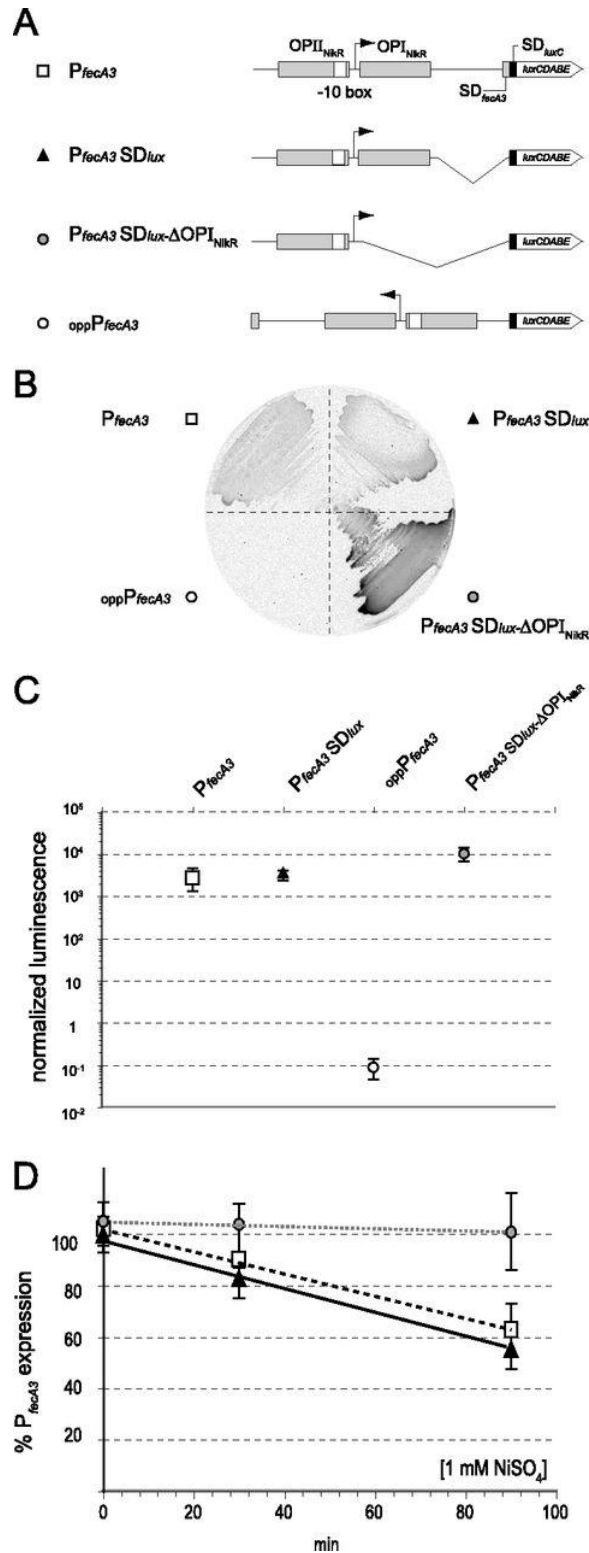
Fig. 10 Reporter assays with the repressible P*fecA3* promoter. (A) Schematic representation of the P*fecA3-lux* fusion constructs, showing the positions of the NikR operators, the −10 box (white box), the transcriptional start site (bent arrow), and the native *fecA3* Shine-Dalgarno (SD) sequences as well as the heterologous SD_{luxC} sequences. (B) Inverted dark-field image of luminescence emitted on plates by *H. pylori* reporter strains carrying the P*fecA3* promoter in either codirectional (G27 P*fecA3-lux*; white squares) or opposite (G27

oppP*fecA3-lux*; white circles) direction with respect to the *luxCDABE* operon, carrying only the heterologous *luxC* ribosome entry site (G27 P*fecA3*SD$_{lux}$-*lux*; black triangles), and a deletion of the NikR OP-I operator important for Ni^{2+}-dependent repression of *fecA3* (G27 P*fecA3*SD$_{lux}$-ΔOPI$_{NikR}$-*lux*; gray circles). Images were acquired through the CCD camera of a laboratory gel imager. (C) Quantification of emitted luminescence (symbols are as described for panel B), measured through a luminometer and normalized according to the optical density (OD$_{600}$) of the cultures. (D) Ni^{2+}-dependent repression of the P*fecA3* promoter verified through the reporter system with the wild-type *fecA3* promoter and 5′UTR (white squares), the SD$_{lux}$-substituted *fecA3* SD$_{lux}$ (black triangles), and the P*fecA3*SD$_{lux}$-ΔOPI$_{NikR}$-*lux* variant with the NikR operator OPI deleted (gray circles).

3.2.5 Utilization of the *lux* reporter for genetic screening

Robust *in vivo* reporter systems greatly facilitate genetic screenings, especially if positive clones can be identified and picked easily over a vast plethora of negative ones.

Strong promoters driving abundant *luxCDABE* expression permitted to spot single luminescent colonies on plates using the CCD camera of a gel imager, a common piece of equipment in most research laboratories (Fig. 8A). However, for weak promoters the integration time needed to acquire a detectable signal had to be increased significantly. This exposed the plates to prolonged periods of suboptimal temperature and unfavorable CO_2 tension, making subsequent recovery of the positive clones demanding. Moreover, it was noticed that in stationary phase, the bioluminescence emitted by *lux* expressing clones has the tendency to drop (data not shown). Thus, to optimize the *lux* reporter system for genetic screening, an alternative high-throughput method based on luminescence monitoring single colonies growing in liquid in 96-well plates was implemented. To validate the method, a blind screen was performed.

Single colonies of G27 *lux*-derivatives carrying the P*pfr* promoter in the *fur* wild-type or knockout background (G27 P*pfr-lux* and P*pfr-lux* Δ*fur*, respectively) were individually cultured in the wells of a microtiter plate. The growth (OD) and luminescence of each clone were monitored at regular time intervals over a period of 72 h within a multilabel plate reader. Recalling the Fur-dependent repression of P*pfr*, discrimination between wild-type and *fur* knockout backgrounds was based solely on the normalized reporter luminescence driven by the Fur-repressed P*pfr* promoter. Out of 30 inoculated clones (15 G27 P*pfr-lux* and 15 G27 P*pfr-lux* Δ*fur*), only one did not

grow. The remaining were promptly classified in two groups according to the weak (repressed P*pfr*) or strong (derepressed P*pfr*) emitted luminescence (Fig. 11). Clones in the first group were judged to have a wild-type background (Fig. 11, black bars), while clones belonging to the second group were predicted by the operator to be Δ*fur* strains (white bars). Notably, all clones were correctly assigned, and viable ones could be effortlessly recovered and expanded even after 72 h of culture, demonstrating that the *lux* reporter system not only may be useful to monitor transcriptional responses but also can be implemented for genetic screening in *H. pylori*.
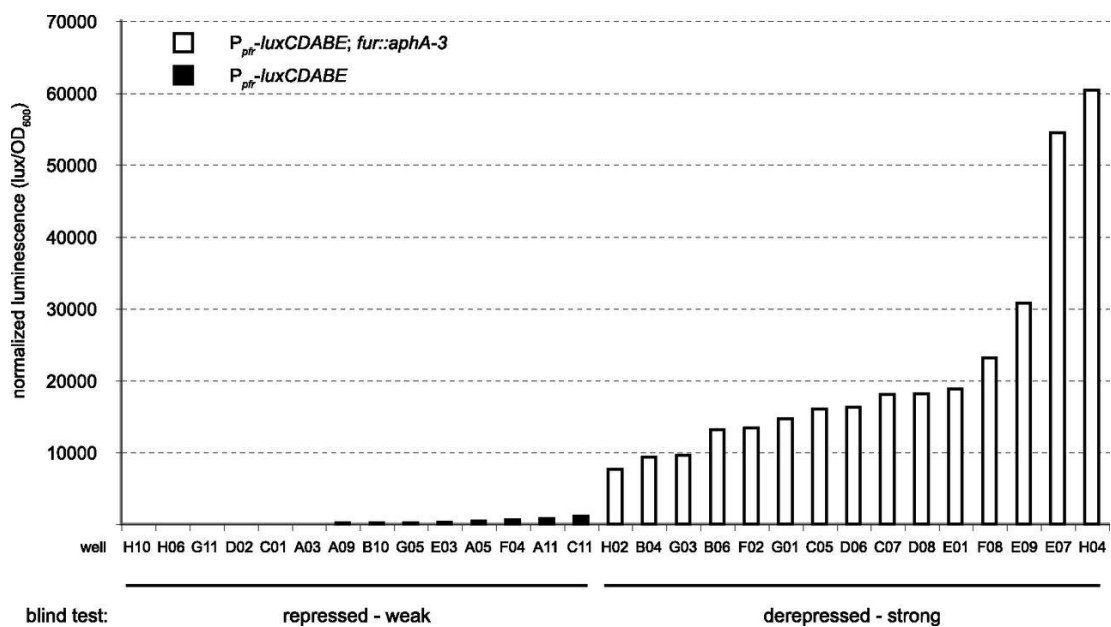
Fig. 11 Genetic screening with the *lux* reporter performed in 96-well culture plates. Genotype prediction blind test of individual *H. pylori* clones expressing the P*pfr-lux* promoter fusion in wild-type (black bars) and Δ*fur* (white bars) genetic backgrounds.

3.3 DISCUSSION

The success of *H. pylori* as a pathogen and its impact on human health depend on the concerted expression of virulence and stress resistance factors, which are controlled by a markedly small number of transcriptional regulators organized in a shallow transcriptional regulatory network (Danielli et al., 2010). In this context, it is clear that the implementation of robust reporter systems for the *in vivo* analysis of gene expression is of pivotal importance.

Measurements of XylE or LacZ enzymatic activities have been used as heterologous reporter systems in many bacteria, and both have been implemented in *H. pylori*. XylE activity is absent from native strains, and the polypeptide encoded by the *xylE* reporter gene appears to be stable when expressed by the bacterium (Karita et al., 1996; Pereira and Hoover, 2005). In contrast, the measurement of the β-galactosidase activity of the LacZ reporter in *H. pylori* has frequently proven critical, with low enzymatic activities detected even in the case of transcriptional fusions with the *ureA* promoter, one of the strongest promoters in *H. pylori* (van Vliet et al., 2001b). Significant advances in the use of *lacZ* have recently been reported in the construction and tweaking of an inducible expression system to engineer conditional mutants (Boneca et al., 2008). However, due to the invasive nature of the enzymatic measurement and their relatively low sensitivity, both *lacZ* and *xylE* appear to be better suited for single- or endpoint assays rather than as a workable *in vivo* resource for the analysis of weak promoters or the implementation of genetic screens.

For the latter purposes, reporter systems based on the promoterless chloramphenicol acetyltransferase *cat* cassette were developed. Fused to promoters of flagellar genes, the *cat* reporter displayed a high sensitivity. However, a major disadvantage of the *cat* reporter system is the well-known high stability of the Cat protein, which makes the system unsuited for the study of transient and dynamic changes in expression over time (Niehus et al., 2002).

The same applies for fluorescent proteins, such as GFP, its cognate derivatives, or DsRed, which give slow responses, with significant rise of the signal occurring only several hours after induction (Hakkila et al., 2002). Another drawback

is their relatively weak sensitivity, leading to detection of the signal at approximately one hundred times higher analyte concentrations than with luminescent proteins (Hakkila et al., 2002). Optimized GFP isoforms with very bright fluorescence and improved folding in bacteria (Cormack et al., 1996) partially resolved this problem and constituted a pivotal tool for construction of reporter systems enabling the analysis of single *H. pylori* cells in culture or in contact with host cells (Carpenter et al., 2007; Josenhans et al., 1998; Kim et al., 2004). However, the high autofluorescence levels of *H. pylori* cells appear to compromise the use of GFP systems, especially in the advanced growth phases (Josenhans et al., 1998).

Here, it has been demonstrated that a bioluminescent reporter system based on the *P. luminescens luxCDABE* operon provides a very convenient reporter to study the kinetics of gene expression in *H. pylori*. The reporter system is constituted by a promoterless *lux* acceptor strain, deriving from of the commonly used G27 parental strain, and of a transforming vector pVCC, in which promoters of interest can be conveniently cloned. The system faithfully reported the iron-inducible Fur regulation of the *pfr* promoter (Fig. 8 and 9), as well as nickel-repressible NikR-dependent regulation of the *fecA3* promoter (Fig. 10), with very low background noise. The high signal-to-background ratio ($\geq 10^3$- to 10^4-fold difference), together with the self-sustainable expression of substrate fuelling the luciferase activity, makes the *luxCDABE* system especially suited for *in vivo* applications in which high sensitivity and continuous monitoring of the reporter output is desirable. It overcomes many of the limitations of fluorescent reporters, e.g., cellular autofluorescence, excessive stability, slow turnover of the fluorescent protein, etc., which have hampered the study of dynamic changes of *H. pylori* gene expression, especially in terms of host-pathogen interactions. For example, it is possible to use this reporter system to monitor differences in the timely activation of specific promoters upon contact with a human AGS cell line (see next section).

Another advantage of the *lux* reporter over other available systems is its robustness, which allowed to correctly assign the genotype of a mutant strain using a high-throughput screening platform (Fig. 11). Moreover, single colonies with strong and constitutively derepressed promoters could be readily detected on plates using

standard laboratory imagers equipped with a CCD camera (Fig. 8), making the selection of positive clones particularly fast and cost-effective.

Given the pervasive occurrence of antisense transcripts in *H. pylori* (Sharma et al., 2010), the *lux* reporter system also has excellent features to monitor putative posttranscriptional regulation mechanisms mediated by these noncoding RNAs. Indeed, the system can be used to verify target regions and pairing cores of putative small RNAs involved in posttranscriptional regulation and also to confirm the presence of predicted transcriptional terminators (see next sections).

On the other hand, several drawbacks in the adaptation of the system to *H. pylori* have been noticed. First, the bioluminescence of the reporter progressively fades when the cultures enter the stationary phase. This is probably due to the high metabolic burden associated with the expression of the large *lux* operon and with the withdrawal of fatty acid metabolites from the central metabolism to synthesize the luciferase aldehyde substrate. This limits the range of workable and reproducible conditions to the mid- and late-exponential phases of growth (Fig. 7). Second, it has been observed that low pH has a negative effect on the emission of luminescence on the promoter tested, hampering to a certain extent the usefulness of the system if acid responses have to be monitored (data not shown). Finally, another pitfall of the system is that the reporter fusion is inserted at the *vacA* locus, so that promoters are not tested at their original positions on the chromosome, while it is acknowledged that the activity of certain promoters may be influenced by the DNA context.

Nevertheless, the many desirable features of the described *lux* reporter system provide a major improvement to the available *H. pylori* toolbox. It is therefore anticipated that they will greatly help the study of kinetic responses in gene expression and implementation of genetic screens in this bacterium.

PART 2:

Transcriptional analysis of the *cag* island

4.1 RESULTS

4.1.1 Mapping of the *cag* promoter

Recent studies on *Helicobacter pylori* have given some insights on the transcriptional organization of the *cag* pathogenicity island, with the mapping of the transcriptional start sites (TSS) located in the *cag* locus and the identification of their promoter regions. In particular 40 putative 5'-end of RNA transcripts were mapped in this DNA region using strain 26695; of these, only 14 5'-end map within 300 bp upstream of *cag* ORFs (Sharma et al., 2010; Ta et al., 2012). To further study transcriptional regulation of the *cag* promoters in *H. pylori* G27 strain, we set up primer extension analyses using oligonucleotides mapping downstream the 14 aforementioned 5'-end of RNA transcripts (Table 6).

With the exception of the transcriptional start sites mapping upstream of the *cagγ* , *cagW* and *cagZ* genes, our primer extension results confirmed the other 11 TSS, suggesting that the *cag* region of G27 strain harbors at least 11 transcriptional units: *cagζεδγ*, *cagVXWYZαβ*, *cagUT*, *cagS*, *cagQ, cagP*, *cagMN*, *cagFGHIL*, *cagCDE*, *cagB* and *cagA* (Fig. 12A).

Nucleotide sequence analyses of these 11 *cag* promoters showed -10 regions with homology to the canonical TATAAT *E. coli* promoter consensus sequence, recognized by the vegetative sigma factor σ^{80} of *H. pylori* (Fig. 12B). In contrast, a -35 TTGACA motif homologue to the *E. coli* -35 consensus sequence was identified only in the P*cagF* promoter region. Notably, *cagζ, cagV, cagU, cagQ, cagM, cagC*, *cagB* and *cagA* exhibited an extended TGn -10 box (Fig 12B – grey boxes), able to ensure transcription even in the absence of a conserved -35 box. Intriguingly, the P*cagS* and P*cagP* promoters show the -10 sequence only, with no upstream -35 and no TG motifs.
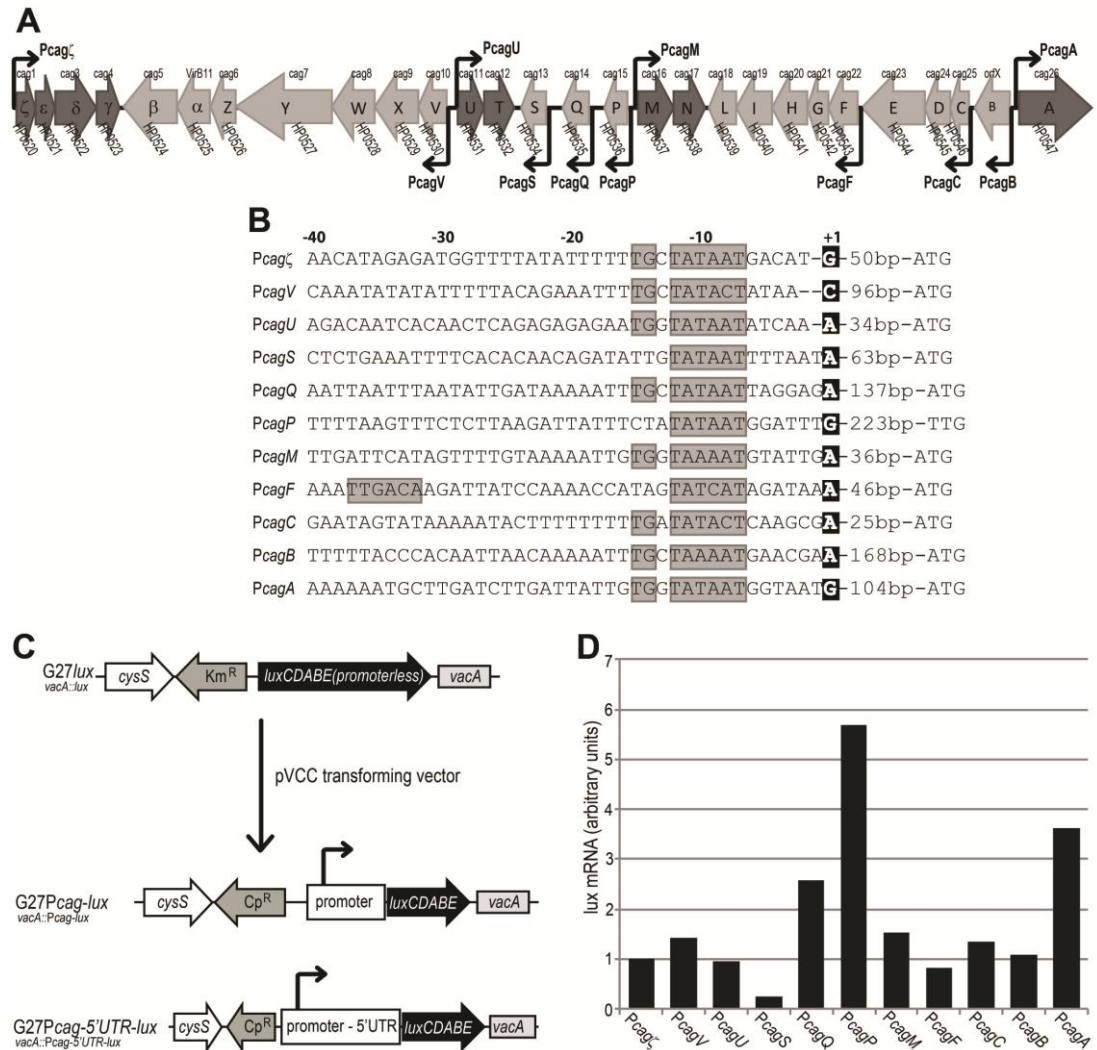
Fig. 12 (A) Gene arrangement of the *cag* pathogenicity island in *H. pylori* G27 strain. The mapped transcriptional start sites (TSS) of each promoter are indicated by a bent arrow and the inferred operon organization is represented in tones of gray. (B) Summary of relevant features within the nucleotide sequences of the 11 mapped P*cag* promoters. The TSSs (+1) are boxed in black boxes and showed in boldface. Sequences corresponding to -10 regions, the extended TGn elements and recognizable -35 region are enlightened in grey boxes. (C) Schematic representation of the P*cag-lux* and P*cag*-5'UTR-*lux* fusion constructs, obtained transforming the G27*lux* acceptor strain with the PVCC vector. The promoter sequences with or without the 5'untranslated regions (5'UTRs) carried by the pVCC vector are inserted upstream the *luxCDABE* operon by double homologous recombination and selected by *cat* chloramphenicol resistance. (D) Comparison of the transcript levels at the P*cag* promoters fused with *lux* reporter genes. mRNA levels of the P*cag-lux* constructs were assayed by primer extension analysis using the oligonucleotide VSluxC1 and quantified with a phospoimager. The mean values from two independent experiments are reported as arbitrary units of ^{32}P counts, normalized on P*cag*ζ.

4.1.2 Analysis of the *cag* transcript levels

To evaluate the transcript levels at the *cag* promoters and compare their relative mRNA abundance, we used *H. pylori* strains harboring the transcriptional fusions of the *cag* promoters with a *lux* reporter operon, as described in the previous sections. Briefly, for each *cag* promoter, the promoter region was cloned upstream the promoterless *lux* operon from *Photorhabdus luminescence*, previously inserted in the chromosomal *vacA* locus of *H. pylori* (Fig. 12C). The P*cag-lux* strains were grown to mid log phase and transcript levels were assayed and quantified by primer extensions. Results normalized on the mRNA level at the P*cag*ζ promoter, are reported in Fig. 12D, showing P*cagQ*, P*cagP* and P*cagA* promoters with the highest mRNA amounts, estimated as 2.6-, 5.7- and 3.6-fold higher than the transcript level at P*cag*ζ promoter. In contrast, P*cagS* exhibited the minimum mRNA level (3.9-fold reduced levels with respect to P*cag*ζ promoter) and the other P*cag* promoters showed transcript levels similar to P*cag*ζ.

Since both P*cagP* and P*cagS* show no conserved -35 or TG elements, we speculate that the observed high transcript level at the P*cagP* promoter and the low level of transcript at the P*cagS* promoter are likely to be exerted by an activator and a repressor, respectively.

4.1.3 Growth-phase regulation of *cag* promoters

To study the transcriptional regulation of the *cag* promoters during growth, we set out a 15 hours time course experiment of *H. pylori* G27 liquid cultures. Cells were collected at different time points and used to extract total RNA for quantitative primer extension experiments at the 11 *cag* promoters of interest (Fig 13). Transcription from the P*cag*ζ, P*cagV*, P*cagF* and P*cagA* promoters showed no significant variation in mRNA levels during the early exponential growth stages of the bacteria (Fig. 13A, lanes 1-3), while their amount increased in late logarithmic growth phase (Fig. 13A, lanes 4, OD=1.7). These extended RNA bands were quantified, normalized with respect to the signal measured at OD=0.2 (Fig. 13A, lane 1) and reported in the graph underneath. As expected, mRNA level from these promoters was unchanged in cultures grown from OD=0.2 to OD=1.1, while at later

time points a two to ten fold increase of transcript levels from P*cagζ*, P*cagV*, P*cagF* and P*cagA* promoters was measured (Fig. 13A, graph).

By contrast, transcription levels from P*cagS*, P*cagP*, P*cagM* and P*cagB* promoters exhibited a reduction of mRNA levels during the time course experiment (Fig. 13B, lane 1-4). Quantification of the primer extensions products, normalized to the signal at OD=0.2 (Fig. 13B, lane 1), showed that the mRNA levels at the P*cagS*, P*cagP*, P*cagM* and P*cagB* promoters progressively decreased over time reaching a 3.4-, 8.1-, 3.1- and 9.7-fold reduction at OD=1.7, respectively (Fig 13B, graph).

Lastly, transcript levels from the P*cagU*, P*cagQ* and P*cagC* promoters showed no significant variation during the time-course experiment (Fig 13C, lanes 1-4 and graph underneath).
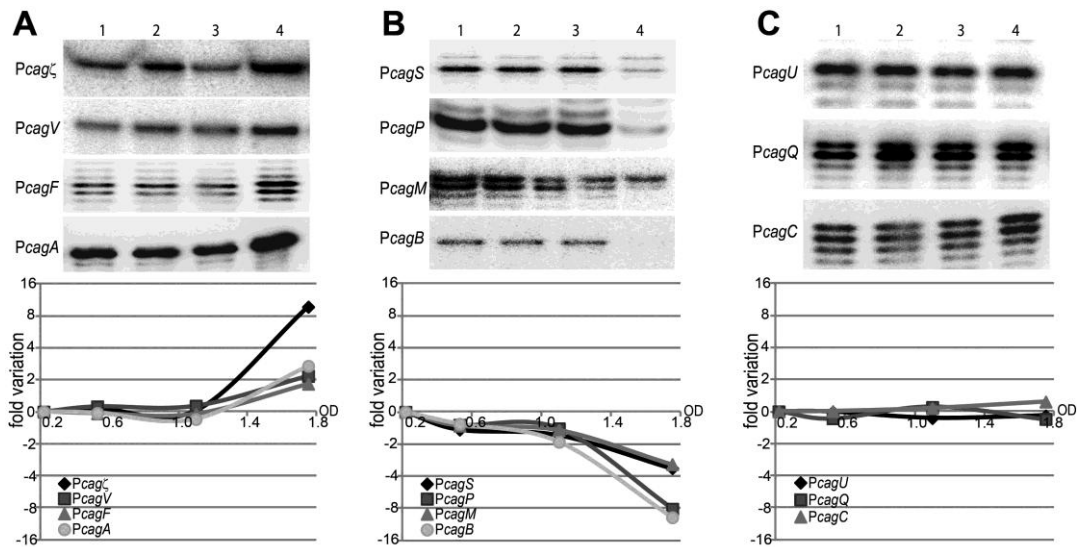
Fig. 13 Growth phase-dependent regulation of the P*cag* promoters. The Pcag promoters are reported in the three panels according to the variations of the transcript levels during bacterial growth, with promoters induced at late logarithmic phase (A), repressed during bacterial growth (B) and not sensitive to growth phase-dependent regulation (C). An overnight culture of wild type strain was diluted to an OD_{600} of 0.08 and cultured for 15 hours. Total RNAs were extracted from equal volumes of cultures at different time points corresponding to OD_{600} of 0.22 (t1), 0.53(t2), 1.06(t3) and 1.75(t4). Primer extension analyses were performed with 0.1 pmol of promoter-specific primers (Table 6) and 12-μg of total RNA. Results from time course experiments are shown in the upper panels. The intensity of the bands from two independent experiments were quantified with Image Quant Software, normalized on signal obtained at t1 and reported in the graphs as the n-fold change.

We conclude that during bacterial growth, transcription from P*cagζ*, P*cagV*, P*cagF* and P*cagA* promoters increases at late log-phase, while transcription from P*cagS*, P*cagP*, P*cagM* and P*cagB* promoters is down-regulated. Likely, the former promoters are induced during the late log-phase, while the latter promoters appear to be repressed at the same growth phase.

4.1.4 Environmental regulation at the *cag* promoters

To study the transcriptional regulation of *cag* promoters in response to environmental signals, we exposed exponentially growing cultures of *H. pylori* G27 strain to various conditions that mimic some of the environmental stresses likely encountered by the bacterium during infections. Total RNA was extracted from treated and untreated control samples and transcript levels at the *cag* promoters were assayed by quantitative primer extensions with the aforementioned *cag*-specific oligonucleotides (Table 6).

In bacterial cultures exposed to heat shock (30 min at 42°C) we observed a 6- to 40-fold reduction of mRNA levels at most *cag* promoters (Fig. 14A), with the of P*cagζ* and P*cagA* promoters that showed unchanged transcript levels (Fig. 14A). To further investigate on heat shock response, we assayed the mRNA levels at all *cag* promoters in knock-out strains for the heat shock transcriptional regulators HspR and HrcA. In comparison to the wild type strain, the Δ*hspR* and Δ*hrcA* mutants, either grown in normal conditions or exposed to heat shock treatment, showed similar mRNA levels at all tested *cag* promoters (data not shown). Therefore, the observed variation in the mRNA levels after heat shock is not under the control of the HspR and HrcA regulators and, likely, is mediated by a still unknown factor or due to changes in the mRNA stability.

Bacterial cultures treated with soluble Fe^{2+} (30 min with 1 mM $(NH_4)_2Fe(SO_4)_2$), iron chelator (30 min with 100 μM 2,2-dipyridyl), or Ni^{2+} (30 min with 1 mM $NiCl_2$), showed no significant variations in the transcript levels from most of the *cag* promoters (data not shown). An exception to this finding was observed at the P*cagA* promoter, showing a slight increase of RNA levels after exposure to Fe^{2+} and a 1.5-fold repression in iron-chlated conditions (Fig. 14B – upper panel). This iron-dependent response is in agreement with previous studies

(Ernst et al., 2005a; Pich et al., 2012). To further investigate on iron- and nickel-dependent regulation, we assayed the mRNA levels at the *cag* promoters in the knock-out mutants of the iron-dependent regulator Fur and the nickel-dependent regulator NikR, exposed to the same conditions as the wild type strain. In RNA from the mutant cultures we observed unchanged transcript levels at the P*cagA* promoter (Fig. 14B – middle panel), as well as at the other *cag* promoters (data not shown). The loss of the iron-dependent response of the P*cagA* promoter in the Δ*fur* mutant strain suggested that Fur can mediate the Fe^{2+}–dependent regulation of at this promoter. In contrast, no iron- and no nickel-dependent responses were observed at the other *cag* promoters.

Since intracellular Fur protein concentration increases during bacterial growth (Danielli et al., 2006), we assayed the iron-dependent response of the P*cagA* promoter in wild type and Δ*fur* cultures grown to late log-phase ($OD_{600}=1.7$), with results reported in Fig. 14B (bottom panel). As expected, in the wild type background, the iron-dependent response of the P*cagA* promoter was observed, with markedly higher differences in the mRNA levels between iron-repleted and iron-depleted conditions, while in the Δ*fur* strain, the transcript levels were unchanged. These results suggested that Fur represses the P*cagA* promoter in response to iron starvation, likely through a direct mechanism.

To demonstrate direct Fur-promoter interaction and map its operators sites, we set up DNaseI footprinting assays using the P*cagA* and P*cagB* promoter regions as probes, and increasing amounts of recombinant Fur protein in Fe^{2+}-repleted (*holo*-Fur) and Fe^{2+}-chelated (*apo*-Fur) conditions, respectively. The protection pattern of *holo*-Fur on the P*cagA*-P*cagB* intergenic region (Fig. 14C) shows four areas of altered DNaseI digestion, two at the minimal protein concentration used (21 nM) and two appearing at a concentration of 84 nM Fur. These results suggest the presence of two high-affinity binding sites, one of 19 bp spanning from position -44 to -63 of P*cagA*, and the other of 29 bp spanning from position -94 to -123 and overlapping with the P*cagB* -35 promoter region. Moreover, two Fur lower-affinity binding sites were detected, one extending from nucleotide +2 to -34 of P*cagA*, and the other spanning from nucleotide -147 to -178 and overlapping with the P*cagB*

transcriptional start site. A DNase I-hypersensitive site is apparent between the two high affinity binding regions.

DNaseI footprinting assay of the *apo*-Fur on the same promoter probe showed four regions with altered DNaseI digestion pattern (Fig. 14D). This finding would suggest for the presence of four *apo*-Fur binding sites, mapping to nucleotide positions +2 to -34 (I), -44 to -63 (II), -94 to -123 (III) and -147 to -178 (IV) of P*cagA*. Regions I and IV showed high affinity binding with *apo*-Fur, while the regions II and III showed low affinity binding. The binding sites of *apo*-Fur on the P*cagA* promoter are consistent with the transcriptional analyses in Fig. 14B and support the hypothesis of the repressive role exerted by *apo*-Fur on the P*cagA* promoter.
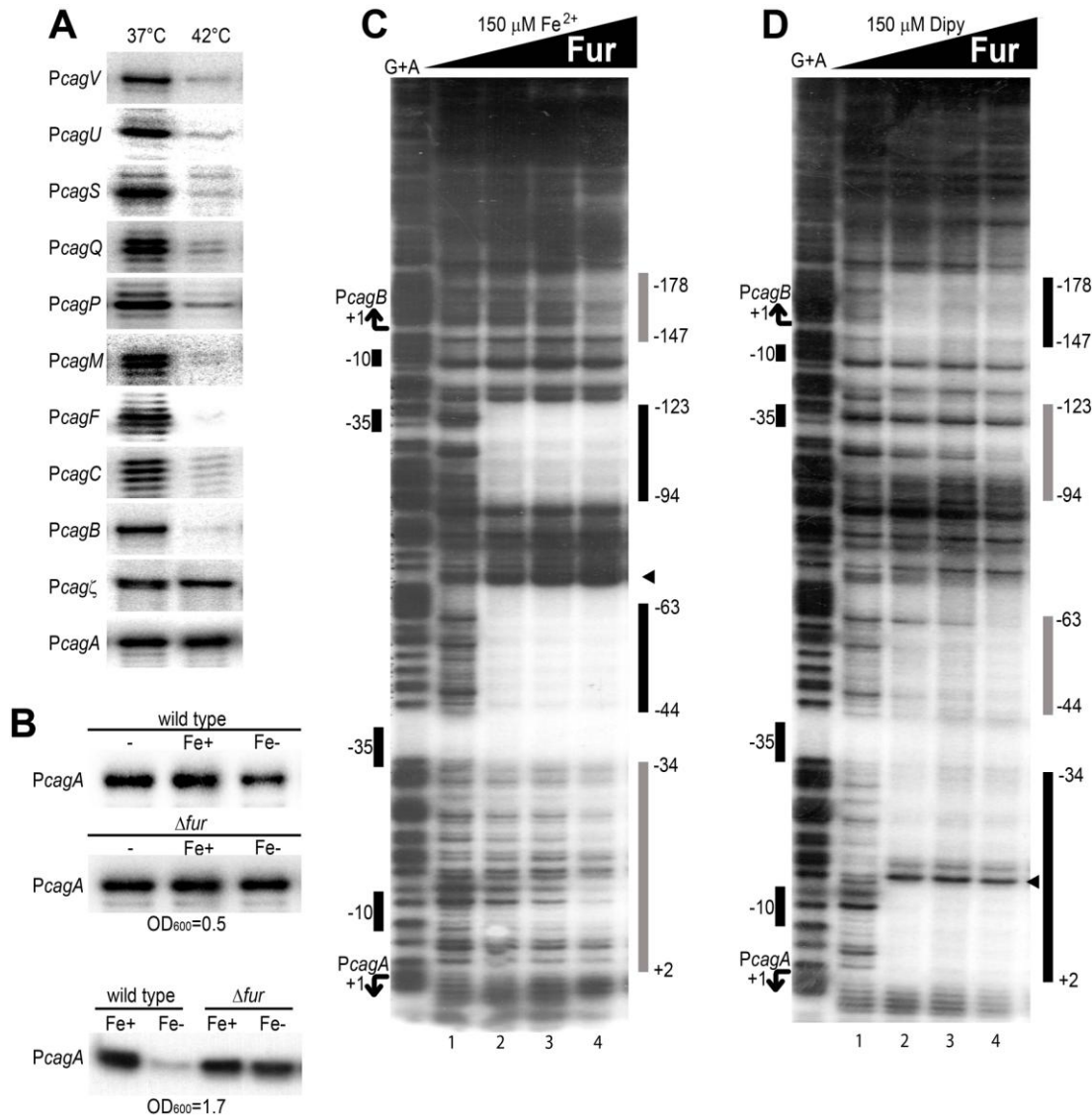
Fig. 14 (A) Heat-shock response of the P*cag* promoters. Primer extension analyses were performed on total RNA extracted from bacterial cultures of *H. pylori* wild type strain grown to exponentially phase and maintained at 37°C or exposed to 42°C for 30 min. (B) Iron-dependent regulation of the P*cagA* promoter. Liquid cultures of wild type and Δ*fur* strains were grown to OD_{600}=0.5 or OD_{600}=1.7 and treated for 30 min with 1 mM $(NH_4)_2Fe(SO_4)_2$ (Fe+), 100μM 2,2-dipyridyl (Fe-) or untreated (-). mRNA levels at the P*cagA* promoter were assayed by quantitative primer extension on the total RNA extracted. (C) In vitro binding of Fur protein to the P*cagB*-P*cagA* promoter region in a DNaseI footprinting assay. The probe used consists of a 462 bp NcoI/SalI fragment containing the P*cagB*-P*cagA* intergenic region 5'-end–labeled on the NcoI site. Approximately 20 fmol the probe was incubated with increasing concentrations of Fur dimer, 0 nM (lane 1), 21 nM (lane 2), 42 nM (lane 3) and 84 nM (lane 4). The binding reaction was performed in a final volume of 50 μL in presence of divalent iron ions as cofactors (150 μM $(NH_4)_2Fe(SO_4)_2$). The vertical grey and black boxes on the right of the panel indicate the areas of partial and complete DNaseI protection, respectively, resulting from binding of Fur on the probe. The numbers aside the boxes indicate the boundaries of the protected regions with respect to the +1 transcriptional start site (TSS) of P*cagA*. An hypersensitivity band that appears at high concentrations of Fur is indicated by a black triangle. On the left side of the panel, the TSS downstream P*cagB* and P*cagA* are indicated with bent arrows, while the relative position of the -10 and -35 regions of the two promoters are indicated as vertical black boxes. The G+A lane is a G+A sequence reaction on the labeled DNA probe used as size marker. (D) DNaseI footprinting of Fur protein to the P*cagB*-P*cagA* promoter region in absence if iron ions. The experimental conditions used for the footprinting assay were the same as described for the panel C, without the supplement of Fe^{2+} ions and with 150 μM 2,2-dipyridyl used to chelate soluble iron.

4.1.5 Acidic shock response

To investigate the acidic shock response, liquid cultures of *H. pylori* grown to mid-log phase were divided in two subcultures and treated for 30 min either with 22 mM HCl to adjust the pH of the medium to a value of 5.2 (acid shock) or with the same volume of sterile water (untreated control sample). The RNAs extracted from three independent cultures were assayed by primer extension experiments with results reported in Fig. 15. Transcript levels from P*cag*ζ, P*cagU*, P*cagF* and P*cagA* promoters increased in cells exposed to acidic shock with respect to the untreated sample (Fig 15A), and quantification of the bands showed a 3.8-, 2.3-, 3.2- and 1.9-fold mRNA increase in the mRNA levels, respectively (Fig. 15A, graph). In contrast, transcript levels from the P*cagS* and P*cagB* promoters decreased after the acid shock (Fig. 15B) with a reduction of mRNA levels to 3.1- and 6.2-fold, respectively (Fig. 15B, graph). Lastly, transcription from the P*cagV*, P*cagQ*, P*cagP*, P*cagM* and P*cagC* showed no significant variation in the mRNA levels after acid-exposure (Fig. 15C).

Subsequently, we assayed the transcript levels at the *cag* promoters after a prolonged acidic shock (90 min), in mid log-phase of growth (OD=0.7-0.8). Interestingly, transcription levels from the P*cagV*, P*cagQ* and P*cagC* promoters increased at 90 min to 1.7-, 3.2-, 6.3-fold, respectively (Fig. 15D), while mRNA levels from the P*cagP* and P*cagM* promoters showed no significant variations (Fig. 15D). All the other promoters showed similar mRNA levels at 30 or 90 min acidic treatment.

We conclude that exposure of bacteria to low-pH induces an immediate or delayed response, leading to variation of mRNA levels from 9 out of 11 *cag* promoters.
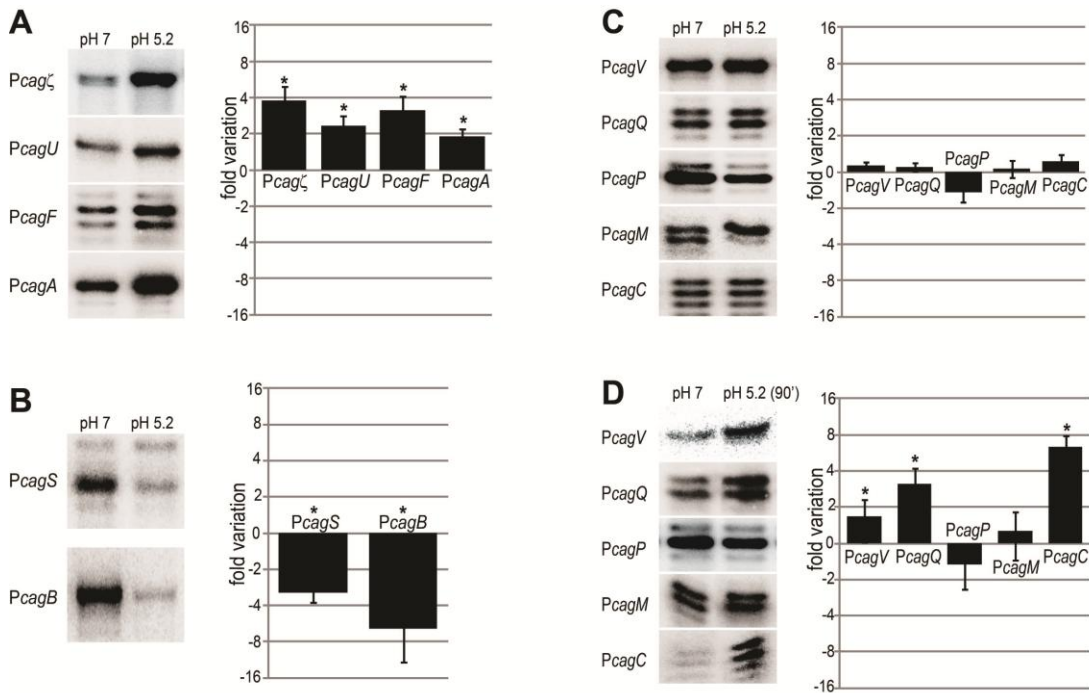
Fig. 15 pH-dependent response of the P*cag* promoters. Primer extension analyses were performed on total RNA extracted from bacterial cultures of *H. pylori* wild type strain, grown to exponential phase and treated for 30 or 90 min with 22 mM HCl to adjust the pH of the medium to 5.2, or maintained at neutral pH (pH 7.0). The intensity of the bands of four independent experiments were quantified and reported in the graphs as n-fold variation of the transcript levels in the acidic-treated samples with respect to the untreated sample. (A) P*cag* promoters with transcript levels increased after an acidic treatment for 30 min; (B) promoters with reduced mRNA levels after the 30min acidic treatment; (C) promoters with unchanged transcript levels after the treatment. Error bars indicate the standard errors and significant variations between treated and untreated samples are marked with asterisks. (D) Response of P*cagV*, P*cagQ*, P*cagP*, P*cagM* and P*cagC* promoters after an acidic treatment of 90 min.

4.1.6 Acid response in mutant strains

It is well established that acidic-response in *H. pylori* is primarily controlled by the ArsRS and FlgRS two-component systems (TCSs) (Pflock et al., 2006a; Wen et al., 2009) and that an indirect role could be exerted by the metal responsive transcriptional regulators NikR and Fur (Valenzuela et al., 2011; van Vliet et al., 2004). To investigate the role of ArsRS, NikR and Fur in acidic response of the P*cag*ζ, P*cagU*, P*cagF*, P*cagA*, P*cagS* and P*cagB* promoters (Fig. 15 A and B), wild type, Δ*fur,* Δ*nikR* and Δ*arsS* strains were grown to mid-log phase, exposed to acidic shock for 30 min and assayed for mRNA levels by quantitative primer extension assays with results reported in Fig. 16.

Intriguingly, P*cagF* and P*cagS* promoters showed a loss of the pH-induced response in the Δ*nikR* mutant, showing unchanged transcript levels after acidic treatment with respect to the untreated sample, while in the Δ*fur* and Δ*arsS* mutants we observed an acid response similar to the wild type strain. This suggests that NikR mediates the acidic response at these promoters.

Similarly, transcript levels at the P*cagB* promoter were unchanged after acidic treatment in the Δ*fur* mutant, while the wild type strain and the other mutants showed a pH-induced reduction in the mRNA levels. These results suggest that Fur can mediate the acid-dependent repression of P*cagB*. On the other hand, P*cag*ζ promoter showed a loss of acidic response in both the Δ*fur* and Δ*nikR* mutants, suggesting that the two regulators can mediate the acidic response of P*cag*ζ. Finally, for P*cagA* and P*cagU* we observed variations of transcript levels in the mutant strains similar to that in the wild type strain, hence acid response of these promoters is mediated by still unknown factors.

To further investigate on the observed loss of the acidic response of some P*cag* promoters in the mutant strains, we performed footprinting assays of recombinant Fur protein on a labeled probe encompassing the P*cag*ζ promoter, while footprinting assays of recombinant NikR were performed on the DNA fragments corresponding to the P*cag*ζ, P*cagS*, P*cagF* promoters. We were not able to detect patterns of protection on the probes tested (data not shown), suggesting that the acidic response mediated by NikR and Fur on these promoters is indirect.
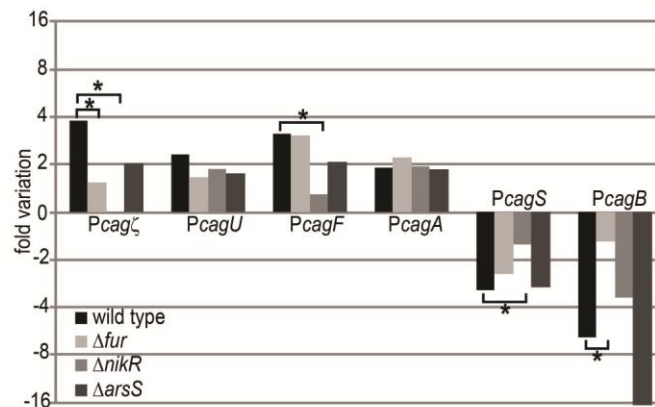
Fig. 16 Acid-dependent response of the P*cag* promoters in Δ*fur*, Δ*nikR* and Δ*arsS* mutant strains. Liquid cultures of G27-derived Δ*fur*, Δ*nikR* and Δ*arsS* mutant strains were grown to exponential phase and exposed to acid-shock (pH=5.2) for 30 min. Transcript levels at the P*cag*ζ, P*cagU*, P*cagF*, P*cagA*, P*cagS* and P*cagB* promoters were assayed by quantitative primer extensions. The intensity of the bands of three independent experiments were quantified and reported in the graphs as n-fold change of the acidic-treated samples with respect to the untreated samples. Error bars indicate the error standards and the significant differences of n-fold variations in the mutant strains with respect to the wild type strain are marked with asterisks.

4.1.7 P*cag* responses to bacterium-host cell contact

Model tissue co-cultures with human gastric adenocarcinoma (AGS) host cells-lines and *H. pylori* cells have been used to study the bacterium responses to the direct contacts with its host cells (Gieseler et al., 2005; Rohde et al., 2003; Sharma et al., 2010). To assess the possible *in vivo* effects exerted by bacterium-host contacts on the transcription of the *cag* promoters, we used co-cultures of AGS cells and *H. pylori* G27-derived strains carrying the P*cag-lux* transcriptional fusions. Bacterial cultures were grown to mid log phase and used to infect AGS cells cultured in 24-well plates (AGS$^+$ sample), while same amounts of bacterial cultures were added to plates containing only the medium (AGS$^-$ sample). During a 6 hours time-course experiment, we measured the luminescence of the samples at regular time intervals using a multilabel reader, and for each time point we calculated the luminescence signal ratio for bacteria grown in presence or in absence of AGS cells (AGS$^+$/AGS$^-$ ratio). The P*cag*ζ-*lux* strain co-cultured with AGS cells exhibited an increase of the luminescence with respect to the cultures grown in the medium only, with AGS$^+$/AGS$^-$ ratio that increased over time reaching a final value of 1.7 at 6 hours

(Fig. 17). In contrast, the other P*cag-lux* strains did not show significant differences between samples cultured with or without the AGS cells, with an AGS$^+$/AGS$^-$ ratio unchanged during the experiment, as showed by the P*cagQ-* and P*cagB-lux* strains (Fig. 17).

We can conclude that under the experimental conditions used, the contact between *H. pylori* and its host cells exerts a positive effect only on expression levels at the P*cag*ζ promoter, hinting that AGS-bacterium interaction could trigger signals that regulate P*cag*ζ promoter through unknown factors.
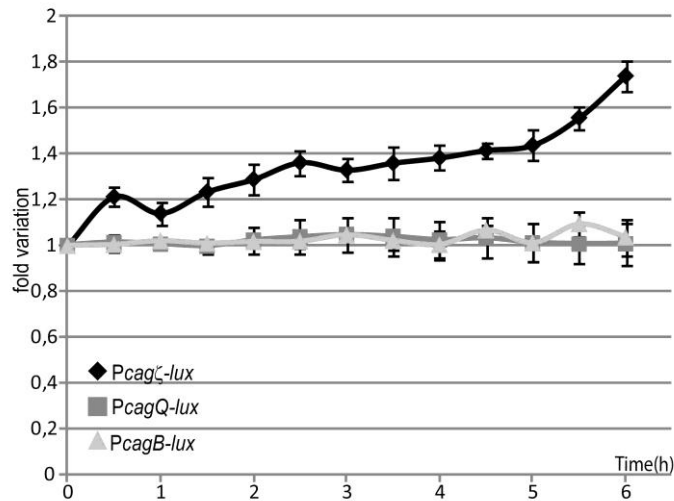
Fig. 17 Reporter assays with the P*cag-lux* strains in bacterium-host contacts. Liquid cultures of P*cag*ζ*-,* P*cagQ-* and P*cagB-lux* strains were added at a multiplicity of infection of 5 to 24-wells plates containing Human gastric adenocarcinoma (AGS) cells or with the medium only. *H. pylori*-AGS were grown in co-culture and luminescence emitted by the reporter strains was recorded at regular time intervals. Signals were normalized on the samples without AGS cells and average values and standard errors were calculated from four independent experiments and reported in the graph.

4.1.8 Post-transcriptional regulation

The analyses of the sequences downstream the transcriptional start sites of the P*cag* promoters showed that each transcript harbors a 5' untranslated region (5'UTR). To assess possible post transcriptional effects mediated by the P*cag*

5'UTRs, we used the previously mentioned strains harboring the P*cag-lux* transcriptional fusions and novel P*cag*-5'UTR-*lux* reporter strains encompassing also the untranslated region downstream of the promoter. The luminescence emitted by these strains was measured at mid-log phase and compared to the luminescence emitted by the P*cag-lux* reporter constructs lacking the 5'UTR region, with results reported in Fig. 18. We observed no significant differences of the signals between the constructs with or without the 5'UTR for P*cagC*, P*cagB*, P*cagF* and P*cagA* promoters (Fig. 18A) with an almost 1:1 ratio, suggesting that in mid-log growing cultures, the 5'UTR downstream these promoters do not affect the translational efficiency of the messengers.

Intriguingly, signals from P*cagP* and P*cagV* promoter constructs, harboring the 5' untranslated regions, decreased 3.2- and 30-fold with respect to the 5'UTR-less constructs (Fig. 18A), suggesting that these sequences may contain elements that reduce the translational efficiency or decrease the mRNA abundance. To investigate this hypothesis, we assayed the mRNA levels of the reporter in these reporter strains. P*cagV*-derived constructs showed similar mRNA levels, while P*cagP*-5'UTR-*lux* strain showed reduced transcript levels with respect to the cognate P*cagP-lux* strain (Fig. 18B). These results suggest that the 5'UTR downstream P*cagV* promoter does not affect mRNA abundance and likely affects the reporter signals, possibly by reducing the translational efficiency. In contrast, the 5'UTR downstream P*cagP* promoter could contain elements that reduce the mRNA stability or reduce the transcription rate. Reporter strains harboring the P*cagU*-, P*cagζ*- and P*cagQ*-5'UTR-*lux* constructs showed a 7-, 19- and 26-fold increase in luminescence with respect to the corresponding 5'UTR-less constructs (Fig. 18A). As before, we assayed the transcript levels of the reporter in these reporter strains, observing that constructs with the P*cagζ* promoter showed differences in the mRNA levels roughly corresponding to the observed variations of the signal of the reporter (Fig. 18C). The other pairs of constructs from P*cagU*, P*cagQ* and P*cagS* showed reduced mRNA levels in the p*cag*-5'UTR-*lux* strains with respect to the cognate P*cag-lux* strains (Fig. 18C). These results suggest that the 5'UTR downstream P*cagζ* may contain elements that enhance mRNA stability or transcription rate, while the 5'UTRs downstream P*cagU*, P*cagQ* and P*cagS* probably affects positively the translational

efficiency. Reporter comparisons with the P*cagS* promoter were excluded from the analysis because the P*cagS*-5'UTR-*lux* strain missed to emit detectable luminescence.
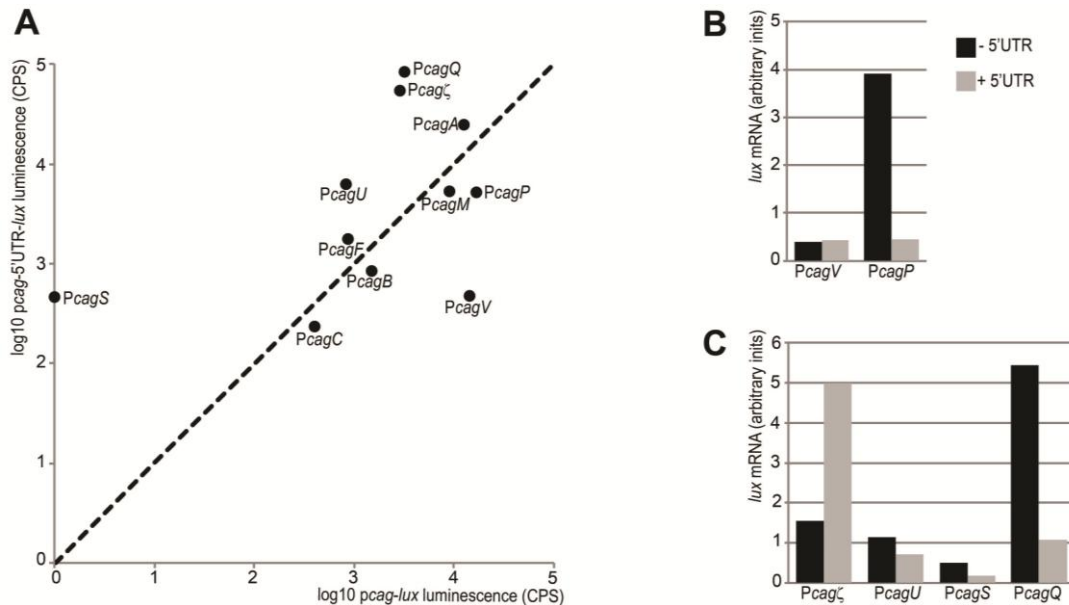
Fig. 18 (A) Bioluminescence of the P*cag-lux* and P*cag*-5'UTR-*lux* reporter fusions. Reporter strains carrying either the P*cag-lux* and P*cag*-5'UTR-*lux* constructs were grown to exponential phase and luminescence emitted was recorded with a multiplate reader. Signals from two independent experiment were normalized according to the optical density of the cultures and the means values were reported in the graph, with P*cag-lux* signals on the X-axis and P*cag*-5'UTR-*lux* signals on the Y-axis. A dashed line was added to the graph, corresponding to the 1:1 ratio of the two signals. (B) Analyses of the mRNA levels at the P*cagV*- and P*cagP*-derived constructs, containing the 5'untranslated regions (grey columns) or without the 5'UTRs (black columns). Each assay was performed on two independent experiments and the mean values are reported in the graph (C) Analyses of the mRNA levels at the P*cagζ*-, P*cagU*-, P*cagS*- and P*cagQ*-derived constructs, containing the 5'untranslated regions (grey columns) or without the 5'UTRs (black columns).

4.2 DISCUSSION

Helicobacter pylori G27 strain harbors a complete and fully functional *cag* pathogenicity island (*cag*-PAI). This chromosomal locus encodes both the toxin CagA and the components of the type IV secretion system (T4SS) that translocate the toxin into gastric epithelial cells during infection.

In order to assess the regulation mechanisms that modulate the concerted expression of the *cag*-PAI genes, we mapped the G27 *cag* primary transcriptional start sites (TSS) and characterized their respective promoter regions. We pinpointed 11 *cag*-PAI promoters, all containing a Pribnow box, homologous to the -10 box sequence of *E. coli* and, with the exception of P*cagP* and P*cagS*, an extended TGn -10 element or a conserved -35 region (Fig. 12B). These findings are consistent with previous analyses (Joyce et al., 2001; Sharma et al., 2010; Spohn et al., 1997; Ta et al., 2012), partitioning the *cag*-PAI ORFs in at least 11 transcriptional units. Minor differences pertain the alternative TSSs located upstream *cagγ*, *cagZ* and *cagW* promoters, which we were unable to confirm, likely due to strain-specific differences in the nucleotide sequences of the promoters or due to low transcription levels. Other previously reported internal and antisense TSSs (Sharma et al., 2010; Ta et al., 2012) deserve dedicated studies and have therefore been excluded from the current analysis. By comparison of the transcript levels of the P*cag* promoters with *lux* reporter fusions, differences of two order of magnitude in the mRNA levels were observed (Fig. 12B). The P*cagA* promoter showed high transcript levels that were consistent with previous reports (Boonjakuakul et al., 2005; Boonjakuakul et al., 2004; Busler et al., 2006; Sharma et al., 2010), likely assuring high expression levels of the of CagA toxin.

The P*cagS*, P*cagQ*, P*cagP* and P*cagB* promoters that direct the transcription of genes coding for disposable T4SS functions (i.e. those unessential for CagA delivery and for IL-8 induction) (Fischer et al., 2001), exhibit extreme values in the mRNA levels, either markedly lower or higher than the remaining *cag* cistrons. In contrast, all the promoters that direct the transcription of T4SS essential components (P*cagζ*, P*cagV*, P*cagU*, P*cagM*, P*cagF* and P*cagC*), exhibited similar transcript

levels, likely reflecting the need to ensure a proper stoichiometric ratio of gene products for the correct T4SS assembly. Previous studies in different *H. pylori* strain recorded different expression levels of the genes downstream of some of these promoters, which led to attribute to P*cagC* and P*cagζ* a 10- to 1000-fold activity with respect to the other *cag* promoters (Boonjakuakul et al., 2005; Boonjakuakul et al., 2004; Busler et al., 2006; Castillo et al., 2008; Eaton et al., 2002; Joyce et al., 2001; Sharma et al., 2010). In our analysis in the G27 strain, the transcription levels observed for the P*cag-lux* reporter fusions are consistent with those of the *cag* promoters at the original chromosomal locus. This suggests that the observed discrepancies may derive from a strain specific regulation of P*cag* promoters.

Adaptive responses to the host environment frequently rely on regulatory networks that control coordinated expression of virulence factors at the transcriptional or post-transcriptional level. In order to identify which signals may modulate *cag* gene expression, we first analyzed the transcript levels at the principal *cag* promoters in a time course experiment (Fig. 13). P*cagS*, P*cagP*, P*cagM* and P*cagB*, promoters are repressed when bacteria enter the stationary phase. On the contrary P*cagζ*, P*cagV*, P*cagF* and P*cagA* promoters, driving the transcription of core structural genes, together with the CagA toxin, its chaperone CagF, and some auxiliary factors important for the T4SS assembly are induced at the late log-phase of growth. Finally, P*cagU*, P*cagQ* and P*cagC* promoters appear not responsive to the phase of growth. These results are consistent with previous observations on P*cagP* and P*cagU*, P*cagζ* and P*cagA* (Boonjakuakul et al., 2005; Karita et al., 1996; Thompson et al., 2003; Vannini et al., 2012). Moreover, the observed repression of P*cagM* promoter during growth reflects the reported repression of the downstream *cagM* and *cagN* genes (Boonjakuakul et al., 2005). The temporal regulation of *cag* promoters during bacterial growth suggests a coordinated transcriptional expression of *cag* operons that can exert a regulatory effects in the pathway of assembly of the *cag*-pathogenicity island encoded Type IV secretion system and its functioning. Intriguingly, the P*cagS*, P*cagP* and P*cagB* promoters whose transcript levels are reduced during time, are upstream genes not fundamental for the T4SS. Hence, it may be possible that these operons could encode for regulatory elements that

modulate the *cag* island expression, similarly to other pathogenic bacteria (Ellermeier et al., 2005; Yahr and Wolfgang, 2006).

Exposure of *H. pylori* to environmental and metabolic stresses enlightened a complex and multifaceted response at the P*cag* promoters, showing altered transcript levels after heath shock and acidic treatments, as well as in response to iron ions availability. In accordance with other studies (Ernst et al., 2005a; Merrell et al., 2003; Pich et al., 2012; Szczebara et al., 1999), we observed an iron-dependent regulation of the P*cagA* promoter, that is repressed under iron-deplete conditions and induced after addiction of soluble Fe^{2+} ions. We demonstrated that the metal-dependent regulator Fur mediates this response, as the *fur* knock out mutant strain (Δ*fur*) showed a loss of the iron-dependent regulation of P*cagA* (Fig. 14B). Moreover, the observed higher repression of P*cagA* in iron-depleted cultures grown to stationary phase correlates with the increase of the Fur protein in this phase of growth (Danielli et al., 2006), suggesting that P*cagA* is repressed by Fur in a direct fashion in the absence of iron cofactor (*apo*-Fur repression). As reported by Pich and colleagues (Pich et al., 2012), the Fe-dependent regulation of Fur on the P*cagA* promoter is likely exerted through a direct binding, and through DNaseI footprinting assays we have shown that Fur binds to the P*cagA*-P*cagB* intergenic region in both *apo*- and *holo*-form (Fig. 14C and 14D). Specifically, *holo*-Fur binds to four sites on the P*cagAB* intergenic region, two with high affinity and two with low affinity, possibly responsible for a cooperative binding of Fur to the promoter regions of *cagA* and *cagB*. The Fur binding site spanning -44 to -63 of P*cagA* contains the previously identified Fur box (Pich et al., 2012) and the other three binding regions show AT-rich sequences with different homologies to the Fur consensus sequence. Footprinting assay of *apo*-Fur on the P*cagAB* intergenic region showed a pattern of protection similar to the binding of *holo*-Fur on the region, but with the high- and low-affinity regions swapped. The two regions protected with high-affinity by *apo*-Fur overlap or map immediately close to the P*cagA* and P*cagB* TSSs respectively. The position of these boxes suggest a repressor role exerted by *apo*-Fur on P*cagA*, in agreement with the *apo*-Fur repression of *cagA* transcripts observed in the primer extension analysis. Moreover, the mapping of the high affinity binding site of *holo*-Fur upstream the -35 region of the P*cagA* promoter suggests that also the *holo*-form

of the protein may regulate the P*cagA* promoter, likely positively, as observed in the transcription analysis. Hence, the Fur-mediated regulation of P*cagA* is likely dependent by a complex binding of *holo-* and *apo-*Fur proteins on the corresponding adjoining operators.

Interestingly, previous footprinting analysis with α-subunit of RNA polymerase showed a protection pattern on the region spanning from -17 to -70 nucleotides of P*cagA* (Spohn et al., 1997), suggesting the presence of an UP element recognized by the CTD domain of the α-subunit of RNA polymerase. We can speculate that the observed iron-dependent regulation of P*cagA* promoter could be exerted not only by the binding of *apo-* and *holo-*Fur on adjoining operators, but also by Fur competing for the binding of the α-subunit to the UP element.

Since *H. pylori* establishes infection in the harsh acidic environment of the human stomach, we assayed the response of the P*cag* promoters to acidic stress (pH 5.2). Interestingly, P*cagζ*, P*cagU*, P*cagF* and P*cagA* promoters were induced by an acid treatment of 30 min, while P*cagS* and P*cagB* promoters were repressed in the same conditions (Fig. 15). The other promoters showed no significant variations, but prolonged exposure (90 min) showed long term adaptive response of P*cagV*, P*cagQ* and P*cagC*. These results partially fit with previous works indicating a strain-dependent response of certain *cag* promoters to acidic stress in different *H. pylori* strains. In particular, an acid-dependent up-regulation of *cagA* (Allan et al., 2001; Barnard et al., 2004; Karita et al., 1996; Scott et al., 2007; Sharma et al., 2010; Wen et al., 2003) and a pleiotropic induction of the majority of the other *cag* genes was reported (Scott et al., 2007; Sharma et al., 2010; Wen et al., 2003). We observed two P*cag* promoters repressed by acidic treatment (P*cagS* and P*cagB*) and two promoters non regulated by acidic exposure (P*cagP* and P*cagM*). Interestingly, these four promoters are the same that are negatively regulated during bacterial growth, hinting at the presence of coordinated regulatory mechanisms on these promoters, and suggesting that the downstream cistrons could encode for *cag*-specific regulatory functions.

To identify the transcriptional regulators that mediate the acidic response of the P*cag* promoters, we assayed the pH response in knock out mutants of known acidic response-mediating regulators. From this analysis we observed that the acidic

response of the P*cag*ζ and P*cagB* promoters is mediated by Fur, while NikR appears to mediate the acidic response of the P*cag*ζ, P*cagF* and P*cagS* promoters (Fig. 16). However, we were able to confirm direct binding only for Fur on P*cagB* promoter (Fig. 14), suggesting that the Fur and NikR pH-dependent responses of the other promoters are mediated by indirect mechanisms. Since *apo-* and *holo-*Fur bind to the corresponding operators on the P*cagB* promoter, it is possible that Fur regulates this promoter within the Fur-mediated acid tolerance response of *H. pylori* (Valenzuela et al., 2011). Further analyses should be carried out to investigate on this regulation. Moreover, our analysis appears to exclude the involvement of the global acid regulator ArsRS system in the pH-dependent responses of the *cag* promoters. With regard to heat shock and stress conditions, a pleiotropic reduction of transcript levels was observed, that was also retained in knock out mutants of the heat-shock regulators *hspR* and *hrcA*. Thus, the observed heat-shock response is likely due to an attenuation of the transcription rates or a reduction of the mRNA stability and likely not mediated by direct HspR and HrcA protein-DNA interactions.

The contact with host cells is a potent elicitor of secretion system gene expression in pathogenic bacteria (Yahr and Wolfgang, 2006). Previous works documented similar effects in *H. pylori*, showing an increase of the *cag*-encoded T4SS needles on the surface of the bacterium, when *H. pylori* is co-cultured with AGS cells (Rohde et al., 2003). In addition, variations of the expression of some *cag* genes during infections in humans, animal models or cell lines co-cultures has been reported (Boonjakuakul et al., 2005; Boonjakuakul et al., 2004; Gieseler et al., 2005; Joyce et al., 2001; Scott et al., 2007; Sharma et al., 2010). However, these studies showed a plethora different, and sometimes contrasting results, suggesting that the host-induced modulations of *cag* gene expression is likely dependent on the *H. pylori* strain, on the host used for the study and on the experimental conditions employed.

In this study, we monitored the P*cag* promoter responses in *H. pylori* G27 strain, co-cultured with AGS cells at regular time intervals in a 6 hour time curse experiment. Using the P*cag-lux* reporter fusions to monitor the dynamics of promoter activity, we observed a significant induction of the P*cag*ζ promoter in response to host cell-contact (Fig. 17). Interestingly, Kim and colleagues reported similar

variations of *cagδ* expression in *H. pylori 69a* strain, co-cultured with AGS cells for 1 hour (Kim et al., 2004). Since *cagδ* belongs to the transcriptional unit downstream the P*cagζ* promoter, these results suggest a conserved regulation of the operon, likely due to the modulation of the P*cagζ* promoter activity. Previous observations of the AGS-induced regulation of *cagA*, *cagP* and *cagS* (Gieseler et al., 2005; Sharma et al., 2010) were not repeated in this study, likely due to strain-specific responses to host-cell contacts.

We concluded our study on the P*cag* promoters analyzing the effects exerted on expression and transcript stabilization by the 5'-UTRs of the first cistron of each *cag* transcriptional unit. Using the *lux* reporter system, we compared cognate constructs harboring only the promoter regions or including also the 5'UTRs. For each construct we assayed both the mRNA levels and the reporter signals, assessing the mRNA abundance and the efficiency of translation, respectively. The 5'UTRs downstream the P*cagC*, P*cagB*, P*cagF* and P*cagA* promoters showed no effects either in mRNA levels or efficiency of translation. Interestingly, the 5'UTR downstream P*cagP* negatively affects the mRNA levels, while the 5-UTR downstream of P*cagζ* positively affects the transcript levels (Fig. 18). In contrast, the *cagV* 5'UTR exerts a negative effect on the translational efficiency of the transcript, while the 5'UTRs of *cagU*, *cagQ* and *cagS* appear to positively affect the translational efficiency (Fig. 18).

PART 3:

Characterization *cag*-encoded *cncR1* sRNA

5.1 RESULTS

5.1.1 The *cncR1* locus

Recent transcriptional analysis conducted by Sharma and colleagues on *Helicobacter pylori* 26695 strain had proven some evidences that *cagP* (HP0536) encodes for a small non coding RNA, corresponding to the 5' untranslated region of *cagP* mRNA (Sharma et al., 2010). Alignments of the *H. pylori cag*-PAI sequences published up to date showed that *cagP* is conserved in all the *cag*-PAI$^+$ strains, with a 95 % sequence homology of the region encompassing both the 5'UTR and the coding sequence (CDS), and a 92% homology of the sequences corresponding to the putative sRNA only, henceforth referred as *cncR1* sRNA.

Since *cncR1* small non-coding RNA corresponds to the 5'UTR of the monocistronic operon *cagP* (Fig. 19A) (Sharma et al., 2010), the 5'-end of the sRNA corresponds to the mapped transcriptional start site (TSS) downstream the P*cagP* promoter (see previous sections). As reported, the P*cagP* promoter harbors a conserved -10 region with homology to the canonical consensus sequence, recognized by the vegetative sigma factor σ^{80} of *H. pylori*, while no upstream -35 nor TG motifs were found (Fig. 19B).

Nevertheless, the analysis of the transcript levels at the P*cag* promoters showed that P*cagP* promoter has the highest mRNA levels, even greater than the P*cagA* promoter, that is responsible for the expression of the abundant toxin CagA. In previous sections, it has been reported the responses of the P*cagP* promoter to various environmental stresses, showing only a progressive repression of the promoter during bacterial growth.

77

A

G27 *cag*-PAI

G27 *cagP-cagM* locus

PcagM

PcagP

B

-40   -30   -20   -10   +1

PcagP TTTTAAGTTTCTCTTAAGATTATTTCTATATAATGGATTTG-223bp-TTG
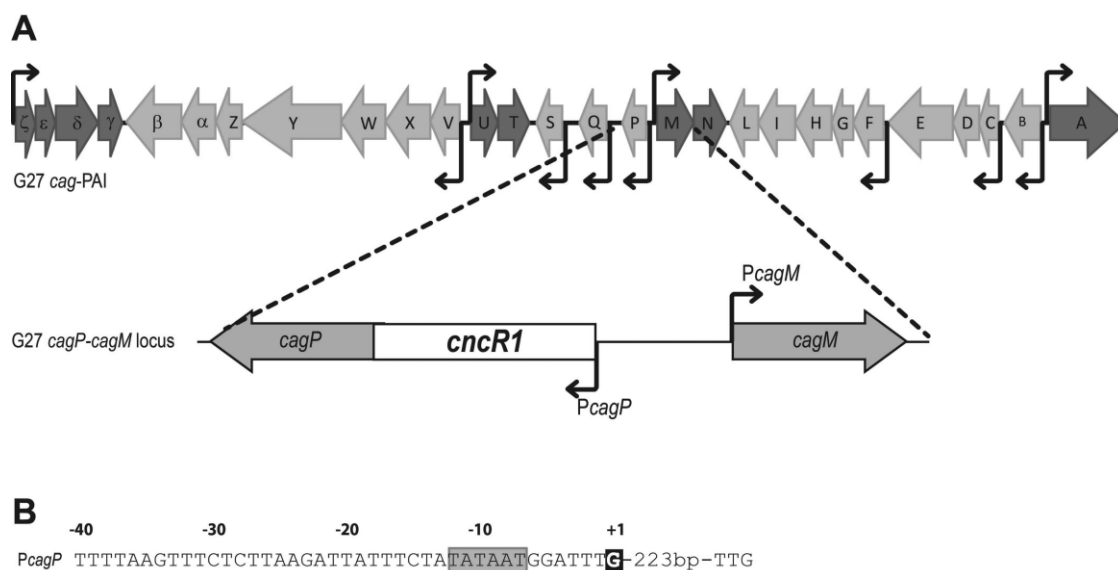
Fig. 19 A) The *cagP-cagM* locus within the *H. pylori* G27 strain *cag* pathogenicity island. Predicted CDS are indicated with grey arrows, the region encoding for the *cncR1* sRNA is represented with a white rectangle and the transcriptional start sites (TSS) of each promoter are indicated by bent arrows. (B) Summary of relevant features within the nucleotide sequences of the P*cagP* promoter. The TSS (+1) is enchased in a black box and sequences corresponding to -10 region are enlightened in grey boxes.

5.1.2 Analysis of the *cncR1* 3'-end

Recent RNA-seq analyses on *H. pylori* 26695 strain showed that transcription from P*cagP* promoter leads to a major *cagP* mRNA population encompassing *cagP* 5'UTR only, and missing the CDS (Sharma et al., 2010). These results were confirmed by northern blot analysis, suggesting a premature end of the transcription process in correspondence of the 3'-end of the *cagP* 5'UTR, or a short mRNA fragment obtained from the processing of a longer *cagP* mRNA. The bioinformatic prediction of an intrinsic terminator of transcription at the 3'-end of the 5'UTR furnished another clue supporting the former hypothesis.

Starting from these observations, a similar study was performed on *H. pylori* G27 strain. Total RNA extracted from wild type strain was assayed by northern blot analysis, using oligonucleotides mapping upstream and downstream the predicted terminator of the *cagP* transcript. The 536pe17 oligonucleotide, mapping upstream the predicted terminator, showed a major band of ~220 nt long (Fig. 20A, lane 1, band marked a1) and a weaker band (data not shown) ~280 nt long, appearing only

after prolonged expositions. In contrast, the probe 536pe20 mapping downstream the predicted terminator produced a single weak band a2 ~280 nt long (Fig. 20A, lane 2, band marked a2). Quantification of the two detected bands estimated the fragment a1 as 8-fold more abundant than a2 (Fig. 20B).
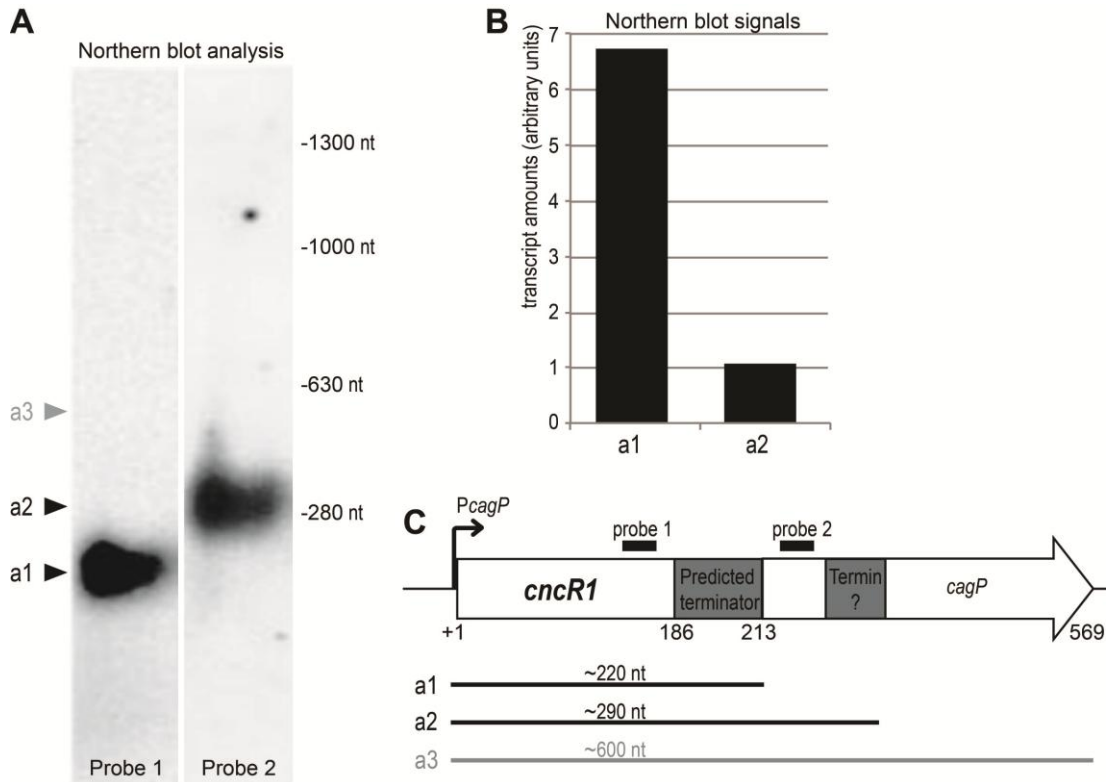
Fig. 20 (A) Northern blot analysis of the mRNAs transcribed from the P*cagP* promoter. About 15 µg of total RNA extracted from G27 wild type strain was separated under denaturing conditions in 1.2% agarose–2.1 M formaldehyde-morpholinepropanesulfonic acid gels, transferred on a Hybond-N+ nylon membrane by capillary transfer and cross-linked to the filter by UV-ray treatment. The membrane was hybridized with the oligonucleotides 536pe17 (probe 1) and 536pe20 (probe 2), mapping on the *cncR1-cagP* mRNA upstream and downstream the predicted terminator sequence, respectively. The membranes were exposed for autoradiography. Black triangles indicate the detected bands: a1 correspond to a ~220 nt RNA transcript, while a2 correspond to a ~290 nt transcript. Grey triangle labeled a3 indicates the putative position of the mRNA encompassing the *cncR1* and *cagP* CDS, based on the results on 26695 strain (Sharma et al., 2010). (B) Quantification of the bands from Northern blot analysis. Signals were acquired with a Storm phosphorimager and quantified using Image Quant Software. Results are reported in arbitrary units of ^{32}P counts. (C) Schematic representation of the *cncR1-cagP* locus, with the regions targeted by the oligos (probes 1 and 2) and the regions with a putative terminator function. Underneath are represented the transcript fragments observed in Northern blot analysis.

Likely, the shorter transcript (a1) corresponds to the products of transcription interrupted in correspondence of the terminator, located ~213 nt downstream the P*cagP* transcriptional start site (Fig. 20C), while the longer transcripts likely correspond to the less abundant products of read-through of the RNA polymerase (Fig. 20C). Interestingly, both the detected RNAs do not cover the entire length of *cagP* CDS, and no full length mRNA was detected (Fig. 20A, putative full length transcript indicated with a3). This results suggest the presence of a further terminator sequence located ~90 nt downstream the start codon of *cagP*. Nevertheless, the detected RNA fragments could also correspond to the processed (a1) and unprocessed or partially processed (a2) RNA fragments of a longer undetected *cagP* mRNA.

5.1.3 Study of the transcriptional terminator in *cncR1*

To grasp information on the nature of the observed major 220 nt transcript, the nucleotide sequence corresponding to the predicted transcriptional terminator spanning 29 bp from position 184 to 213 of the *cncR1* sRNA, was submitted to bioinformatic analysis. Search for sequence conservation among different *H. pylori* strains revealed that this hypothetical terminator is conserved, including strain G27 (Fig. 21A). The bioinformatic prediction of the secondary structure of the RNA region corresponding to the terminator, was performed with the online resource RNA-fold (http://rna.tbi.univie.ac.at/cgi-bin/RNAfold.cgi). Results of the analysis are reported in Fig. 21B, showing a low free-energy RNA stem-loop structure (-20.1 KJ/mol), followed by an uracil stretch with no base-paring. The secondary structure is consistent with the classic structure of the intrinsic transcription terminators (Castillo et al., 2008).

To verify the *in vivo* functionality of the *cncR1* terminator sequence, the *lux* reporter system was used. The parental G27-*lux* strain, carrying the promoterless *P. luminescens luxCDABE* operon cloned in the *vacA* locus (see previous section), was transformed with the PVCC::P*cagP*-5'UTR vector to obtain the G27 P*cagP*-5'UTR-*lux* strain (Fig. 21C), that carries the *cncR1* sRNA, along with its natural promoter P*cagP*, fused with the *lux* operon (P*cagP-cncR1-lux*). Moreover, using PVCC::P*cagP*-5'UTRΔterm vector, it was obtained the G27 P*cagP*-5'UTRΔterm-*lux*

mutant strain (Fig. 21C), carrying the same transcriptional fusion, with the deletion of the a 26 bp sequence corresponding to the predicted terminator (P*cagP*-*cncR1*Δterm-*lux*). The two G27 *lux*-derived mutant strains were grown to exponential phase and the luminescence emitted by the cultures was recorded using Victor3V (1420) multilabel reader (Perkin Elmer). Signals were normalized according to the optical density (OD_{600}) of the cultures and reported in Fig. 21D. The luminescence emitted by the mutant carrying the P*cagP*-*cncR1*Δterm-*lux* construct is 3.3-fold higher with respect to the cognate P*cagP*-*cncR1*-*lux* construct, suggesting that the region deleted in the former mutant harbors sequences that reduce the levels of the *lux* reporter.
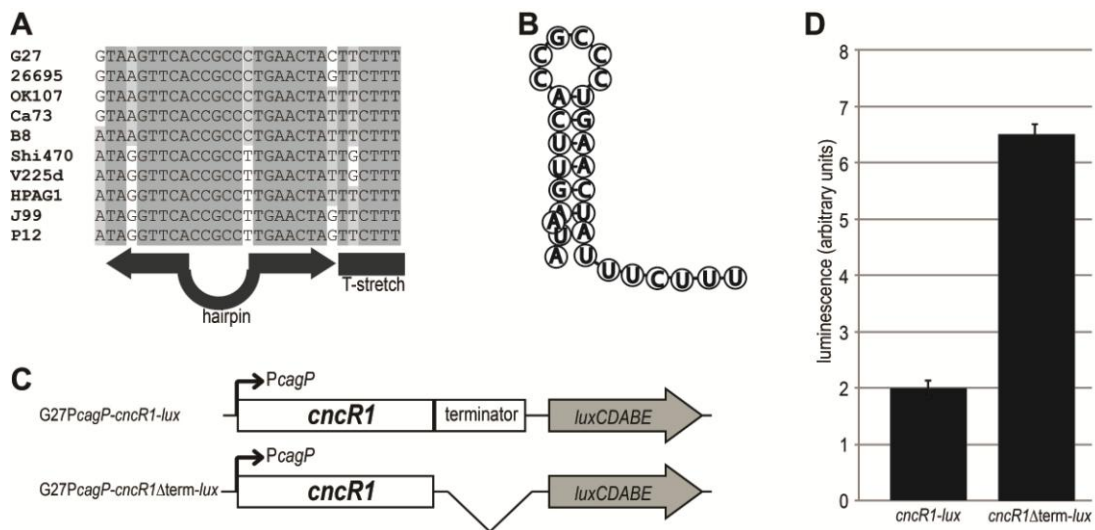
Fig. 21 (A) Sequence alignment of the predicted *cncR1* terminator sequence. The nucleotide sequence spanning 29 bp from position 184 to 213 of the *cncR1* sRNA (the predicted intrinsic transcriptional terminator) from 10 *H. pylori* strains was aligned with Vector-AlignX program to assess conserved motifs. (B) Bioinformatic prediction of the secondary structure assumed by the nucleotide sequence corresponding to the predicted terminator region in G27 strain. The online program RNA-fold was employed for the analysis. (C) Schematic representation of the P*cagP*-*cncR1*-*lux* and P*cagP*-*cncR1*Δterm-*lux* reporter strains, obtained transforming the G27 *lux* acceptor strain with the PVCC::P*cagP*-5'UTR and PVCC::P*cagP*-5'UTRΔterm vectors, respectively (D) Comparison of the reporter levels in the G27 strains harboring the P*cagP*-*cncR1*-*lux* and P*cagP*-*cncR1*Δterm-*lux* constructs. Luminescence emitted by the bacterial cultures was recorded with a multiplate reader and normalized according to the optical density of the cultures. Mean values from two independent experiments are reported in the graph.

Since bioinformatic analysis predicted an intrinsic terminator element within the deleted sequence, the observed variations are likely due to the negative effect exerted by the terminator on the transcriptional activity of the RNA polymerase. However, the possibility that the 26 bp sequence could contain elements that enhance the processing of the primary transcript, leading to trunked mRNAs and hence the reduction of the expression of the downstream genes, cannot be excluded.

5.1.4 Construction of the isogenic *cncR1* mutant

To initiate studies on the role exerted by *cncR1* sRNA in the regulation of *H. pylori* genes, an isogenic *cncR1* knock-out mutant was constructed. For this purpose, *H. pylori* strain G27 was transformed with the vector pBS::Δ*cncR1*, in which most of the sequence encoding for *cncR1* and 79 bp of the upstream P*cagP* promoter were replaced with the chloramphenicol resistance *cat* gene (Fig. 22A). Mutants carrying the correct replacement of the wild type sequences with the *cat* cassette were confirmed by PCR and expanded for the analyses. To further characterize the G27 *cncR1::cat* strain (Δ*cncR1*), liquid cultures of Δ*cncR1* and the parental wild type strains were harvested and the extracted RNAs were assayed for the expression of *cncR1* and the divergent *cagM* transcripts by primer extension analysis.
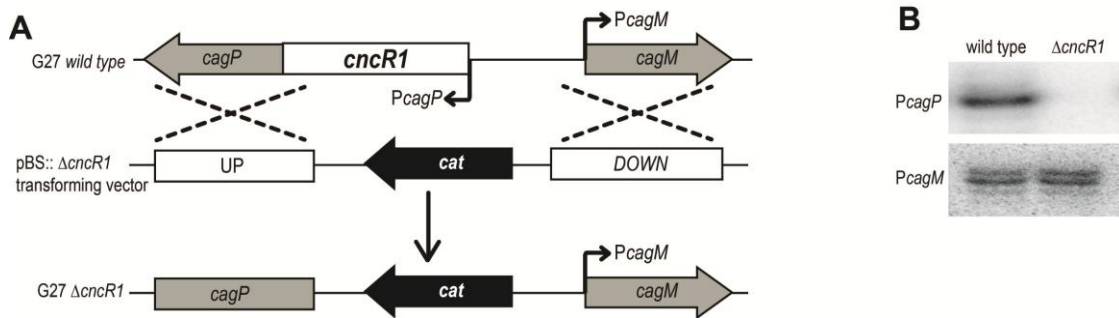
Fig. 22 (A) Schematic representation of the procedure to obtain the *cncR1* knock out mutant. The pBS::Δ*cncR1* vector carries the 574 bp "UP" region of homology with the sequences downstream *cncR1*, the 442 bp "DOWN" region of homology with the sequences upstream *cncR1*, and the *cat* cassette inserted between these two fragments. By transformation of the G27 wild type strain with pBS::Δ*cncR1* vector, the *cat* selected Δ*cncR1* strains harbor the sequence spanning 287 bp from position -79 to 208 of the *cncR1* sRNA replaced by the *cat* cassette. (B) Primer extension analysis of transcript levels at the P*cagP* and P*cagM* promoters in the wild type and Δ*cncR1* strains. Primer extensions were performed with 12-μg of total RNA and 0.1 pmol of labeled 536pe17 and 537pe8 primers (Table 6) to target transcript from P*cagP* and P*cagM* promoters, respectively.

As shown in Fig. 22B , the *cncR1* levels observed in the wild type strain are completely lost in the Δ*cncR1* strain, while *cagM* showed same transcript levels in the two strains, suggesting that the replacement of *cncR1* fully abrogate the *cncR1* expression but does not affect the expression of the divergent operon *cagMN*.

5.1.5 *cncR1* transcriptome analysis

To identify *H. pylori* genes regulated by *cncR1* sRNA, a genome-wide transcriptional analysis of the Δ*cncR1* mutant was carried out through DNA macroarray approach. Total RNAs isolated from exponentially growing cultures of the Δ*cncR1* mutant and the parental G27 wild type strain (OD$_{600}$=0.6) were used for *in vitro* synthesis of ^{33}P-labeled cDNAs, that were subsequently hybridized to *H. pylori* Panorama ORF arrays (Sigma-Genosys). The arrays were exposed for autoradiography, then the images were acquired with a Storm phosphor-imager (Amersham-GE). Each of the 1681 spots of the array was quantified using the Image Quant Software (Molecular Dynamics) and associated to the corresponding gene of *H. pylori* 26695 and J99 strains. For each *H. pylori* gene, signals were reported as per cent values of the total signal detected in the array and Δ*cncR1*/wild-type expression ratio was calculated from two independent hybridization experiments. The results were filtered according to both statistical significance of the variations (P ≤ 0.1) and the selected threshold limit of quantification (Materials and Methods).

As reported in Table 2, 66 genes are significantly deregulated at least 1.5-fold in the Δ*cncR1* strain with respect to the wild type strain, with 29 genes up-regulated and 37 genes down-regulated. The *cncR1*-regulated genes were grouped into several categories according to their cellular functions, as internal metabolism, cellular processes and signaling, transcription and DNA processing, motility and chemotaxis, as well as *H. pylori*-specific proteins of unknown function. Among the genes up-regulated in the Δ*cncR1* mutant strain, a clustering of the genes encoding for proteins involved in regulation and assembly of the flagellar apparatus was observed, with 10 out 26 genes belonging to this category. These results suggested a coordinate co-regulation of these genes in the knock out *cncR1* mutant. In contrast, no obvious clusters of co-regulated genes were observed among the genes down-regulated in the Δ*cncR1* mutant strain. However, expression level of the heat-inducible transcription

repressor *hrcA* (HP0111) is reduced in the Δ*cncR1* strain and at least 4 genes related to host-pathogen interaction showed down-regulated expression, with *omp17* (HP0725) and HP1392 (fibronectin/fibrinogen-binding protein) involved in cell adhesion processes, and *napA* (HP0243) and *tsaA* (HP1563) linked to the resistance to oxygen toxicity.

Interestingly, analysis of the de-regulated genes showed that 19 out 29 genes that are up-regulated in the Δ*cncR1* mutant belong to operons preceded by σ^{54} consensus promoter sequences, indicating that transcription from these promoters is likely under the control of the alternative σ^{54} factor (Niehus et al., 2004; Pereira et al., 2006; Spohn and Scarlato, 1999b). In contrast, no σ^{54} consensus sequence was found upstream of genes down-regulated in the mutant strain. In agreement with this observation, the HP1122 ORF, whose promoter (P$_{HP1122}$) was previously reported as being under the control of both the alternative σ^{54} and σ^{28} factors (Josenhans et al., 2002), in *H. pylori* G27 strain it harbors a disrupted σ^{54} consensus sequence. Therefore, it is likely that this promoter is under the control of the sole σ^{28} factor.

To date, the known regulome of the σ^{54} factor in *H. pylori* consists of 10 operons: *flaB*-HP0114; *flgE*; HP0367-HP0368; *flgE-hypA-mua*; *fliK-flgD-flgE*; HP1076; HP1120-*flgK*; *fliW-murG*; HP1233; *flgB-flgC-fliE* (Niehus et al., 2004; Pereira et al., 2006; Spohn and Scarlato, 1999b). The *fliA-fliM* operon, formerly reported as member of σ^{54} regulome (Niehus et al., 2004), has been recently reported as not controlled by σ^{54} (Niehus et al., 2004; Sharma et al., 2010). In the reported macroarray analysis, all the known σ^{54}-dependent genes are up-regulated in the Δ*cncR1* mutant with respect to the wild type strain. The *fliE* gene was not included in this analysis as signals were below the selected threshold of validity, >0,0015%. These results suggest that *cncR1* exerts a negative regulation of the expression of the entire σ^{54} regulome.

Functional category	Genome ORF	Fold change in Δ*cncR1*	Promoter	Description
UP-regulated genes				
Chemotaxis and motility	HP0115	2,1	σ^{54}	flagellin B (*flaB*)
	HP0295	2,0	σ^{54}	flagellar hook-associated protein (*flgL*)
	HP0870	1,8	σ^{54}	flagellar hook protein (*flgE*)
	HP0906	3,0	σ^{54}	flagellar hook lenght control protein (*fliK*)
	HP0907	1,9	σ^{54}	flagellar basal body rod modification protein (*flgD*)
	HP0908	1,7	σ^{54}	flagellar hook protein (*flgE*)
	HP1119	3,1	σ^{54}	flagellar hook-associated protein (*flgK*)
	HP1154	1,9	σ^{54}	flagellar assembly protein (*fliW*)
	HP1558	1,5	σ^{54}	flagellar basal-body rod protein (*flgC*)
	HP1559	2,5	σ^{54}	flagellar basal-body rod protein (*flgB*)
Internal metabolism	HP0483	1,7		cytosine specific DNA methyltransferase
	HP0966	1,6		conserved hypothetical protein
	HP1036	1,6		7, 8-dihydro-6-hydroxymethylpterin-pyrophosphokinase (*folK*)
	HP1045	2,0		acetyl-CoA synthetase (*acoE*)
	HP1155	1,7	σ^{54}	transferase, peptidoglycan synthesis (*murG*)
	HP1193	1,5		aldo-keto reductase
Cellular processes and signaling	HP0366	2,4	σ^{54}	spore coat polysaccharide biosynthesis protein C
	HP0869	1,7	σ^{54}	hydrogenase expression/formation protein (*hypA*)
	HP1129	1,7		biopolymer transport protein (*exbD*)
Transcription and DNA processing	HP0868	1,5	σ^{54}	nickel-binding protein (*Mua*)
	HP1541	1,6		transcription-repair coupling factor (*trcF*)
Unknown/ Hypothetical	HP0114	2,0	σ^{54}	*H. pylori* predicted coding region HP0114
	HP0367	2,9	σ^{54}	*H. pylori* predicted coding region HP0367
	HP0469	1,5		*H. pylori* predicted coding region HP0469
	HP0688	1,7		*H. pylori* predicted coding region HP0688
	HP1076	5,3	σ^{54}	*H. pylori* predicted coding region HP1076
	HP1120	2,0	σ^{54}	*H. pylori* predicted coding region HP1120
	HP1162	1,7		*H. pylori* predicted coding region HP1162
	HP1233	2,0	σ^{54}	*H. pylori* predicted coding region HP1233
DOWN-regulated genes				
Internal metabolism	HP0265	-1,5		cytochrome c biogenesis protein (*ccdA*)
	HP0370	-1,5		biotin carboxylase (*accC*)
	HP0724	-3,3		anaerobic C4-dicarboxylate transport protein (*dcuA*)
	HP0799	-1,6		molybdenum cofactor biosynthesis protein (*mogA*)
	HP0839	-1,7		outer membrane protein P1 (*ompP1*)
	HP1229	-1,6		aspartate kinase (*lysC*)
Cellular processes and	HP0022	-1,7		lipid A phosphoethanolamine transferase
	HP0243	-1,8		neutrophil activating protein (*napA*)

signaling				(bacterioferritin)
	HP0725	-1,9		outer membrane protein (*omp17*)
	HP0970	-1,8		nickel-cobalt-cadmium resistance protein (*nccB*)
	HP1335	-1,7		nicotinate-nucleotide pyrophosphorylase
	HP1392	-1,5		fibronectin/fibrinogen-binding protein
	HP1563	-1,5		alkyl hydroperoxide reductase (*tsaA*)
Transcription and DNA processing	HP0111	-1,8		heat-inducible transcription repressor (*hrcA*)
	HP0223	-1,6		DNA repair protein (*radA*)
	HP1231	-1,6		DNA polymerase III delta prime subunit (*holB*)
Translation and protein fate	HP0182	-1,8		lysyl-tRNA synthetase (*lysS*)
	HP0825	-1,9		thioredoxin reductase (*trxB*)
	HP1497	-1,6		peptidyl-tRNA hydrolase (*pth*)
Unknown/ Hypothetical	HP0120	-1,6		*H. pylori* predicted coding region HP0120
	HP0155	-1,9		*H. pylori* predicted coding region HP0155
	HP0234	-1,8		*H. pylori* predicted coding region HP0234
	HP0258	-1,7		*H. pylori* predicted coding region HP0258
	HP0282	-1,8		*H. pylori* predicted coding region HP0282
	HP0308	-1,6		*H. pylori* predicted coding region HP0308
	HP0350	-1,8		*H. pylori* predicted coding region HP0350
	HP0395	-1,9		*H. pylori* predicted coding region HP0395
	HP0487	-1,6		*H. pylori* predicted coding region HP0487
	HP0677	-1,5		*H. pylori* predicted coding region HP0677
	HP0764	-1,6		*H. pylori* predicted coding region HP0764
	HP0773	-1,6		*H. pylori* predicted coding region HP0773
	HP0892	-1,5		*H. pylori* predicted coding region HP0892
	HP0946	-1,6		*H. pylori* predicted coding region HP0946
	HP1122	-1,8	$(\sigma^{54})\ \sigma^{28}$	*H. pylori* predicted coding region HP1122
	HP1163	-2,0		*H. pylori* predicted coding region HP1163
	HP1207	-1,9		*H. pylori* predicted coding region HP1207
	HP1579	-4,2		*H. pylori* predicted coding region HP1579

Table 2: Genes listed are those whose transcription differed more than 1.5-fold in the Δ*cncR1* mutant compared to the parental G27 wild type strain in the macroarray analysis; results are filtered according to the parameters reported in Material and Methods. ORF numbers are based on the genome sequences of *H. pylori* 26695, while the functional annotation of the genes and the subsequent grouping in functional categories was derived from literature reports. σ^{54} and σ^{28} annotations indicate genes belonging to operons whose transcription depend on the alternative σ^{54} and σ^{28} sigma factors, respectively.

5.1.6 Primer extension analysis of *cncR1*-regulated genes and *cag*-PAI genes

To validate the results of the transcriptomic analysis, 4 promoters controlling the expression of 11 detected up-regulated genes were selected, and the transcript levels at these promoters were assayed by quantitative primer extension experiments,

comparing the expression in the Δ*cncR1* strain with respect to the wild type strain. The promoters assayed in this analysis were P*flaB*, P*flgE*, P*fliK* and P*flgB*, upstream the *flaB*-HP0114, *flgE*, *fliK-flgD-flgE* and *flgB-flgC-fliE* operons, respectively. All selected promoters are under the control of the σ^{54} sigma factor, and the downstream operons encode for structural or regulatory flagellar proteins. Results of the primer extension assay are reported in Fig. 23, showing increased mRNA levels at all the tested promoters in the Δ*cncR1* mutant, with respect to the wild type strain. The specific signals of the primer extension assays were quantified, showing in the Δ*cncR1* strain 2.7-, 1.7-, 2.4- and 1.7-fold increased mRNA levels, with respect to the wild type strain, at the P*flaB*, P*flgE*, P*fliK* and P*flgB* promoters, respectively. The observed variations of the transcript levels in the primer extension assays are in agreement to the differential expressions detected in the macroarray analysis (Table 2), confirming that *cncR1* exerts a negative regulation of the σ^{54} regulome.

To further confirm the specificity of the *cncR1*-dependent response, the Δ*cncR1* strain was used to construct the complementing *vacA::cncR1* strain, harboring the region encompassing the *cncR1* sRNA and the upstream P*cagP* promoter cloned in the *vacA* locus. Through primer extension analysis were assayed the transcript levels at the P*flaB*, P*flgE*, P*fliK* and P*flgB* promoters, showing reduced transcript levels with respect to the Δ*cncR1* and unchanged levels with respect to the wild type strain (data not shown). Hence, the novel copy of P*cagP-cncR1* inserted in the Δ*cncR1* strain was able to restore the transcript levels of at least four σ^{54}-dependent promoters to values unchanged with respect to the wild type, likely complementing the strain Δ*cncR1*.

Since it has been shown that in many pathogenic bacteria dedicated transcriptional regulators are frequently encompassed within the PAIs of type III and type IV secretion systems (Ellermeier et al., 2005; Yahr and Wolfgang, 2006), expression of the *cag*-PAI genes was assayed in the Δ*cncR1* mutants to assess possible *cncR1*-mediated regulation. While the macroarray transcriptional analyses showed unchanged transcript levels for most of the *cag* genes, some transcripts (*cagζ*, *cagZ*, *cagV*, *cagS*, *cagQ*, and *cagL*) had signals under the limit of quantification. Hence, expression levels of *cagζ*, *cagV*, *cagS* and *cagQ* were assayed by primer extension assay in Δ*cncR1* and the wild type strain, showing unchanged

levels (data not shown). These results suggest that the *cncR1* sRNA does not regulate the transcript levels of the *cag* genes under normal growing conditions.
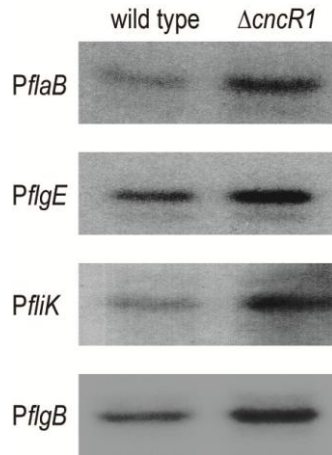
Fig. 23 Primer extension analysis of transcript levels at four σ^{54}-dependent promoters in the wild type and Δ*cncR1* strains. Primer extensions were performed with 12 μg of total RNA and 0.1 pmol of labeled oligos to target the transcripts at the corresponding promoters: VSflaB (P*flaB* promoter), VSflgE (P*flgE* promoter), VS958p1 (P*fliK* promoter) and VSflgB (P*flgB* promoter).

5.1.7 *cncR1*-dependent modulation of the *H. pylori* motility

Since most of the genes up-regulated in the Δ*cncR1* strain are involved in the flagella assembly and regulation, the effect of the knock out was tested on the motility of the bacteria, by assaying the ability of the cells to spread on soft agar plates. The strains selected for the assay were the parental G27 wild type, Δ*cncR1*, Δ*cncR1 vacA::cncR1* (complemented strain) and Δ*hspR* strains (non-motile control). Cells were grown to exponential phase, spotted onto low-concentration agar plates and incubated for 72-96 h at 37°C under microaerophilic conditions. As reported in Fig. 24, the areas of spreading of the Δ*cncR1* strain were augmented with respect to the area covered by the wild-type strain, thus showing increased motility functions. In contrast, the Δ*cncR1* complemented strain (Δ*cncR1 vacA::cncR1*) restored wild type spreading. Consequently, we conclude that *cncR1* exerts a negative effect on the regulation of the *H. pylori* motility functions.
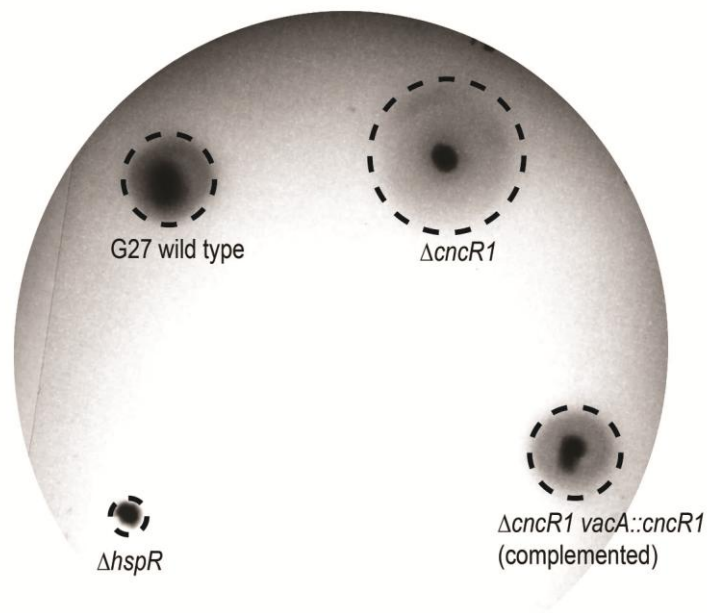
Fig. 24 Bacterial motility assay. Bacteria were stab inoculated with a pipette tip into semisolid agar plates and incubated for 72 h at 37°C under microaerophilic conditions. The strains used in this assay are indicated as follows: G27 wild type, Δ*cncR1* (G27 *cncR1*::*cat*), Δ*cncR1 vacA*::*cncR1* (G27 *cncR1*::*cat vacA*::*cncR1* - complemented strain) and Δ*hspR* (G27 *hspR*::*km*).

5.1.8 *cncR1*-dependent regulation of σ^{54}-interacting factors

It is well established that the transcriptional activity of the alternative σ^{54} factor on its regulome in *H. pylori* is positively regulated by the FlgRS two-component systems (HP0703, HP0244), FlhA (HP1041), FlhF (HP1035) and FlgZ (HP0958), while is repressed by FlgM (HP1122) and FliK (HP0906) (Brahmachary et al., 2004; Douillard et al., 2009; Niehus et al., 2004; Pereira and Hoover, 2005; Pereira et al., 2011; Ryan et al., 2005; Spohn and Scarlato, 1999b; Wen et al., 2009). To investigate possible regulatory effects exerted by the *cncR1* sRNA on the aforementioned regulators, the mRNA levels of the corresponding genes were compared in the Δ*cncR1* mutant with respect to the wild type strain. In the global transcriptional analysis with DNA macroarrays, *flgR*, *flgS*, *flhA*, *flhF* and *flgZ*

showed unchanged transcript levels, while mRNA levels of *fliK* and *flgM* were increased and decreased, respectively in the Δ*cncR1* strain (Table 2). Afterwards, the transcript levels of *flgR*, *flgS* and *flgZ* genes were assayed by dot-blot analysis. Results showed unchanged transcript levels in *flgR*, *flgS* (data not shown), while *flgZ* showed 1.8-fold increased levels in the Δ*cncR1* strain (Fig. 25A), which was not detected in macroarray analysis. Since *fliK*, *flgZ* and *flgM* are de-regulated in the Δ*cncR1* strain, it is possible that the negative regulation exerted by *cncR1* sRNA on the σ^{54} regulome could be mediated by one or more of these factors.

A bioinformatic screening of putative targets of the *cncR1* sRNA on the genome of *H. pylori* G27 strain was carried out using the online resource RNAtarget (http://cs.wellesley.edu/~btjaden/TargetRNA2/). This analysis was based on finding of short (at least 7 bp) and imperfect base-pairing of the G27 *cncR1* most conserved sequences with the whole *H. pylori* G27 predicted transcriptome. Results of the screening were filtered according to the energy of hybridization and relative positions of the two putative complementary RNAs. The analysis enlisted many bacterial mRNAs showing a significant base-pairing with short regions of the *cncR1* sRNA. Among high scored results is reported the *fliK* mRNA (HP0906), showing a base-pairing of the sequence from position 525 to 537 bp of the former with the *cncR1* sRNA (Fig. 25B). To assess if this predicted short base-paring between *cncR1* and *fliK* mRNA is part of a more extensive long-range base-paring, a bioinformatic analysis with the online resource RNAhybrid (http://bibiserv.techfak.uni-bielefeld.de/rnahybrid/submission.html) was performed, showing an extensive discontinued and imperfect complementarity between the two RNAs (Fig. 25C). The predicted short and long imperfect base-pairing regions between *cncR1* and *fliK* mRNA are consistent with a typical *trans* sRNA-mediated regulation mechanism of the corresponding mRNA target. If confirmed by further analyses, these interactions can support the regulatory effect exerted by *cncR1* sRNA on the *fliK* mRNA that was observed in the transcriptional analysis.
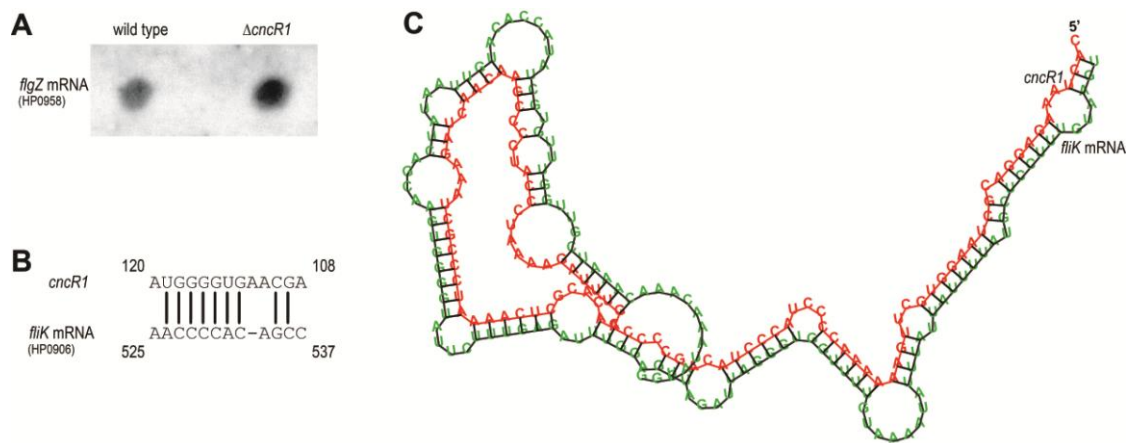
Fig. 25 (A) Dot-blot analysis of the *flgZ* transcript levels in the Δ*cncR1* and wild type strains. About 15 µg of total RNA was spotted on a Hybond-N+ nylon membrane by means of a Bio-Dot microfiltration apparatus (Bio-Rad) and cross-linked to the filter by UV-ray treatment. The membrane was hybridized with the oligonucleotide VS958p1 (Table 6), mapping on the *flgZ* mRNA. (B) Bioinformatic prediction of short low-energy base-pairing between *cncR1* sRNA and *fliK* RNA. The analysis was performed with RNAtarget program (C) Bioinformatic prediction of long discontinuous base-pairing between *cncR1* sRNA and *fliK* RNA, using RNAhybrid program.

5.2 DISCUSSION

For a successful infection of the host or survival in the environment, bacteria have to rapidly adapt their gene expression in response to changing conditions. Besides regulation at the transcriptional level, post-transcriptional regulation is an important layer of control in both prokaryotes and eukaryotes. Together with several RNA binding proteins which influence RNA structure and stability, the bacterial small RNAs (sRNAs) act as post-transcriptional regulators under various stress and growth conditions (Papenfort and Vogel, 2010; Storz et al., 2011; Waters and Storz, 2009). In this context, *H. pylori* is a peculiar organism: on one hand it is particularly poor in numbers of transcriptional regulators (Scarlato et al., 2001; Tomb et al., 1997), which has been traditionally attributed to reductive evolution due to the constrained gastric habitat, on the other hand this situation is balanced by the very high numbers of antisense transcripts and putative sRNAs recently described (Pernitzsch and Sharma, 2012; Sharma et al., 2010). Despite the extensive regulatory potential offered by asRNA and sRNA regulation, in *H. pylori*, only few examples have been described to date (Sharma et al., 2010; Wen et al., 2011), likely due to the relative novelty of these findings.

The *cag*-encoded *cncR1* sRNA is a peculiar non coding RNA, since it is observed only in *H. pylori* strains with a conserved *cag*-PAI island. In particular, all sequenced *cag*$^+$ strains harbor the *cncR1* locus (both the sRNA and the upstream promoter P*cagP*), with a 92% sequence homology, a conservation that is higher than for most other *cag* genes (Azuma et al., 2004). This conservation suggests a possible functional role exerted by the *cncR1* sRNA in *H. pylori* gene regulation, maybe at the level of the *cag*-dependent virulence pathways. The *cncR1* sRNA corresponds to the 5'UTR of the *cagP* gene (Fig. 19), that, in contrast, is less conserved, and frequently disrupted by frameshift mutations, as for example in the G27 strain. Moreover, *cagP* is not fundamental for the functioning of the *cag*-encoded T4SS, and mutagenic studies missed to identify a function (Fischer et al., 2001).

The 5'-end of *H. pylori* G27 strain *cncR1* sRNA has been mapped by primer extension analysis, while the position of the 3'-end was inferred from Northern blot

assays, showing a major transcript of 218 nucleotides, corresponding to the *cncR1* sRNA (Fig. 20). Transcription beyond the *cncR1* 3'-end drops dramatically, likely due to a transcriptional terminator. The bioinformatic analysis of the putative terminator sequences predicted secondary structures compatible with an intrinsic transcriptional terminator. In addition, the functionality of these sequences as terminators were confirmed with the aid of transcriptional fusions with a *lux* reporter (Fig. 21). Interestingly, the low levels of expression of *cagP* reported in many studies (Boonjakuakul et al., 2005; Eaton et al., 2002) are explained by the presence of the transcriptional terminator at the 3'-end of the *cncR1* sRNA, that reduces the downstream transcription into of the putative *cagP* coding sequence.

The *cncR1* sRNA is under the control of P*cagP* promoter, and the nucleotide sequence of the promoter indicates a conserved -10 box recognized by the vegetative σ^{80} factor, without extended TGn element or a -35 box. Quantification assays of the expressed *cncR1* sRNA in normal physiological conditions showed that it is the most abundant RNA coded by the *H. pylori cag*-island (Fig. 12). Transcriptional studies on the P*cagP* promoter revealed that the expression of *cncR1* sRNA is not under the control of either the pleiotropic metal-dependent transcriptional regulators Fur and NikR, nor the heat-shock regulators HrcA and HspR (see previous sections). Moreover, *cncR1* levels do not change in response of most of the tested stimuli (environmental stresses, acidic pH and contact with AGS host cells). Interestingly, *cncR1* levels change during bacterial growth, with reduced expression levels in the advanced growth phase (Fig. 13). This result suggests that the possible negative effect (typical of sRNA regulation) exerted by *cncR1* may drop when *H. pylori* approaches the stationary phase.

A clear negative effect exerted by *cncR1* was observed for all genes under the control of the alternative σ^{54} factor RpoN (Table 2). Since the mRNA levels of the *rpoN* gene are unchanged between the *cncR1* deletion mutant and the wild type strain, *cncR1* is likely not affecting the expression of *rpoN*, but rather influencing post-transcriptionally the activity of the RNA polymerase-σ^{54} holoenzyme. The latter is modulated by different factors, affecting either the affinity of the RNAP holoenzyme with the promoter sequences, or the availability of the σ^{54} sigma factor. In particular, FlhA, FlhF and the activated form of the FlgRS two-component system

are all required for the expression of the σ^{54}-dependent genes (Brahmachary et al., 2004; Niehus et al., 2004; Spohn and Scarlato, 1999b; Wen et al., 2009), likely by direct interaction with the RNA polymerase-σ^{54} holoenzyme or by binding with specific sequences on the promoter, that alter the DNA bending (Xu and Hoover, 2001). Similarly, FliK and FlgM reduce the activity of the holoenzyme likely with similar mechanisms or by interaction with the aforementioned positive regulators (Douillard et al., 2009; Niehus et al., 2004; Ryan et al., 2005). In contrast, FlgZ acts as a molecular chaperon of σ^{54} protein, promoting its accumulation in the cytoplasm (Pereira and Hoover, 2005; Pereira et al., 2011).

In the transcriptional analysis of the *cncR1* mutant strain, the mRNA levels of *flgZ*, *fliK* and *flgM* resulted de-regulated with respect to the wild type strain (Fig. 25 and Table 2), suggesting that the effect exerted by *cncR1* on the transcriptional activity of σ^{54} is likely mediated by one or more of these factors. In particular, *flgZ* is up-regulated in the *cncR1* knock-out strain, and since FlgZ positively affects σ^{54}, the global up-regulation of the σ^{54} promoters in the mutant strain would be explained. Similarly, *flgM* is down-regulated in the *cncR1* mutant. This result fits with the up-regulation of the σ^{54}-regulon since FlgM has been reported to negatively regulates σ^{54} (Niehus et al., 2004). In contrast, the possible mechanism mediated by FliK is more elusive, since this factor represses the activity of σ^{54} in a feedback loop, and appears to be up-regulated in the *cncR1* mutant along with all other σ^{54} promoters. Nevertheless the functioning of *H. pylori* FliK factor is poorly understood and it is possible that it acts with alternate mechanisms that fit with the speculation of a *cncR1*-mediated regulation of σ^{54}.

Finally, since *cncR1* inversely correlates with bacterial motility (Fig. 24), and the *cncR1* expression decreases in the advanced growth phase, we can speculate that *H. pylori* may use *cncR1* to modulate the motility during gastric infections. In particular, as long as there are few bacteria that can grow in nearly log phase, the *cncR1* is highly expressed and bacterial motility is reduced. When the bacteria are locally too abundant and the culture proceeds to stationary phase, the expression of *cncR1* is likely repressed and the motility enhanced, in order to permit the bacteria to reach less populated niches.

CONCLUSIONS

The transcriptional analysis of the *H. pylori cag*-pathogenicity island has been conducted to identify regulatory factors that underlie the coordinated expression of *cag* gene products, needed to assemble the *cag*-encoded type 4 secretion system apparatus.

The study has enlightened 11 *cag* transcriptional units, for which a plethora of responses affecting to environmental stresses and growth conditions were reported. In particular, the mechanism of iron-dependent regulation of the P*cagA* promoter has been successfully cleared, as we were able to demonstrate a direct involvement of the ferric uptake regulator Fur. In contrast, the other observed transcriptional responses of P*cag* promoters were not directly linked to any other known transcriptional regulator, suggesting that they may be due to pleiotropic responses of the bacterium or under the control of unknown regulators.

In this respect, the extensive presence of putative antisense transcripts and small non coding RNAs suggests that post-transcriptional regulation mechanisms might be responsible for the regulation of the *cag* genes. The *cncR1* sRNA, characterized in detail in this study, is a primary candidate for this task, as it is coded by the *cag*-PAI island itself. Notably, in the Δ*cncR1* mutant strain the expression levels of most *cag* genes is unchanged with respect to the wild type strain. Thus, the regulation mediated by *cncR1*-should be exerted at the post-transcriptional level, acting on the translatability of the target mRNA. Hence, dedicated studies should be undertaken to clarify the possible antisense- and sRNA-mediated regulatory mechanisms on the *cag*-PAI.

MATERIALS and METHODS

7.1.1 Bacterial strains and growth conditions

All *H. pylori* strains used are listed in Table 3. Bacteria were recovered from -80°C glycerol stocks and propagated on Columbia agar plates containing 5% defibrinated horse blood (Oxoid) or on BBL Brucella (BD) agar plates containing 5% fetal calf serum (Oxoid), both supplemented with 0.2% cyclodextrin and Dent's or Skirrow's antibiotic supplement. Bacteria were grown for 24-48 hours at 37°C in a water-jacketed thermal incubator (9% CO_2, 91% air atmosphere, and 95% humidity) or in jars using CampyGen™ (Oxoid) gas-packs. Liquid cultures were grown in BBL Brucella Broth supplemented with 5% fetal calf serum and Dent's or Skirrow's antibiotic supplement at 37°C with gentle agitation (125 rpm), in glass or tissue-culture flasks with vented cap. When required, Brucella agar plates or liquid broth were supplemented with chloramphenicol (30μg/ml) and kanamycin (25μg/ml).

To measure the metal-dependant transcriptional response, cultures of the wild-type and mutant strains were grown to mid-log phase (optical density at 600nm [OD_{600}] 0.5-0.6) and treated for 30 minutes with either 1 mM $(NH_4)_2Fe(SO_4)_2$, 1 mM $NiSO_4$, or 100 μM 2,2-dipyridyl (Sigma-Aldrich) prior to RNA extraction or the measurement at regular time intervals for the emission of bioluminescence. For acid exposure experiment, mid-log phase cultures of the wild-type and mutant strains were divided in two subcultures and treated with either 1M HCl to adjust the pH from 7.0 to 5.2 (acid shock) or equal volume of sterile water (control sample). Subcultures were grown for 30-90 minutes than harvested for RNA extraction. The volume of 1 M HCl required to achieve a pH of 5.2 was determined on aliquots of the growing cultures. For heat-shock experiments, mid-log phase culture was split into 10-ml aliquots that were heat shocked at 42°C in a water bath for 30 min or maintained at 37°C, then harvested for total RNA extraction. To follow the expression of *cag* genes over times, an overnight culture of wild type strain was diluted to a starting OD_{600} of 0.08 and cultured to an OD_{600} of 1.75. Aliquots of the master culture were obtained at different time points for measurement of luminescence and optical density, as well as for total RNA extraction. For growth in 96-well plates (Orange Scientific) or in an Isoplate-96 TC (optimized for luminescence reading; Perkin Elmer), single *H. pylori* colonies were picked and inoculated in single wells containing 100 μl BBL Brucella broth. Plates (with loose lids) were agitated at 700 rpm with an MS3 digital shaker (IKA), placed inside the thermal incubator, and measured at regular time intervals with a multilabel reader (see below). Colonies cultured in single wells could be recovered and expanded on Brucella agar plates up to 72 to 96 h after the initial inoculum.

Motility of *H. pylori* strains was assayed by stab-inoculating bacteria with a pipette tip into 0.3 % Brucella agar plates supplemented with 10% fetal calf serum and Dent's or Skirrow's antibiotic supplement.

H. pylori transformants were obtained by double homologous recombination of the naturally competent G27 strain: freshly grown overnight cultures were spotted onto plates and grown for a further 5 h, at which point 5 μg of plasmid DNA was added onto the growing strain and incubated overnight. Positive clones were selected on Brucella agar plates supplemented with chloramphenicol or kanamycin, according to the resistance phenotype conferred by the *Campylobacter coli cat* (Cm[R]) and *aphA3* (Km[R]) cassettes, respectively.

E. coli strains DH5α cultures were grown in Luria-Bertani (LB) agar or in LB broth. When required, ampicillin, kanamycin and chloramphenicol were added at final concentration of 100μg/ml, 25μg/ml, and 30μg/ml, respectively.

Table 3. Strains used in this study

Strain or Plasmid	Genotype or description	Source/reference
***E. coli* strains**		
DH5α	supE44 ΔlacU169 (φ80 lacZΔM15) hsdR17 recA1 endA1 gyrA96 thi-1 relA1β	(Hanahan, 1983)
***H. pylori* strains**		
G27	Clinical isolate; wild-type parental strain	(Xiang et al., 1995)
G27(*fur::km*)	G27 derivative; bp 25 to 434 of the *fur (HP1027)* coding sequence replaced by a *km* cassette; Km^R	(Delany et al., 2001a)
G27(*nikR::km*)	G27 derivative; bp 88 to 417 of the *nikR (HP1338)* coding sequence replaced by a *km* cassette; Km^R	(Pflock et al., 2005)
G27(*hspR::km*)	G27 derivative; bp 66 to 334 of the *hspR (HP1025)* coding sequence replaced by a *km* cassette; Km^R	(Spohn and Scarlato, 1999a)
G27(*hrcA::km*)	G27 derivative; bp 156 to 375 of the *hrcA (HP0111)* coding sequence replaced by a *km* cassette; Km^R	(Spohn et al., 2004)
G27(*arsS::cp*)	G27 derivative; bp 3 to 1290 of the *arsS (HP0164-HP0165)* coding sequence replaced by a *cat* cassette; Cm^R	This study
G27(*cncR1::cp*)	G27 derivative; bp -79 to 208 of the *cncR1 (HP0536 5'UTR)* sequence replaced by a *cat* cassette; Cm^R	This study
G27*lux*	G27 derivative carrying the *km* cassette and the promoterless *Photorhabdus luminescens luxCDABE* operon in the *vacA* locus; Km^R	(Vannini et al., 2012)
G27 P$_{pfr}$-*lux*	*vacA::cat*-P$_{pfr}$*luxCDABE*; G27*lux* derivative obtained by double omologous recombination with plasmid PVCC::P$_{pfr}$; Cm^R	(Vannini et al., 2012)
G27 oppP$_{pfr}$-*lux*	*vacA::cat*-opp P$_{pfr}$*luxCDABE*; G27*lux* derivative obtained by double homologous recombination with plasmid PVCC::oppP$_{pfr}$; Cm^R	(Vannini et al., 2012)
G27 P$_{pfr}$-*lux* Δ*fur*	*vacA::cat*-P$_{pfr}$*luxCDABE fur::aphA-3*; G27*lux* P$_{pfr}$ derivative carrying a deletion of the *fur* gene, obtained by double homologous recombination with plasmid pFur::km; Km^R Cm^R	(Vannini et al., 2012)
G27 P$_{fecA3}$-*lux*	*vacA::cat*-P$_{fecA3}$*luxCDABE*; G27*lux* derivative obtained by double homologous recombination with plasmid PVCC::P$_{fecA3}$; Cm^R	(Vannini et al., 2012)
G27 oppP$_{fecA3}$-*lux*	*vacA::cat*-opp P$_{fecA3}$*luxCDABE*; G27*lux* derivative obtained by double homologous recombination with	(Vannini et al., 2012)

plasmid PVCC::oppP$_{fecA3}$; Cm^R

G27 P$_{fecA3}$SD$_{lux}$-*lux*	*vacA::cat-P$_{fecA3}$SD$_{lux}$luxCDABE*; G27*lux* derivative obtained by double homologous recombination with plasmid PVCC::P$_{fecA3}$SD$_{lux}$; Cm^R	(Vannini et al., 2012)
G27 P$_{fecA3}$SD$_{lux}$-ΔOPI$_{NikR}$-*lux*	*vacA::cat-P$_{fecA3}$SD$_{lux}$-ΔOPI$_{NikR}$luxCDABE*; G27*lux* derivative obtained by double homologous recombination with plasmid PVCC::P$_{fecA3}$SD$_{lux}$-ΔOPI$_{NikR}$; Cm^R	(Vannini et al., 2012)
G27 P$_{cagζ}$-*lux*	*vacA::cat-P$_{cagζ}$luxCDABE*; G27*lux* derivative obtained by double homologous recombination with plasmid PVCC::P$_{cagζ}$; Cm^R	This study
G27 P$_{cagζ}$-5'UTR-*lux*	*vacA::cat-P$_{cagζ}$-cagζ5'UTR-luxCDABE*; G27*lux* derivative obtained by double homologous recombination with plasmid PVCC::P$_{cagζ}$-5'UTR; Cm^R	This study
G27 P$_{cagV}$-*lux*	*vacA::cat-P$_{cagV}$luxCDABE*; G27*lux* derivative obtained by double homologous recombination with plasmid PVCC::P$_{cagV}$; Cm^R	This study
G27 P$_{cagV}$-5'UTR-*lux*	*vacA::cat-P$_{cagV}$-cagV5'UTR-luxCDABE*; G27*lux* derivative obtained by double homologous recombination with plasmid PVCC::P$_{cagV}$-5'UTR; Cm^R	This study
G27 P$_{cagU}$-*lux*	*vacA::cat-P$_{cagU}$luxCDABE*; G27*lux* derivative obtained by double homologous recombination with plasmid PVCC::P$_{cagU}$; Cm^R	This study
G27 P$_{cagU}$-5'UTR-*lux*	*vacA::cat-P$_{cagU}$-cagU5'UTR-luxCDABE*; G27*lux* derivative obtained by double homologous recombination with plasmid PVCC::P$_{cagU}$-5'UTR; Cm^R	This study
G27 P$_{cagU}$-5'UTRtr-*lux*	*vacA::cat-P$_{cagU}$-cagU5'UTRtr-luxCDABE*; G27*lux* derivative obtained by double homologous recombination with plasmid PVCC::P$_{cagU}$-5'UTRtr; Cm^R	This study
G27 P$_{cagQ}$-*lux*	*vacA::cat-P$_{cagQ}$luxCDABE*; G27*lux* derivative obtained by double homologous recombination with plasmid PVCC::P$_{cagQ}$; Cm^R	This study
G27 P$_{cagQ}$-5'UTR-*lux*	*vacA::cat-P$_{cagQ}$-cagQ5'UTR-luxCDABE*; G27*lux* derivative obtained by double homologous recombination with plasmid PVCC::P$_{cagQ}$-5'UTR; Cm^R	This study
G27 P$_{cagS}$-*lux*	*vacA::cat-P$_{cagS}$luxCDABE*; G27*lux* derivative obtained by double homologous recombination with plasmid PVCC::P$_{cagS}$; Cm^R	This study
G27 P$_{cagS}$-5'UTR-*lux*	*vacA::cat-P$_{cagS}$-cagS5'UTR-luxCDABE*; G27*lux* derivative obtained by double homologous	This study

plasmid PVCC::P$_{cagA}$; Cm^R

| G27 P$_{cagA}$-5'UTR-*lux* | *vacA::cat-P$_{cagA}$-cagA*5'UTR-*luxCDABE*; G27*lux* derivative obtained by double homologous recombination with plasmid PVCC::P$_{cagA}$-5'UTR; Cm^R | This study |

Table 4. Plasmids used in this study

Plasmid	Description	Source/ reference
pBluescript KS II	Cloning vector, Ap^R	Stratagene
pGEM-T	Cloning vector, Ap^R	Promega
pGEM-T Easy	Cloning vector, Ap^R	Promega
pSB1075	Plasmid vector containing the 5.8-kb Photorhabdus luminescens luxCDABE operon cassette; Ap^R	(Winson et al., 1998b)
pBS::*cat*	pBluescript KS II derivative carrying a HincII *Campylobacter coli cat* cassette from pDT2548 (Wang and Taylor, 1990) cloned into the SmaI site of the vector; Ap^R, Cm^R	(Vannini et al., 2012)
pP$_{hpn2}$	pGEM-T derivative carrying a 280-bp BamHI-PstI fragment encompassing the intergenic region upstream of *hpn2* (HP1432), amplified with oligonucleotides 1431DxD and 1431DxS; Ap^R	(Vannini et al., 2012)
pFur::km	pGEM3Z derivative carrying the *C. coli aphA-3* cassette flanked by upstream and downstream regions for double homologous recombination in the *fur* locus; Ap^R, Km^R	(Delany et al., 2001a)
pBS::Δ*arsS*	pBluescript KS II derivative, carrying a 460 bp XbaI-BglII fragment amplified on chromosomal DNA of *H. pylori* with oligos 163f_Xba and 163r_Bgl, BglI/BamHI *cat* cassette and a 616 bp BglII-HindIII fragment amplified with 166f_Bgl and 166r_Hin; Ap^R, Cm^R	This study
pBS::Δ*cncR1*	pBluescript KS II derivative, carrying a 574 bp XbaI-BglII fragment amplified on chromosomal DNA of *H. pylori* with oligos VS536U-F and VS536U-R, BglI/BamHI *cat* cassette and a 442 bp BglII-HindIII fragment amplified with VS536D2F and VS536D-R; Ap^R, Cm^R	This study
pGEM-P$_{cagAB}$	pGEM-T Easy derivative, carrying a 403 bp fragment amplified on chromosomal DNA of *H. pylori* with oligos Lux547R and Lux546F, encompassing P$_{cagA}$-P$_{cagB}$ promoter regions; Ap^R, Cm^R	This study
pVAC::km	pGEM3Z derivative containing the *C. coli aphA-3* cassette flanked by upstream and downstream regions for double homologous recombination in the *vac* locus;	(Delany et al., 2002)

Ap^R, Km^R

pVC	pVAC derivative lacking the 779-bp 3'-end region of homology to *vacA*, altered with a 1,045-bp BamHI-HindIII fragment of pSB1075 encompassing the 5'-end of the *luxCDABE* cassette, including the RBS, the translation start codon, and the first 1,013 bp of the *luxC* cistron; Ap^R	(Vannini et al., 2012)
pVCC	Suicide transformation vector for promoter-*lux* fusions; Ap^R, Cm^R	(Vannini et al., 2012)
PVCC::P$_{pfr}$	pVCC derivative carrying a 180-bp fragment, amplified with oligonucleotides PpfrF and PpfrR, encompassing a codirectional P$_{pfr}$ promoter upstream of *luxC*; Ap^R, Cm^R	(Vannini et al., 2012)
PVCC::oppP$_{pfr}$	pVCC derivative carrying the 180-bp P$_{pfr}$ promoter fragment, cloned in opposite direction with respect to *luxC*; Ap^R, Cm^R	(Vannini et al., 2012)
PVCC::P$_{fecA3}$	pVCC derivative carrying a 182-bp fragment, amplified with oligonucleotides A3.4 and A3.5B, encompassing a codirectional P$_{fecA3}$ promoter upstream of *luxC*; Ap^R, Cm^R	(Vannini et al., 2012)
PVCC::oppP$_{fecA3}$	pVCC derivative carrying the P$_{fecA3}$ promoter fragment, cloned in opposite direction with respect to *luxC*; Ap^R, Cm^R	(Vannini et al., 2012)
PVCC::P$_{fecA3}$SD$_{lux}$	pVCC derivative carrying a 109-bp fragment, amplified with oligonucleotides A3.4 and A3.1B, encompassing a codirectional P$_{fecA3}$ promoter with a shortened 5'UTR devoid of the *fecA3* RBS, cloned upstream of the *lux* operon; Ap^R, Cm^R	(Vannini et al., 2012)
PVCC::P$_{fecA3}$SD$_{lux}$-ΔOPI$_{NikR}$	pVCC derivative carrying a 66-bp fragment, amplified with oligonucleotides A3.4 and A3.3B, encompassing a codirectional P$_{fecA3}$ promoter missing the *fecA3* 5'UTR and the NikR OPI operator, cloned upstream of the *lux* operon; Ap^R, Cm^R	(Vannini et al., 2012)
PVCC::P$_{cagζ}$	pVCC derivative carrying a 122 bp BamHI/BglII fragment amplified on chromosomal DNA of *H. pylori* with oligos Lux519F and Lux520RS, encompassing 115 bp of the P$_{cagζ}$ promoter and the first 7 bp of the *cagζ* 5'UTR cloned upstream of *luxC*; Ap^R, Cm^R	This study
PVCC::P$_{cagζ}$-5'UTR	pVCC derivative carrying a 166 bp BamHI/BglII fragment from Lux519F and Lux520RL oligos, encompassing 115 bp of the P$_{cagζ}$ promoter and the *cagζ* 5'UTR (51 bp) cloned upstream of *luxC*; Ap^R, Cm^R	This study
PVCC::P$_{cagV}$	pVCC derivative carrying a 306 bp BamHI/BglII fragment from VS530FS and VS531RL oligos, encompassing 300 bp of the P$_{cagV}$ promoter and the first	This study

	6 bp of the cagV 5'UTR cloned upstream of *luxC*; Ap^R, Cm^R	
PVCC::P*cagV*-5'UTR	pVCC derivative carrying a 366 bp BamHI/BglII fragment from VS530FL and VS531RS oligos, encompassing 269 bp of the P*cagV* promoter and the *cagV* 5'UTR (97 bp) cloned upstream of *luxC*; Ap^R, Cm^R	This study
PVCC::P*cagU*	pVCC derivative carrying a 366 bp BamHI/BglII fragment from VS530FL and VS531RS oligos, encompassing 361 bp of the P*cagU* promoter and the first 5 bp of the *cagU* 5'UTR cloned upstream of *luxC*; Ap^R, Cm^R	This study
PVCC::P*cagU*-5'UTR	pVCC derivative carrying a 306 bp BamHI/BglII fragment from VS530FS and VS531RL oligos, encompassing 270 bp of the P*cagU* promoter with the *cagU* 5'UTR (35 bp) cloned upstream of *luxC*; Ap^R, Cm^R	This study
PVCC::P*cagU*-5'UTRtr	pVCC derivative carrying a 373 bp BamHI/BglII fragment from Lux530F2 and Lux531R2 oligos, encompassing 338 bp of the P*cagU* promoter and the first 24 bp of the *cagU* 5'UTR cloned upstream of *luxC*; Ap^R, Cm^R	(Vannini et al., 2012)
PVCC::P*cagS*	pVCC derivative carrying a 180 bp BamHI/BglII fragment from VS534FS and VS534R2 oligos, encompassing 177 bp of the P*cagS* promoter and the first 3 bp of the *cagS* 5'UTR cloned upstream of *luxC*; Ap^R, Cm^R	This study
PVCC::P*cagS*-5'UTR	pVCC derivative carrying a 241 bp BamHI/BglII fragment from VS534F and VS534R2 oligos, encompassing 177 bp of the P*cagS* promoter and the *cagS* 5'UTR (64 bp) cloned upstream of *luxC*; Ap^R, Cm^R	This study
PVCC::P*cagQ*	pVCC derivative carrying a 304 bp BamHI/BglII fragment from VS535FS and VS535R oligos, encompassing 301 bp of the P*cagQ* promoter and the first 3 bp of the *cagQ* 5'UTR cloned upstream of *luxC*; Ap^R, Cm^R	This study
PVCC::P*cagQ*-5'UTR	pVCC derivative carrying a 439 bp BamHI/BglII fragment from VS535F and VS535R oligos, encompassing 301 bp of the P*cagQ* promoter and the *cagQ* 5'UTR (138 bp) cloned upstream of *luxC*; Ap^R, Cm^R	This study
PVCC::P*cagP*	pVCC derivative carrying a 204 bp BamHI/BglII fragment from VS536FS and VS537RL oligos, encompassing 201 bp of the P*cagP* promoter and the first 3 bp of the *cagP* 5'UTR cloned upstream of *luxC*; Ap^R, Cm^R	This study

PVCC::P$_{cagP}$-5'UTR	pVCC derivative carrying a 394 bp BamHI/BglII fragment from VS536FL and Lux537R2 oligos, encompassing 170 bp of the P$_{cagP}$ promoter and the *cagP* 5'UTR (224 bp) cloned upstream of *luxC*; Ap^R, Cm^R	This study
PVCC::P$_{cagP}$-5'UTRtr	pVCC derivative carrying a 383 bp BamHI/BglII fragment Lux536F2 and Lux537R2 oligos, encompassing 170 bp of the P$_{cagP}$ promoter and the first 213 bp of the *cagP* 5'UTR cloned upstream of *luxC*; Ap^R, Cm^R	(Vannini et al., 2012)
PVCC::P$_{cagM}$	pVCC derivative carrying a 394 bp BamHI/BglII fragment from VS536FL and Lux537R2 oligos, encompassing 388 bp of the P$_{cagM}$ promoter and the first 6 bp of the *cagM* 5'UTR cloned upstream of *luxC*; Ap^R, Cm^R	This study
PVCC::P$_{cagM}$-5'UTR	pVCC derivative carrying a 204 bp BamHI/BglII fragment from VS536FS and VS537RL oligos, encompassing 167 bp of the P$_{cagM}$ promoter and the *cagM* 5'UTR (37 bp) cloned upstream of *luxC*; Ap^R, Cm^R	This study
PVCC::P$_{cagF}$	pVCC derivative carrying a 308 bp BamHI/BglII fragment from VS543FS and VS543R oligos, encompassing 305 bp of the P$_{cagF}$ promoter and the first 3 bp of the *cagF* 5'UTR cloned upstream of *luxC*; Ap^R, Cm^R	This study
PVCC::P$_{cagF}$-5'UTR	pVCC derivative carrying a 352 bp BamHI/BglII fragment from VS543F and VS543R oligos, encompassing 305 bp of the P$_{cagF}$ promoter and the *cagF* 5'UTR (47 bp) cloned upstream of *luxC*; Ap^R, Cm^R	This study
PVCC::P$_{cagC}$	pVCC derivative carrying a 276 bp BamHI/BamHI fragment VS546FS and VS546R oligos, encompassing 274 bp of the P$_{cagC}$ promoter and the first 2 bp of the *cagC* 5'UTR cloned upstream of *luxC*; Ap^R, Cm^R	This study
PVCC::P$_{cagC}$-5'UTR	pVCC derivative carrying a 300 bp BamHI/BamHI fragment from VS546F and VS546R oligos, encompassing 274 bp of the P$_{cagC}$ promoter and the *cagC* 5'UTR (26 bp) cloned upstream of *luxC*; Ap^R, Cm^R	This study
PVCC::P$_{cagB}$	pVCC derivative carrying a 261 bp BamHI/BglII fragment from VSorfxFS and VS547RL oligos, encompassing 257 bp of the P$_{cagB}$ promoter and the first 4 bp of the *cagB* 5'UTR cloned upstream of *luxC*; Ap^R, Cm^R	This study
PVCC::P$_{cagB}$-5'UTR	pVCC derivative carrying a 324 bp BamHI/BglII fragment from VSorfxFL and VS547RS oligos, encompassing 155 bp of the P$_{cagB}$ promoter and the *cagB* 5'UTR (169 bp) cloned upstream of *luxC*; Ap^R, Cm^R	This study

PVCC::P$_{cagA}$	pVCC derivative carrying a 324 bp BamHI/BglII fragment from VSorfxFL and VS547RS oligos, encompassing 321 bp of the P$_{cagA}$ promoter and the first 3 bp of the *cagA* 5'UTR cloned upstream of *luxC*; Ap^R, Cm^R	This study
PVCC::P$_{cagA}$-5'UTR	pVCC derivative carrying a 261 bp BamHI/BglII fragment from VSorfxFS and VS547RL oligos, encompassing 156 bp of the P$_{cagA}$ promoter and the *cagA* 5'UTR (105 bp) cloned upstream of *luxC*; Ap^R, Cm^R	This study
PVCC::P$_{cagP}$-5'UTRΔterm	pVCC derivative carrying a 261 bp BamHI/BglII fragment from VSorfxFS and VS547RL oligos, encompassing 156 bp of the P$_{cagA}$ promoter and the *cagA* 5'UTR (105 bp) cloned upstream of *luxC*; Ap^R, Cm^R	This study

Table 5. Oligonucleotides used for cloning

Name	Sequence (5'-3')[a]	Source	Restr site
163f_Xba	GCCCATGGTCGGTGTCTAGACAAAAACACAAATCCGC	This study	XbaI
163r_Bgl	GAAAATTTGAGATCTGTGAGCGGAGTGAAGGG	This study	BglII
166f_Bgl	CTTAAAAAAGATAGAGAGATCTAAAACCCCTTAACTC	This study	BglII
166r_Hin	CATGTAACCAAGCTTGATGAGCCATATACCGGC	This study	HindIII
VS536D2F	AGAAAAACATAGATCTATAAGACCTG	This study	BglII
VS536D-R	CCATAAGCTTTTGACTTAGCAGTAAG	This study	HindIII
VS536U-F	CACTCTAGATGTAGAATTATTTTTAAAAAACG	This study	XbaI
VS536U-R	GCCCTGAACTAGATCTTTAAAAAC	This study	BglII
PpfrF	GTTTTGGATCCTATTGATGCCAACCC	(Vannini et al., 2012)	BamHI
PpfrR	GTTTTAGATCTTGTCCCATAATTATAGCATA	(Vannini et al., 2012)	BglII
A3.4	CGGGATCCAAAAGATTTTCA	(Danielli et al., 2009)	BamHI
A3.5B	ACTTAGATCTGCAACACAAACTC	(Vannini et al., 2012)	BglII
A3.1B	TCACAGATCTAACGAACGCCTAT	(Vannini et al., 2012)	BglII
A3.3B	AAAAAGATCTAATTCGCAGAAT	(Vannini et al., 2012)	BglII
Lux519F	TATAAGATCTAGTCCTTTTACAATTTGAGC	This study	BglII
VS520RS	ACTAGGATCCAAATTCATGTCATTATAGC	This study	BamHI
VS520RL	TGTGGGATCCATAGTGTTACCTCCATAAG	This study	BamHI
VS530FS	CTTAGGATCCTTTCAGTTATAGTATAG	This study	BamHI
VS530FL	TCCCGGATCCGCGACAGCTTTATTGTTTAG	This study	BamHI
Lux530F2	TGTTTAGATCTTGGTTTGTTGGTTGCAAAAC	(Vannini et al., 2012)	BglII
VS531RS	ATTGAGATCTTGTTTTGATATTATACCATTC	This study	BglII

VS531RL	TATC<u>AGATCT</u>GAAATTCCTTTCAAGAATTAAATTG	This study	BglII
Lux531R2	TAATA<u>GGATCC</u>AAGAATTAAATTGAGAAATTG	(Vannini et al., 2012)	BamHI
VS534FS	CGTA<u>GGATCC</u>TATATTAAAATTATACAATATC	This study	BamHI
VS534F	TATT<u>GGATCC</u>ATCGCTCTTGATCCCTTCAGTG	This study	BamHI
VS534R2	AAATA<u>GATCT</u>ATTAAAACTTTTTTAAATCG	This study	BglII
VS535FS	TTTT<u>GGATCC</u>TATCTCCTAATTATAG	This study	BamHI
VS535F	TAGG<u>GGATCC</u>TTCACAATAGCATACCTAAAG	This study	BamHI
VS535R	AAAA<u>AGATCT</u>CTTATGATTCGTTCAAAAATTTC	This study	BglII
VS536FS	ATCT<u>GGATCC</u>CACAAATCCATTATATAG	This study	BamHI
VS536FL	GGTT<u>GGATCC</u>TTTTGGTTTTTAAAGAAG	This study	BamHI
Lux536F2	AATATA<u>GGATCC</u>AAAGAAGTAGTTCAGGGCG	(Vannini et al., 2012)	BamHI
Lux537R2	TTATA<u>GATCT</u>AAATATCAATACATTTTACC	(Vannini et al., 2012)	BglII
VS537RL	TTGCAA<u>AGATCT</u>TATAGTTTTTGTAACC	This study	BglII
VS543FS	CAAG<u>GGATCC</u>TATTTATCTATGATACTATG	This study	BamHI
VS543F	TTT<u>GGGATCC</u>TTTAATACTCCTCTATTGTTG	This study	BamHI
VS543R	TCAC<u>AGATCT</u>TTTGGCTTGCCCTATTGCTG	This study	BglII
VS546FS	ATT<u>GGGATCC</u>ATCGCTTGAGTATATC	This study	BamHI
VS546F	AAAA<u>GGATCC</u>GCGTTTCCTTTCAAATTGAAATC	This study	BamHI
VS546R	TCTA<u>GGATCC</u>TGCTTAAAATGGAGCTTTATTC	This study	BamHI
VSOrfXFS	TTCT<u>GGATCC</u>AAATTCGTTCATTTTAG	This study	BamHI
VSOrfXFL	TGTT<u>GGATCC</u>GTGAATCACAAACGCTTAATTG	This study	BamHI
VS547RS	CATG<u>AGATCT</u>AACATTACCATTATACCAC	This study	BglII
VS547RL	CGTT<u>AGATCT</u>TGTTTCTCCTTACTATAC	This study	BglII
Lux546F	TATA<u>GGATCC</u>TATATACTTTATGGTAAGC	This study	BamHI
Lux547R	TATA<u>GATCT</u>ACCTAGTTTCATACCTATC	This study	BglII
VSsteDF1	<u>GGATCC</u>GGGGAATTCAGGCTTG	This study	BamHI
VSstemR1	TACAAAGGAGCATAAAATAATAAATATTTTAC	This study	-

[a] Restriction site added for cloning purposes are underlined

Table 6. Oligonucleotides used for primer extension and hybridization assays

Name	Sequence (5'-3')[a]	Source	Target
520pe2	CTAATGAATCATAACGCTTGTC	This study	*cagζ* (HP0520)
530pe1	ACCAAATTTTCATCAATCAAG	This study	*cagV* (HP0530)
531pe4	CATGATGCTCTGTTGTATC	This study	*cagU* (HP0531)
534pe3	GTTTTCGCATGTTATTACTC	This study	*cagS* (HP0534)
535pe1	ATAAGTAGCCACCAATCGCAAAC	This study	*cagQ* (HP0535)
536pe20	TTTGCTAATTTGGTTGTTCC	(Vannini et al., 2012)	*cagP* (HP0536)
536pe17	AACGATTTGTTTGTTTATGC	(Vannini et al., 2012)	*cagP* (HP0536)
537pe8	CTCCAAACGCAACCAATGAG	This study	*cagM* (HP0537)
543pe3	GTTCACGCAAATTTTGTTTC	This study	*cagF* (HP0543)

546pe1	ACAACTTTCTTGTAGCTGTC	This study	*cagC* (HP0546)
OrfX	GCAACTCCATAGACCACTAAAG	(Spohn et al., 1997)	*cagB*
cagN	GTCAATGGTTTCGTTAGTC	(Spohn et al., 1997)	*cagA* (HP0547)
VSLuxC1	CAACCTGGCCGTTAATAATG	This study	*luxC*
VSflgE	GACACCAGACCATAAAGACC	(Spohn and Scarlato, 1999b)	*flgE* (HP0870)
VS906pe7	GGATTAATAGGAGATGGCATG	(Spohn and Scarlato, 1999b)	*fliK* (HP0906)
VSflaB	GCATGAGAAGTTAAAGCGGC	(Spohn and Scarlato, 1999b)	*rpoN* (HP0115)
VS958p1	GGCTCTAAAGAGTCAATTTC	This study	*flgZ* (HP0958)
VSflgB	AAGACCGATAATCCAACGCC	(Spohn and Scarlato, 1999b)	*flgB* (HP1559)

7.1.2 DNA manipulation

DNA amplification, restriction digests and ligations were all carried out with standard molecular techniques (Sambrook, 1989), with enzymes purchased from New England Biolabs. Preparations of plasmid DNA were carried out with a Qiagen Miniprep Spin Kit (Qiagen, Inc.) or a NucleoBond Xtra Midi plasmid purification kit (Macherey-Nagel). DNA fragments for cloning purposes were extracted and purified from agarose gel using a Qiagen Gel Extraction Kit (Qiagen, Inc.)

7.1.3 Construction of an isogenic *arsS⁻* mutant

H. pylori G27-derivative *arsS* knock-out mutant was obtained using a pBluescriptKS(-) vector carrying DNA regions flanking the *arsS* gene (ORF HP0164/HP0165) on the *H. pylori* chromosome, in attrition to a *cat* chloramphenicol resistance cassette. Primers 163f_Xba and 163r_Bgl (Table 5) were used to amplify and clone a 460 bp XbaI-BglII fragment encompassing the region upstream *arsS*, that correspond to 359 bp of the 5' region of the HP0163 open reading frame (ORF), 9 bp of the intergenic region and the 57 bp of the 3' region of HP0164. The primer couple 166f_Bgl and 166r_Hin were used for amplification and cloning of a 616 bp BglII-HindIII fragment encompassing the region downstream *arsS*, that correspond to 585 bp of the 3' region of the HP0166 ORF and 25bp of the intergenic region downstream the HP0165 ORF. The *cat* cassette derived as BglII-BamHI fragment from pBS::*cat* was inserted between these two fragments and the final construct (Table 4) was used to transform *H. pylori*. The chloramphenicol-selected mutant strains (Table 3) were confirmed by PCR.

7.1.4 Construction of an isogenic *cncR1⁻* mutant

H. pylori G27-derivative *cncR1* knock-out mutant was obtained using a pBluescriptKS(-) vector carrying DNA regions flanking the *cncR1*-encoding region (corresponding to the annotated 5'UTR of HP0536) on the *H. pylori* chromosome, as well as a *Campylobacter coli cat* chloramphenicol resistance cassette. Primers VS536U-F and VS536U-R (Table 5) were used for amplification and cloning of a 574 bp Xba-BglII fragment encompassing the region downstream *cncR1*, that correspond to the last 16 bp of *cncR1*, the *cagP* CDS (345 bp) and 213 bp downstream *cagP*. The primer couple VS536D2F and VS536D-R were used to amplify and clone a 442 bp BglII-Hind fragment encompassing the region upstream *cncR1*, that correspond to 85 bp of the divergent P*cagM* promoter, the 5'UTR of *cagM* (37 bp) and the first 320 bp of the *cagM* CDS. The *cat* cassette derived as

BglII-BamHI fragment from pBS::*cat* was inserted between these two fragments and the final construct (Table 4) was used to transform *H. pylori*. The chloramphenicol-selected mutant strains (Table 3) were confirmed by PCR.

7.1.5 Generation of the promoterless *luxCDABE* acceptor strain

To construct the *H. pylori vacA::luxCDABE* acceptor strain, a promoterless *Photorhabdus luminescens luxCDABE* operon cassette was isolated as a 5.8-kb BamHI fragment from plasmid pSB1075 (Winson et al., 1998a; Winson et al., 1998b) (Table 4) and cloned into pPhpn2, a pGEM-T (Promega) derivative containing a 280-bp PCR PstI-BamHI fragment encompassing the intergenic region between *ksgA* (HP1431) and *hpn2* (HP1432), generating pP*hpn2-luxCDABE* (Table 4). A unique EcoRI site in pP*hpn2-luxCDABE* upstream of the *luxCDABE* ribosome binding site (RBS) served to insert the *aphA-3* cassette, conferring kanamycin resistance (Trieu-Cuot et al., 1985). The resulting plasmid was used to recover a 7.3-kb BamHI fragment, encompassing the *aphA-3* and *luxCDABE* operons, which was cloned in the pVAC suicide vector (Delany et al., 2002), generating pVAC::*aphA-3-luxCDABE* (Table 4). This plasmid includes the promoterless *lux* operon and the selectable Km^R marker in divergent orientation, flanked by regions allowing double homologous recombination in the *vacA* locus of *H. pylori* G27. After transformation (as described above), recombinant colonies of the resulting G27 *vacA::aphA-3-luxCDABE* strain (G27*lux* for short) were expanded and confirmed by PCR (Table 3).

7.1.6 Generation of the pVCC transformation vector

Starting from pVAC (Delany et al., 2002), a 779-bp BamHI-HindIII fragment, containing the 3′ end of the *vacA* locus (the right region of homology to *vacA*), was replaced with a 1,045-bp BamHI-HindIII fragment derived from pSB1075, encompassing the 5′ end of the *luxCDABE* operon (the RBS, the translation start, and the first 1,013 bp of the *luxC* cistron), generating pVC (Table 4). A *Campylobacter coli cat* chloramphenicol resistance cassette, derived as a BglII-BamHI fragment from pBS::*cat*, was cloned into the unique BamHI site of pVC, generating pVCC. This vector bears unique BamHI, KpnI, SacI, and SnaBI sites upstream of the *lux* RBS, which can be used to clone promoters of interest through cohesive or blunt-end ligation. The nucleotide sequence of pVCC (Table 4) has been deposited in GenBank under accession number HQ207194.

7.1.7 Generation of the G27 P*pfr-lux* and P*fecA3-lux* reporter strains

The promoter regions of *pfr* (HP0653) and *fecA3* (HP1400) were PCR amplified from *H. pylori* G27 genomic DNA using primer pairs with either BglII or BamHI overhangs and cloned into the unique BamHI site of pVCC. Due to cohesive BglII and BamHI ends, the promoter sequence could be cloned randomly in both directions, disrupting the BamHI site on either end of the insert. This feature was used to check the orientation of the promoter. Constructs with promoters diverging in orientation with respect to the *lux* operon (oppP) were used as negative controls.

The primer couple PpfrF and PpfrR was used for amplification and cloning of the P*pfr* promoter (180 bp), generating pVCC::P*pfr* and pVCC::oppP*pfr*. For the P*fecA3* promoter, several constructs were created: (i) the full-length *fecA3* promoter, encompassing the −10 box, the RBS, and the start codon of *fecA3*, was amplified with oligonucleotides A3.4 and A3.5B and cloned in pVCC, generating pVCC::P*fecA3* and pVCC::oppP*fecA3*; (ii) a 3′-shortened promoter, devoid of the native *fecA3* RBS and start codon, was amplified with oligonucleotides A3.4 and A3.1B, giving rise to pVCC::P*fecA3*SD*lux*; and (iii) a mutant promoter lacking the native *fecA3* RBS and start codon, as well as the OPI NikR operator

responsible for Ni2$^+$-dependent repression of P*fecA3*, was amplified with oligonucleotides A3.4 and A3.3B and cloned, generating pVCC::P*fecA3*SD*lux*-ΔOPI*NikR*. All constructs were checked for correct insertion by sequencing. pVCC derivatives containing wild-type, oppP, and mutant promoters were then used to transform the G27*lux* acceptor strain by double homologous recombination. Positive transformants carrying the *cat* cassette were selected on chloramphenicol and were sensitive to kanamycin due to swapping of the resistance cassette. Finally, a *fur* deletion mutant, carrying the P*pfr-luxCDABE* transcriptional fusion, was obtained by double homologous recombination of the G27 *vacA*::*cat*-P*pfr-luxCDABE* strain with the pFur::km suicide vector (Delany et al., 2001a) and subsequent selection on Km^R/Cm^R Columbia agar plates. pVCC-derivative constructs used for *H. pylori* transformation are enlisted in Table 4 and the corresponding mutant strains are reported in Table 3.

7.1.8 Generation of the reporter strains P*cag-lux* and P*cag*-5'UTR-*lux*

H. pylori G27-derivative strains carrying the transcriptional fusions of the P*cag* promoter regions with the *luxCDABE* operon were obtained with the same procedures described above. For P*cag*ζ, P*cagV*, P*cagS*, P*cagQ*, P*cagM*, P*cagF*, P*cagC*, P*cagB* and P*cagA* promoters, two variants were derived, with or without the 5'untranlsated regions (5'UTRs), respectively. In particular, the P*cag-lux* strains were obtained from PVCC::P*cag-lux* carrying the P*cag* promoter regions and the first 2-6 bases of the of the 5'UTRs cloned upstream the *luxC* gene, while P*cag*-5'UTR-*lux* strains were obtained from the PVCC::P*cag*-5'UTR-*lux* constructs carrying the promoters and theirs corresponding 5'UTR cloned upstream *luxC*. For P*cagU* and P*cagP* promoters, three variants were derived: beside the aforementioned the P*cag-lux* and P*cag*-5'UTR-*lux* strains, the P*cag*-5'UTRtr-*lux* strains were derived, carrying the promoter regions and trunked 5' untranslated regions cloned upstream the *lux* reporter. The detailed description of the pVCC-derivative constructs used for *H. pylori* transformation with the oligonucleotides used for cloning are reported in Table 4, while the corresponding mutant strains are enlisted in Table 3.

Using the phosphorylated oligonucleotides (150 pmol oligos, 1.5 nmol ATP, 2.5U T4 Polynucleotide Kinase, 1X PNK buffer) VSsteDF1 and VSstemR1, and the PVCC::P*cagP* vector as template for a site-direct mutagenic PCR, a DNA fragment was obtained that, after a blunt-end ligation, gave rise to the PVCC::P*cagP*-5'UTRΔterm construct. This vector carries the P*cagP* promoter region plus its 5'UTR deleted in the putative region of intrinsic transcription terminator (29 bp from position 184 to 213 downstream the P*cagP* transcriptional start site) and, after G27*lux* transformation, generated the G27*lux*:: P*cagP*-5'UTRΔterm strain.

7.1.9 Luminometry and data processing

The luminescence of *lux* strains streaked on Columbia agar plates was captured through a Fluoromax Imager (Bio-Rad), with an integration time of 10 min. In the case of liquid cultures growing in flasks and treated with metal ions or chelator, samples of 0.5 to 1.0 ml were taken at regular time intervals, gently pipetted into prewarmed luminometry vials (Promega), and immediately measured in a TD-20/20 luminometer (Turner Designs), with an integration time of 60 s. Data were normalized according to the culture volume and the optical density of the culture by measuring the OD at 600 nm (OD$_{600}$) of the sample with a Beckman spectrophotometer. Luminescence in multiwell plates was assayed in a Victor3V (1420) multilabel reader (Perkin Elmer), with the bottom trail preheated at 37°C. Plates were first shaken with a linear 2-s pulse (shaking diameter, 0.1 mm), thereafter the luminescence of each well was measured with an integration time of 2 s (normal aperture) in the absence of

optical filters. To normalize the data, the optical density was assessed by measuring for 1 s the absorbance of each well through a 595-nm-length continuous-wave lamp filter.

Data sets were processed with Genework 2.0, Wallac, and Excel software. The luminescence and OD values of vials/wells filled with growth medium were used as blank controls and were subtracted from the values of the experimental samples. Three to eight independent replicates were performed for each experiment, and average values and standard deviations were calculated. The threshold of significance was set 3 standard deviations above the average value of the blank controls both for OD and luminescence. Experimental samples with an OD below this threshold were excluded from the analysis; samples with luminescence below the threshold were judged to be negative (null). The luminescence values, normalized according to the OD of the sample, were averaged and plotted on graphs. In the course of the blind test, the maximum value of normalized reporter luminescence, measured at regular time intervals over a period of 72 h, was used to discriminate between weak (repressed) and strong (derepressed) promoters.

7.1.10 RNA preparation (Hot phenol procedure)

Bacterial cells were harvested pipetting 10 ml of liquid cultures into a 15 ml conical tube containing 1.25 ml of ice-cold EtOH/Phenol stop solution (5 % water-saturated phenol pH 4.5 in ethanol). Cells were spun down at 8,000 rpm for 2 min at 4 °C, then bacterial pellets were resuspended in 800 μl of lysis buffer (10 mM Tris-HCl pH 8.0, 1 mM EDTA pH 8.0, 0.5 mg/ml lysozyme) and transferred in 2 ml microfuge tubes. Samples were treated with 80 μl 10% SDS, placed in water bath at 64 °C for 2 min before addition of 88 μl 1 M NaOAc pH5.2 and 1 ml of water saturated phenol pH 4.5. The tubes were incubated in 64 °C water bath for 6 min, inverting 6-10 times every 40 s, than placed on ice to chill and centrifuged at max speed (14,000 rpm) for 10 min at 4 °C. The aqueous layer was transferred to a fresh 2 ml microfuge tube, extracted with 1 ml of chloroform and divided into two 1.5 ml microfuge tubes containing 1/10 volume of 3M NaOAc pH 5.2 and 2 volumes of cold 100% EtOH. Samples were stored at –20 °C. Prior to use, an aliquot of each RNA samples was collected by centrifugation, quantified, and loaded on a 1% agarose gel to assess RNA purity and integrity.

7.1.11 Primer extension analysis

The oligonucleotides used for primer extension reactions are listed in Table 6. The primer (5pmol) was 5'-end labeled using 6 pmol [γ-^{32}P]-ATP (Perkin Elmer) with T4 polynucleotide kinase (NEB) at 37°C for 45 min. Unincorporated radiolabeled nucleotide was removed with a G-50 microspin column (GE Healthcare). Labeled primer (0.1 pmol) was then added to 12 μg of total RNA, 2 μl of 2 mM dNTPs and 2 μl of 5X AMV reverse transcriptase buffer (Promega) to make up a final volume of 9.5 μl. The reaction mixture was incubated at 100°C for 3 min, cooled to 42°C, before addition of 0.5 μl of AMV reverse transcriptase. Reverse transcriptase (5 U, Promega) was added, and incubation continued at 42°C for a further 60 min. After cDNA synthesis, samples were incubated for 10 min at room temperature with 1 μl of RNase A (10μg/μl), extracted once with an equal volume of phenol–chloroform (1:1), ethanol precipitated and resuspended in 5 μl of formamide loading buffer (99% formamide, 0.1% bromophenol blue, 10 mM EDTA pH 8.0). After denaturation at 100°C for 3 min, samples were subjected to electrophoresis on denaturing (6 M urea) 6% polyacrylamide gels in TBE buffer (90 mM Tris, 90 mM boric acid, 2.5 mM EDTA; pH 8.0) at 1600 V, dried and autoradiographed. Signals for quantitative primer extension experiments were acquired with a Storm phosphor-imager (Amersham-GE) and quantified using the Image Quant Software (Molecular Dynamics).

7.1.12 RNA dot blot and Northern blot analysis

For dot blot analysis, 15 μg of RNA was ethanol precipitated, resuspended in 200 μl of RNA denaturing buffer (50% formamide, 7% formaldehyde, 15 mM Na_3-citrate, 150 mM NaCl), denatured at 65°C for 15 min. The samples were chilled on ice, mixed with 400 μl of 20× SSC (1X SSC: 0.15 M NaCl, 0.015 M sodium citrate; pH 7.0), spotted on a Hybond-N+ nylon membrane (Amersham, U.K.) by means of a Bio-Dot microfiltration apparatus (Bio-Rad) and cross-linked to the filter by UV-ray treatment. The filter was prehybridized in 5 ml of hybridization buffer (6X SSC, 5X Denhardt's Solution [0.1% Ficoll 400, 0.1% polyvinylpyrrolidone-90, 0.1% bovine serum albumin], 0.5% SDS, 100 μg/ml denatured fragmented salmon sperm DNA) for 2 h and then hybridized in the same buffer with 1 pmol of radioactively labeled oligonucleotide 958p 51°C for 20 h. The membranes were washed twice for 2 min with wash buffer A (2X SSC, 0.1% SDS) at room temperature, twice for 5 min with wash buffer A at temperatures of hybridization and exposed to Kodak Biomax XAR films for autoradiography.

For Northern blot analysis, samples of total RNA were separated under denaturing conditions in 1.2% agarose–2.1 M formaldehyde-morpholinepropanesulfonic acid gels, stained with ethidium bromide, and transferred to the Hybond-N+ nylon membrane by capillary transfer with 20X SSC buffer. Membranes were treated as described for dot blot experiments. Hybridization reactions were carried out with end-labeled oligonucleotides 536pe17 and 536pe20 at 45°C for 18 h. The Northern blot was washed four times with wash buffer A (2X SSC, 0.1% SDS), twice with wash buffer B (1X SSC, 0.1% SDS) and twice with wash buffer C (0.2X SSC, 0.1% SDS). Each wash was performed for 2 min at room temperature, than the membranes were exposed to X-ray film for autoradiography.

7.1.13 Transcriptome analyses with microarrays

Total RNA was extracted from cells of both wild-type G27 and Δ$cncR1$ strains grown to an OD_{600} of 0.6, by following a hot-phenol extraction procedure described above. Prior to reverse transcription, 60 μg RNAs were treated with 60 U RQ1 RNase-free DNase (Promega) in presence 80 U RNase inhibitor RNasin [Promega] at 37°C for 30 min, phenol-chloroform extracted, and ethanol precipitated. Integrity of the DNA-free RNA was assessed on 1% agarose gels prior to cDNA synthesis and labeling carried out in a thermal cycler (Roche). Forty micrograms of RNA was mixed with 150 pmol random 6-mer hexamers (Invitrogen) for 30-μl reactions, denatured for 3 min at 94°C and annealed for 5 min at 37°C. Then, 20 μl of reverse transcriptase labeling mix (40 U avian myeloblastosis virus reverse transcriptase [Promega], 40 μCi [α-^{33}P]dATP, 80 U RNasin) was added, and reverse transcription was allowed to proceed for 3 h. The reaction was stopped by the addition of 2 μl 0.5 M EDTA, and RNA was degraded by alkaline treatment with 8 μl 1 M NaOH for 15 min at 37°C and thereafter neutralized with 17.5 μl 1 M Tris-HCl (pH 7.5). The cDNAs were purified from unincorporated label by use of Chromaspin-TE spin columns (Clontech) and hybridized to *H. pylori* Panorama ORF arrays (Sigma-Genosys) according to the manufacturer's instructions. Briefly, membranes of gene arrays were prehybridized in hybridization solution (5 X SSPE, 2% SDS, 5X Denhardt's Solution, 100 μg/ml denatured salmon sperm DNA) for 1 h at 65°C, prior to the addition of labeled cDNA. Hybridization was carried out overnight at 65°C, than the membranes were washed with wash solution (0.5 X SSPE, 0.2% SDS) 3 times for 20 min at 65°C and autoradiographed. Each experiment was originated from at least two biological replicates, and each replica was hybridized twice on the arrays. Images were acquired with a Storm phosphorimager (Molecular Dynamics) and the intensities of the spots on the arrays were quantified with Image Quant 5.2 software (Molecular Dynamics), processed with Microsoft Excel, and normalized by expressing values as percentages of the total gene specific intensity. To avoid background noise, spots with levels of intensity of <0.0015% were not considered. For data analysis, genes with

mutant strain/wild-type strain expression ratios of ≥1.5 or ≤−1.5 and Bayesian P values of ≤0.1 were considered to be significantly deregulated.

7.1.14 Overexpression and purification of recombinant His_6-Fur

Recombinant His_6-Fur was overexpressed and purified under native conditions as previously described (Delany et al., 2001b). Thrombin protease (10 U/mg) was used to remove the N-terminal histidine tag according to the instructions of the manufacturer (Amersham GE Healthcare). The purified, untagged protein was dialyzed overnight against the binding buffer (10 mM Tris-Cl, pH 7.85, 50 mM NaCl, 10mM KCl, 0.02% Igepal CA-630, 10% glycerol, 0.1 mM dithiothreitol) prior to the DNA binding experiments. A Bradford colorimetric assay kit (Bio-Rad) was used to quantify the protein fractions with bovine serum albumin as the standard (Sambrook, 1989).

7.1.15 Probe preparation and DNase I footprinting

P*cagAB* probe preparation was carried out with previously described methods (Delany et al., 2001b). Briefly, 1 pmol of pGEM-P*cagAB* vector was linearized with NcoI, dephosphorylated with calf intestinal phosphatase and labeled at the 5′ ends with 2 pmol of $[\gamma\text{-}^{32}P]$ATP (6,000 Ci/mmol; PerkinElmer) by using T4 polynucleotide kinase. The labeled DNA probe was further digested with SalI and the products were separated by native polyacrylamide 6% gel electrophoresis and eluted in 1.5 ml of elution buffer (10 mM Tris-HCl, pH 8.0, 1 mM EDTA, 300 mM sodium acetate, pH 5.2, 0.2% SDS) at 37°C overnight. The eluted probes were then extracted once with an equal volume of phenol–chloroform (1:1), ethanol precipitated and resuspended in 50 ml of milliQ water. The binding reactions between approximately 20 fmol of labeled probe and increasing concentrations of Fur were carried out at room temperature for 15 min in a final volume of 50 μl in the footprinting buffer (10 mM Tris-Cl, pH 7.85, 50 mM NaCl, 10 mM KCl, 0.02% Igepal CA-630, 10% glycerol, 5 mM dithiothreitol) containing an excess of $(NH_4)_2Fe(SO_4)_2$ (150 μM) or 2,2-dipyridyl (150 μM) and with 300 ng of salmon sperm DNA (Invitrogen) as a nonspecific competitor. Afterwards, DNase I (0.08 U), diluted in footprinting buffer 1X containing 10 mM $CaCl_2$ and 5 mM $MgCl_2$ was added to the reaction mixture and digestion was allowed to occur for 85 s. The reaction was stopped by adding 140 μl of stop buffer (192 mM NaOAc pH 5.2, 32 mM EDTA pH 8.0, 0.14 % SDS, 64 μg/ml sonicated salmon sperm DNA), extracted once with an equal volume of phenol–chloroform (1:1), ethanol precipitated and resuspended in 5 μl of formamide loading buffer. Samples were denatured at 100°C for 3 min, separated on 8 M urea-6% acrylamide sequencing gels in TBE buffer and autoradiographed. A modified G+A sequencing ladder protocol (Liu and Hong, 1998) was employed to map the binding sites.

7.1.16 AGS cell culture and infection assay

AGS cells, a human adenocarcinoma epithelial cell line (ATCC CRL 1739), were grown in RPMI-1650 medium with 10% fetal bovine serum (FBS) in tissue-culture flasks. For the infection assay, cells were seeded in 24-well plates (Orange Scientific) and cultured for 1-2 days to reach 60-80% confluency. Before infection, the medium was replaced with fresh RPMI-1650 with 5% FBS conditioned in the bacterial incubator (9% CO_2, 91% air atmosphere, and 95% humidity). Cells were infected with P*cag-lux* strains at a multiplicity of infection (MOI) of 5, while other 24-well plates filled with medium but without AGS cells were inoculated with the same amount of bacterial cells and used as control samples. The plates were placed inside the bacterial incubator and luminescence was measured at regular time intervals with Victor3V (1420) multilabel reader (Perkin Elmer), with bottom trail pre heated at 37°C. Luminescence was measured with an integration time of 2 seconds (normal

aperture) in the absence of optical filters. The luminescence values of wells filled with plain growth medium were used as blank controls and subtracted from the values of the experimental samples. Each infection assay was performed in quadruplicate and the assay was repeated in three to six independent experiment. Average values and standard deviations were calculated.

7.1.17 Bioinformatic analyses

The RNAfold online program was used to predict the secondary structure of RNA sequences.
http://rna.tbi.univie.ac.at/cgi-bin/RNAfold.cgi

The online resource RNAtarget was employed to identify putative targets of the *cncR1* sRNA through the identification of low-hybridization energy short base-pairing.
http://cs.wellesley.edu/~btjaden/TargetRNA2/

The RNAhybrid online program was used to identify long discontinued base pairing between *cncR1* sRNA and mRNAs target.
http://bibiserv.techfak.uni-bielefeld.de/rnahybrid/submission.html

REFERENCES

Abraham, L.O., Li, Y., and Zamble, D.B. (2006). The metal- and DNA-binding activities of Helicobacter pylori NikR. Journal of inorganic biochemistry *100*, 1005-1014.

Aiba, H. (2007). Mechanism of RNA silencing by Hfq-binding small RNAs. Current opinion in microbiology *10*, 134-139.

Akada, J.K., Shirai, M., Takeuchi, H., Tsuda, M., and Nakazawa, T. (2000). Identification of the urease operon in Helicobacter pylori and its control by mRNA decay in response to pH. Molecular microbiology *36*, 1071-1084.

Akopyants, N.S., Clifton, S.W., Kersulyte, D., Crabtree, J.E., Youree, B.E., Reece, C.A., Bukanov, N.O., Drazek, E.S., Roe, B.A., and Berg, D.E. (1998). Analyses of the cag pathogenicity island of Helicobacter pylori. Molecular microbiology *28*, 37-53.

Al-Ghoul, L., Wessler, S., Hundertmark, T., Kruger, S., Fischer, W., Wunder, C., Haas, R., Roessner, A., and Naumann, M. (2004). Analysis of the type IV secretion system-dependent cell motility of Helicobacter pylori-infected epithelial cells. Biochemical and biophysical research communications *322*, 860-866.

Allan, E., Clayton, C.L., McLaren, A., Wallace, D.M., and Wren, B.W. (2001). Characterization of the low-pH responses of Helicobacter pylori using genomic DNA arrays. Microbiology *147*, 2285-2292.

Allen, K.J., and Griffiths, M.W. (2001). Effect of environmental and chemotactic stimuli on the activity of the Campylobacter jejuni flaA sigma(28) promoter. FEMS microbiology letters *205*, 43-48.

Allison, C.C., Kufer, T.A., Kremmer, E., Kaparakis, M., and Ferrero, R.L. (2009). Helicobacter pylori induces MAPK phosphorylation and AP-1 activation via a NOD1-dependent mechanism. Journal of immunology *183*, 8099-8109.

Alm, R.A., Ling, L.S., Moir, D.T., King, B.L., Brown, E.D., Doig, P.C., Smith, D.R., Noonan, B., Guild, B.C., deJonge, B.L.*, et al.* (1999). Genomic-sequence comparison of two unrelated isolates of the human gastric pathogen Helicobacter pylori. Nature *397*, 176-180.

Alvarez-Martinez, C.E., and Christie, P.J. (2009). Biological diversity of prokaryotic type IV secretion systems. Microbiol Mol Biol Rev *73*, 775-808.

Amieva, M.R., and El-Omar, E.M. (2008). Host-bacterial interactions in Helicobacter pylori infection. Gastroenterology *134*, 306-323.

Andrzejewska, J., Lee, S.K., Olbermann, P., Lotzing, N., Katzowitsch, E., Linz, B., Achtman, M., Kado, C.I., Suerbaum, S., and Josenhans, C. (2006). Characterization of the pilin ortholog of the Helicobacter pylori type IV cag pathogenicity apparatus, a surface-associated protein expressed during infection. Journal of bacteriology *188*, 5865-5877.

Azuma, T., Yamakawa, A., Yamazaki, S., Ohtani, M., Ito, Y., Muramatsu, A., Suto, H., Yamazaki, Y., Keida, Y., Higashi, H.*, et al.* (2004). Distinct diversity of the cag pathogenicity island among Helicobacter pylori strains in Japan. Journal of clinical microbiology *42*, 2508-2517.

Backert, S., Fronzes, R., and Waksman, G. (2008). VirB2 and VirB5 proteins: specialized adhesins in bacterial type-IV secretion systems? Trends in microbiology *16*, 409-413.

Backert, S., and Meyer, T.F. (2006). Type IV secretion systems and their effectors in bacterial pathogenesis. Current opinion in microbiology *9*, 207-217.

Backert, S., Moese, S., Selbach, M., Brinkmann, V., and Meyer, T.F. (2001). Phosphorylation of tyrosine 972 of the Helicobacter pylori CagA protein is essential for induction of a scattering phenotype in gastric epithelial cells. Molecular microbiology *42*, 631-644.

Backert, S., and Selbach, M. (2005). Tyrosine-phosphorylated bacterial effector proteins: the enemies within. Trends in microbiology *13*, 476-484.

Backert, S., and Selbach, M. (2008). Role of type IV secretion in Helicobacter pylori pathogenesis. Cellular microbiology *10*, 1573-1581.

Backert, S., Tegtmeyer, N., and Selbach, M. (2010). The versatility of Helicobacter pylori CagA effector protein functions: The master key hypothesis. Helicobacter *15*, 163-176.

Balazsi, G., and Oltvai, Z.N. (2005). Sensing your surroundings: how transcription-regulatory networks of the cell discern environmental signals. Sci STKE *2005*, pe20.

Baltrus, D.A., Amieva, M.R., Covacci, A., Lowe, T.M., Merrell, D.S., Ottemann, K.M., Stein, M., Salama, N.R., and Guillemin, K. (2009). The complete genome sequence of Helicobacter pylori strain G27. Journal of bacteriology *191*, 447-448.

Barnard, F.M., Loughlin, M.F., Fainberg, H.P., Messenger, M.P., Ussery, D.W., Williams, P., and Jenks, P.J. (2004). Global regulation of virulence and the stress response by CsrA in the highly adapted human gastric pathogen Helicobacter pylori. Molecular microbiology *51*, 15-32.

Barrick, J.E., Sudarsan, N., Weinberg, Z., Ruzzo, W.L., and Breaker, R.R. (2005). 6S RNA is a widespread regulator of eubacterial RNA polymerase that resembles an open promoter. Rna *11*, 774-784.

Benanti, E.L., and Chivers, P.T. (2007). The N-terminal arm of the Helicobacter pylori Ni2+-dependent transcription factor NikR is required for specific DNA binding. J Biol Chem *282*, 20365-20375.

Bereswill, S., Greiner, S., van Vliet, A.H., Waidner, B., Fassbinder, F., Schiltz, E., Kusters, J.G., and Kist, M. (2000). Regulation of ferritin-mediated cytoplasmic iron storage by the ferric uptake regulator homolog (Fur) of Helicobacter pylori. Journal of bacteriology *182*, 5948-5953.

Bereswill, S., Lichte, F., Vey, T., Fassbinder, F., and Kist, M. (1998). Cloning and characterization of the fur gene from Helicobacter pylori. FEMS microbiology letters *159*, 193-200.

Bijlsma, J.J., Waidner, B., Vliet, A.H., Hughes, N.J., Hag, S., Bereswill, S., Kelly, D.J., Vandenbroucke-Grauls, C.M., Kist, M., and Kusters, J.G. (2002). The Helicobacter pylori homologue of the ferric uptake regulator is involved in acid resistance. Infection and immunity *70*, 606-611.

Blaser, M.J. (1990). Helicobacter pylori and the pathogenesis of gastroduodenal inflammation. The Journal of infectious diseases *161*, 626-633.

Boisset, S., Geissmann, T., Huntzinger, E., Fechter, P., Bendridi, N., Possedko, M., Chevalier, C., Helfer, A.C., Benito, Y., Jacquier, A*., et al.* (2007). Staphylococcus aureus RNAIII coordinately represses the synthesis of virulence factors and the transcription regulator Rot by an antisense mechanism. Genes Dev *21*, 1353-1366.

Boneca, I.G., Ecobichon, C., Chaput, C., Mathieu, A., Guadagnini, S., Prevost, M.C., Colland, F., Labigne, A., and de Reuse, H. (2008). Development of inducible

systems to engineer conditional mutants of essential genes of Helicobacter pylori. Applied and environmental microbiology *74*, 2095-2102.

Boonjakuakul, J.K., Canfield, D.R., and Solnick, J.V. (2005). Comparison of Helicobacter pylori virulence gene expression in vitro and in the Rhesus macaque. Infection and immunity *73*, 4895-4904.

Boonjakuakul, J.K., Syvanen, M., Suryaprasad, A., Bowlus, C.L., and Solnick, J.V. (2004). Transcription profile of Helicobacter pylori in the human stomach reflects its physiology in vivo. The Journal of infectious diseases *190*, 946-956.

Boughan, P.K., Argent, R.H., Body-Malapel, M., Park, J.H., Ewings, K.E., Bowie, A.G., Ong, S.J., Cook, S.J., Sorensen, O.E., Manzo, B.A.*, et al.* (2006). Nucleotide-binding oligomerization domain-1 and epidermal growth factor receptor: critical regulators of beta-defensins during Helicobacter pylori infection. J Biol Chem *281*, 11637-11648.

Bourzac, K.M., and Guillemin, K. (2005). Helicobacter pylori-host cell interactions mediated by type IV secretion. Cellular microbiology *7*, 911-919.

Bouvard, V., Baan, R., Straif, K., Grosse, Y., Secretan, B., El Ghissassi, F., Benbrahim-Tallaa, L., Guha, N., Freeman, C., Galichet, L.*, et al.* (2009). A review of human carcinogens--Part B: biological agents. Lancet Oncol *10*, 321-322.

Brahmachary, P., Dashti, M.G., Olson, J.W., and Hoover, T.R. (2004). Helicobacter pylori FlgR is an enhancer-independent activator of sigma54-RNA polymerase holoenzyme. Journal of bacteriology *186*, 4535-4542.

Brandt, S., Kwok, T., Hartig, R., Konig, W., and Backert, S. (2005). NF-kappaB activation and potentiation of proinflammatory responses by the Helicobacter pylori CagA protein. Proceedings of the National Academy of Sciences of the United States of America *102*, 9300-9305.

Brennan, R.G., and Link, T.M. (2007). Hfq structure, function and ligand binding. Current opinion in microbiology *10*, 125-133.

Buhrdorf, R., Forster, C., Haas, R., and Fischer, W. (2003). Topological analysis of a putative virB8 homologue essential for the cag type IV secretion system in Helicobacter pylori. International journal of medical microbiology : IJMM *293*, 213-217.

Bundock, P., den Dulk-Ras, A., Beijersbergen, A., and Hooykaas, P.J. (1995). Trans-kingdom T-DNA transfer from Agrobacterium tumefaciens to Saccharomyces cerevisiae. The EMBO journal *14*, 3206-3214.

Busler, V.J., Torres, V.J., McClain, M.S., Tirado, O., Friedman, D.B., and Cover, T.L. (2006). Protein-protein interactions among Helicobacter pylori cag proteins. Journal of bacteriology *188*, 4787-4800.

Caron, M.P., Lafontaine, D.A., and Masse, E. (2010). Small RNA-mediated regulation at the level of transcript stability. RNA biology *7*, 140-144.

Carpenter, B.M., Gancz, H., Gonzalez-Nieves, R.P., West, A.L., Whitmire, J.M., Michel, S.L., and Merrell, D.S. (2009). A single nucleotide change affects fur-dependent regulation of sodB in H. pylori. PLoS One *4*, e5369.

Carpenter, B.M., McDaniel, T.K., Whitmire, J.M., Gancz, H., Guidotti, S., Censini, S., and Merrell, D.S. (2007). Expanding the Helicobacter pylori genetic toolbox:

modification of an endogenous plasmid for use as a transcriptional reporter and complementation vector. Applied and environmental microbiology *73*, 7506-7514.

Cascales, E., and Christie, P.J. (2003). The versatile bacterial type IV secretion systems. Nature reviews Microbiology *1*, 137-149.

Castillo, A.R., Arevalo, S.S., Woodruff, A.J., and Ottemann, K.M. (2008). Experimental analysis of Helicobacter pylori transcriptional terminators suggests this microbe uses both intrinsic and factor-dependent termination. Molecular microbiology *67*, 155-170.

Cendron, L.Z., G. (2011). Structural and functional aspects of unique type IV secretory components in the Helicobacter pylori cag pathogenicity island. FEBS J *278*, 9.

Chao, Y., and Vogel, J. (2010). The role of Hfq in bacterial pathogens. Current opinion in microbiology *13*, 24-33.

Chevalier, C., Huntzinger, E., Fechter, P., Boisset, S., Vandenesch, F., Romby, P., and Geissmann, T. (2008). Staphylococcus aureus endoribonuclease III purification and properties. Methods Enzymol *447*, 309-327.

Choi, Y.W., Park, S.A., Lee, H.W., Kim, D.S., and Lee, N.G. (2008). Analysis of growth phase-dependent proteome profiles reveals differential regulation of mRNA and protein in Helicobacter pylori. Proteomics *8*, 2665-2675.

Christie, P.J. (1997). Agrobacterium tumefaciens T-complex transport apparatus: a paradigm for a new family of multifunctional transporters in eubacteria. Journal of bacteriology *179*, 3085-3094.

Churin, Y., Al-Ghoul, L., Kepp, O., Meyer, T.F., Birchmeier, W., and Naumann, M. (2003). Helicobacter pylori CagA protein targets the c-Met receptor and enhances the motogenic response. The Journal of cell biology *161*, 249-255.

Churin, Y., Kardalinou, E., Meyer, T.F., and Naumann, M. (2001). Pathogenicity island-dependent activation of Rho GTPases Rac1 and Cdc42 in Helicobacter pylori infection. Molecular microbiology *40*, 815-823.

Contreras, M., Thiberge, J.M., Mandrand-Berthelot, M.A., and Labigne, A. (2003). Characterization of the roles of NikR, a nickel-responsive pleiotropic autoregulator of Helicobacter pylori. Molecular microbiology *49*, 947-963.

Corbel, M.J. (1997). Brucellosis: an overview. Emerging infectious diseases *3*, 213-221.

Cormack, B.P., Valdivia, R.H., and Falkow, S. (1996). FACS-optimized mutants of the green fluorescent protein (GFP). Gene *173*, 33-38.

Couturier, M.R., Tasca, E., Montecucco, C., and Stein, M. (2006). Interaction with CagF is required for translocation of CagA into the host via the Helicobacter pylori type IV secretion system. Infection and immunity *74*, 273-281.

Covacci, A., Censini, S., Bugnoli, M., Petracca, R., Burroni, D., Macchia, G., Massone, A., Papini, E., Xiang, Z., Figura, N.*, et al.* (1993). Molecular characterization of the 128-kDa immunodominant antigen of Helicobacter pylori associated with cytotoxicity and duodenal ulcer. Proceedings of the National Academy of Sciences of the United States of America *90*, 5791-5795.

Cover, T.L., Tummuru, M.K., Cao, P., Thompson, S.A., and Blaser, M.J. (1994). Divergence of genetic sequences for the vacuolating cytotoxin among Helicobacter pylori strains. J Biol Chem *269*, 10566-10573.

Croxen, M.A., Sisson, G., Melano, R., and Hoffman, P.S. (2006). The Helicobacter pylori chemotaxis receptor TlpB (HP0103) is required for pH taxis and for colonization of the gastric mucosa. Journal of bacteriology *188*, 2656-2665.

Cussac, V., Ferrero, R.L., and Labigne, A. (1992). Expression of Helicobacter pylori urease genes in Escherichia coli grown under nitrogen-limiting conditions. Journal of bacteriology *174*, 2466-2473.

Danielli, A., Amore, G., and Scarlato, V. (2010). Built shallow to maintain homeostasis and persistent infection: insight into the transcriptional regulatory network of the gastric human pathogen Helicobacter pylori. PLoS pathogens *6*, e1000938.

Danielli, A., Romagnoli, S., Roncarati, D., Costantino, L., Delany, I., and Scarlato, V. (2009). Growth phase and metal-dependent transcriptional regulation of the fecA genes in Helicobacter pylori. Journal of bacteriology *191*, 3717-3725.

Danielli, A., Roncarati, D., Delany, I., Chiarini, V., Rappuoli, R., and Scarlato, V. (2006). In vivo dissection of the Helicobacter pylori Fur regulatory circuit by genome-wide location analysis. Journal of bacteriology *188*, 4654-4662.

de Reuse, H., and Bereswill, S. (2007). Ten years after the first Helicobacter pylori genome: comparative and functional genomics provide new insights in the variability and adaptability of a persistent pathogen. FEMS immunology and medical microbiology *50*, 165-176.

Delany, I., Pacheco, A.B., Spohn, G., Rappuoli, R., and Scarlato, V. (2001a). Iron-dependent transcription of the frpB gene of Helicobacter pylori is controlled by the Fur repressor protein. Journal of bacteriology *183*, 4932-4937.

Delany, I., Spohn, G., Rappuoli, R., and Scarlato, V. (2001b). The Fur repressor controls transcription of iron-activated and -repressed genes in Helicobacter pylori. Molecular microbiology *42*, 1297-1309.

Delany, I., Spohn, G., Rappuoli, R., and Scarlato, V. (2002). Growth phase-dependent regulation of target gene promoters for binding of the essential orphan response regulator HP1043 of Helicobacter pylori. Journal of bacteriology *184*, 4800-4810.

Dietz, P., Gerlach, G., and Beier, D. (2002). Identification of target genes regulated by the two-component system HP166-HP165 of Helicobacter pylori. Journal of bacteriology *184*, 350-362.

Ding, W., Wang, H., and Griffiths, M.W. (2005). Probiotics down-regulate flaA sigma28 promoter in Campylobacter jejuni. Journal of food protection *68*, 2295-2300.

Douillard, F.P., Ryan, K.A., Hinds, J., and O'Toole, P.W. (2009). Effect of FliK mutation on the transcriptional activity of the {sigma}54 sigma factor RpoN in Helicobacter pylori. Microbiology *155*, 1901-1911.

Dreiseikelmann, B. (1994). Translocation of DNA across bacterial membranes. Microbiol Rev *58*, 293-316.

Du, M.Q., and Isaccson, P.G. (2002). Gastric MALT lymphoma: from aetiology to treatment. Lancet Oncol *3*, 97-104.

Dunn, B.E., Cohen, H., and Blaser, M.J. (1997). Helicobacter pylori. Clin Microbiol Rev *10*, 720-741.

Eaton, K.A., Gilbert, J.V., Joyce, E.A., Wanken, A.E., Thevenot, T., Baker, P., Plaut, A., and Wright, A. (2002). In vivo complementation of ureB restores the ability of Helicobacter pylori to colonize. Infection and immunity *70*, 771-778.

Eaton, K.A., Suerbaum, S., Josenhans, C., and Krakowka, S. (1996). Colonization of gnotobiotic piglets by Helicobacter pylori deficient in two flagellin genes. Infection and immunity *64*, 2445-2448.

Ellermeier, C.D., Ellermeier, J.R., and Slauch, J.M. (2005). HilD, HilC and RtsA constitute a feed forward loop that controls expression of the SPI1 type three secretion system regulator hilA in Salmonella enterica serovar Typhimurium. Molecular microbiology *57*, 691-705.

Ernst, F.D., Bereswill, S., Waidner, B., Stoof, J., Mader, U., Kusters, J.G., Kuipers, E.J., Kist, M., van Vliet, A.H., and Homuth, G. (2005a). Transcriptional profiling of Helicobacter pylori Fur- and iron-regulated gene expression. Microbiology *151*, 533-546.

Ernst, F.D., Homuth, G., Stoof, J., Mader, U., Waidner, B., Kuipers, E.J., Kist, M., Kusters, J.G., Bereswill, S., and van Vliet, A.H. (2005b). Iron-responsive regulation of the Helicobacter pylori iron-cofactored superoxide dismutase SodB is mediated by Fur. Journal of bacteriology *187*, 3687-3692.

Ernst, F.D., Kuipers, E.J., Heijens, A., Sarwari, R., Stoof, J., Penn, C.W., Kusters, J.G., and van Vliet, A.H. (2005c). The nickel-responsive regulator NikR controls activation and repression of gene transcription in Helicobacter pylori. Infection and immunity *73*, 7252-7258.

Ernst, F.D., Stoof, J., Horrevoets, W.M., Kuipers, E.J., Kusters, J.G., and van Vliet, A.H. (2006). NikR mediates nickel-responsive transcriptional repression of the Helicobacter pylori outer membrane proteins FecA3 (HP1400) and FrpB4 (HP1512). Infection and immunity *74*, 6821-6828.

Faucher, S.P., Friedlander, G., Livny, J., Margalit, H., and Shuman, H.A. (2010). Legionella pneumophila 6S RNA optimizes intracellular multiplication. Proceedings of the National Academy of Sciences of the United States of America *107*, 7533-7538.

Fehri, L.F., Rechner, C., Janssen, S., Mak, T.N., Holland, C., Bartfeld, S., Bruggemann, H., and Meyer, T.F. (2009). Helicobacter pylori-induced modification of the histone H3 phosphorylation status in gastric epithelial cells reflects its impact on cell cycle regulation. Epigenetics : official journal of the DNA Methylation Society *4*, 577-586.

Fischer, W. (2011). Assembly and molecular mode of action of the Helicobacter pylori Cag type IV secretion apparatus. The FEBS journal *278*, 1203-1212.

Fischer, W., Puls, J., Buhrdorf, R., Gebert, B., Odenbreit, S., and Haas, R. (2001). Systematic mutagenesis of the Helicobacter pylori cag pathogenicity island: essential genes for CagA translocation in host cells and induction of interleukin-8. Molecular microbiology *42*, 1337-1348.

Fischer, W., Windhager, L., Rohrer, S., Zeiller, M., Karnholz, A., Hoffmann, R., Zimmer, R., and Haas, R. (2010). Strain-specific genes of Helicobacter pylori: genome evolution driven by a novel type IV secretion system and genomic island transfer. Nucleic Acids Res *38*, 6089-6101.

Foynes, S., Dorrell, N., Ward, S.J., Stabler, R.A., McColm, A.A., Rycroft, A.N., and Wren, B.W. (2000). Helicobacter pylori possesses two CheY response regulators and a

histidine kinase sensor, CheA, which are essential for chemotaxis and colonization of the gastric mucosa. Infection and immunity *68*, 2016-2023.

Fronzes, R., Schafer, E., Wang, L., Saibil, H.R., Orlova, E.V., and Waksman, G. (2009). Structure of a type IV secretion system core complex. Science *323*, 266-268.

Gancz, H., Censini, S., and Merrell, D.S. (2006). Iron and pH homeostasis intersect at the level of Fur regulation in the gastric pathogen Helicobacter pylori. Infection and immunity *74*, 602-614.

Gerrits, M.M., van Vliet, A.H., Kuipers, E.J., and Kusters, J.G. (2006). Helicobacter pylori and antimicrobial resistance: molecular mechanisms and clinical implications. Lancet Infect Dis *6*, 699-709.

Giedroc, D.P., and Arunkumar, A.I. (2007). Metal sensor proteins: nature's metalloregulated allosteric switches. Dalton transactions, 3107-3120.

Gieseler, S., Konig, B., Konig, W., and Backert, S. (2005). Strain-specific expression profiles of virulence genes in Helicobacter pylori during infection of gastric epithelial cells and granulocytes. Microbes and infection / Institut Pasteur *7*, 437-447.

Gottesman, S. (2005). Micros for microbes: non-coding regulatory RNAs in bacteria. Trends in genetics : TIG *21*, 399-404.

Grohmann, E., Muth, G., and Espinosa, M. (2003). Conjugative plasmid transfer in gram-positive bacteria. Microbiol Mol Biol Rev *67*, 277-301, table of contents.

Hakkila, K., Maksimow, M., Karp, M., and Virta, M. (2002). Reporter genes lucFF, luxCDABE, gfp, and dsred have different characteristics in whole-cell bacterial sensors. Analytical biochemistry *301*, 235-242.

Hamilton, H.L., Dominguez, N.M., Schwartz, K.J., Hackett, K.T., and Dillard, J.P. (2005). Neisseria gonorrhoeae secretes chromosomal DNA via a novel type IV secretion system. Molecular microbiology *55*, 1704-1721.

Hanahan, D. (1983). Studies on transformation of Escherichia coli with plasmids. Journal of molecular biology *166*, 557-580.

Handa, O., Naito, Y., and Yoshikawa, T. (2007). CagA protein of Helicobacter pylori: a hijacker of gastric epithelial cell signaling. Biochemical pharmacology *73*, 1697-1702.

Hatakeyama, M. (2008). Linking epithelial polarity and carcinogenesis by multitasking Helicobacter pylori virulence factor CagA. Oncogene *27*, 7047-7054.

Hatakeyama, M., and Higashi, H. (2005). Helicobacter pylori CagA: a new paradigm for bacterial carcinogenesis. Cancer science *96*, 835-843.

Hohlfeld, S., Pattis, I., Puls, J., Plano, G.V., Haas, R., and Fischer, W. (2006). A C-terminal translocation signal is necessary, but not sufficient for type IV secretion of the Helicobacter pylori CagA protein. Molecular microbiology *59*, 1624-1637.

Homuth, G., Domm, S., Kleiner, D., and Schumann, W. (2000). Transcriptional analysis of major heat shock genes of Helicobacter pylori. Journal of bacteriology *182*, 4257-4263.

Huntzinger, E., Boisset, S., Saveanu, C., Benito, Y., Geissmann, T., Namane, A., Lina, G., Etienne, J., Ehresmann, B., Ehresmann, C*., et al.* (2005). Staphylococcus aureus

RNAIII and the endoribonuclease III coordinately regulate spa gene expression. The EMBO journal *24*, 824-835.

Jimenez-Soto, L.F., Kutter, S., Sewald, X., Ertl, C., Weiss, E., Kapp, U., Rohde, M., Pirch, T., Jung, K., Retta, S.F.*, et al.* (2009). Helicobacter pylori type IV secretion apparatus exploits beta1 integrin in a novel RGD-independent manner. PLoS pathogens *5*, e1000684.

Josenhans, C., Beier, D., Linz, B., Meyer, T.F., and Suerbaum, S. (2007). Pathogenomics of helicobacter. International journal of medical microbiology : IJMM *297*, 589-600.

Josenhans, C., Friedrich, S., and Suerbaum, S. (1998). Green fluorescent protein as a novel marker and reporter system in Helicobacter sp. FEMS microbiology letters *161*, 263-273.

Josenhans, C., Niehus, E., Amersbach, S., Horster, A., Betz, C., Drescher, B., Hughes, K.T., and Suerbaum, S. (2002). Functional characterization of the antagonistic flagellar late regulators FliA and FlgM of Helicobacter pylori and their effects on the H. pylori transcriptome. Molecular microbiology *43*, 307-322.

Josenhans, C., and Suerbaum, S. (2002). The role of motility as a virulence factor in bacteria. International journal of medical microbiology : IJMM *291*, 605-614.

Joyce, E.A., Gilbert, J.V., Eaton, K.A., Plaut, A., and Wright, A. (2001). Differential gene expression from two transcriptional units in the cag pathogenicity island of Helicobacter pylori. Infection and immunity *69*, 4202-4209.

Judd, P.K., Kumar, R.B., and Das, A. (2005). Spatial location and requirements for the assembly of the Agrobacterium tumefaciens type IV secretion apparatus. Proceedings of the National Academy of Sciences of the United States of America *102*, 11498-11503.

Kaparakis, M., Turnbull, L., Carneiro, L., Firth, S., Coleman, H.A., Parkington, H.C., Le Bourhis, L., Karrar, A., Viala, J., Mak, J.*, et al.* (2010). Bacterial membrane vesicles deliver peptidoglycan to NOD1 in epithelial cells. Cellular microbiology *12*, 372-385.

Karita, M., Tummuru, M.K., Wirth, H.P., and Blaser, M.J. (1996). Effect of growth phase and acid shock on Helicobacter pylori cagA expression. Infection and immunity *64*, 4501-4507.

Kassem, II, Sanad, Y., Gangaiah, D., Lilburn, M., Lejeune, J., and Rajashekara, G. (2010). Use of bioluminescence imaging to monitor Campylobacter survival in chicken litter. Journal of applied microbiology *109*, 1988-1997.

Kavermann, H., Burns, B.P., Angermuller, K., Odenbreit, S., Fischer, W., Melchers, K., and Haas, R. (2003). Identification and characterization of Helicobacter pylori genes essential for gastric colonization. J Exp Med *197*, 813-822.

Keates, S., Keates, A.C., Warny, M., Peek, R.M., Jr., Murray, P.G., and Kelly, C.P. (1999). Differential activation of mitogen-activated protein kinases in AGS gastric epithelial cells by cag+ and cag- Helicobacter pylori. Journal of immunology *163*, 5552-5559.

Keates, S., Sougioultzis, S., Keates, A.C., Zhao, D., Peek, R.M., Jr., Shaw, L.M., and Kelly, C.P. (2001). cag+ Helicobacter pylori induce transactivation of the epidermal growth factor receptor in AGS gastric epithelial cells. J Biol Chem *276*, 48127-48134.

Kelana, L.C., and Griffiths, M.W. (2003). Use of an autobioluminescent Campylobacter jejuni to monitor cell survival as a function of temperature, pH, and sodium chloride. Journal of food protection *66*, 2032-2037.

Kim, N., Marcus, E.A., Wen, Y., Weeks, D.L., Scott, D.R., Jung, H.C., Song, I.S., and Sachs, G. (2004). Genes of Helicobacter pylori regulated by attachment to AGS cells. Infection and immunity *72*, 2358-2368.

Kim, S.Y., Lee, Y.C., Kim, H.K., and Blaser, M.J. (2006). Helicobacter pylori CagA transfection of gastric epithelial cells induces interleukin-8. Cellular microbiology *8*, 97-106.

Kutter, S., Buhrdorf, R., Haas, J., Schneider-Brachert, W., Haas, R., and Fischer, W. (2008). Protein subassemblies of the Helicobacter pylori Cag type IV secretion system revealed by localization and interaction studies. Journal of bacteriology *190*, 2161-2171.

Kwok, T., Zabler, D., Urman, S., Rohde, M., Hartig, R., Wessler, S., Misselwitz, R., Berger, J., Sewald, N., Konig, W.*, et al.* (2007). Helicobacter exploits integrin for type IV secretion and kinase activation. Nature *449*, 862-866.

Lai, E.M., and Kado, C.I. (2000). The T-pilus of Agrobacterium tumefaciens. Trends in microbiology *8*, 361-369.

Lamb, A., Yang, X.D., Tsang, Y.H., Li, J.D., Higashi, H., Hatakeyama, M., Peek, R.M., Blanke, S.R., and Chen, L.F. (2009). Helicobacter pylori CagA activates NF-kappaB by targeting TAK1 for TRAF6-mediated Lys 63 ubiquitination. EMBO reports *10*, 1242-1249.

Lasa, I., Toledo-Arana, A., Dobin, A., Villanueva, M., de los Mozos, I.R., Vergara-Irigaray, M., Segura, V., Fagegaltier, D., Penades, J.R., Valle, J.*, et al.* (2011). Genome-wide antisense transcription drives mRNA processing in bacteria. Proceedings of the National Academy of Sciences of the United States of America *108*, 20172-20177.

Lawley, T.D., Klimke, W.A., Gubbins, M.J., and Frost, L.S. (2003). F factor conjugation is a true type IV secretion system. FEMS microbiology letters *224*, 1-15.

Lessl, M., and Lanka, E. (1994). Common mechanisms in bacterial conjugation and Ti-mediated T-DNA transfer to plant cells. Cell *77*, 321-324.

Lessl, M., Pansegrau, W., and Lanka, E. (1992). Relationship of DNA-transfer-systems: essential transfer factors of plasmids RP4, Ti and F share common sequences. Nucleic Acids Res *20*, 6099-6100.

Li, Y., and Zamble, D.B. (2009). pH-responsive DNA-binding activity of Helicobacter pylori NikR. Biochemistry *48*, 2486-2496.

Liu, S.T., and Hong, G.F. (1998). Three-minute G + A specific reaction for DNA sequencing. Analytical biochemistry *255*, 158-159.

Macnab, R.M. (2003). How bacteria assemble flagella. Annu Rev Microbiol *57*, 77-100.

Madan Babu, M., Teichmann, S.A., and Aravind, L. (2006). Evolutionary dynamics of prokaryotic transcriptional regulatory networks. Journal of molecular biology *358*, 614-633.

Marais, A., Mendz, G.L., Hazell, S.L., and Megraud, F. (1999). Metabolism and genetics of Helicobacter pylori: the genome era. Microbiol Mol Biol Rev *63*, 642-674.

Marshall, B.J., and Warren, J.R. (1984). Unidentified curved bacilli in the stomach of patients with gastritis and peptic ulceration. Lancet *1*, 1311-1315.

Mathy, N., Hebert, A., Mervelet, P., Benard, L., Dorleans, A., Li de la Sierra-Gallay, I., Noirot, P., Putzer, H., and Condon, C. (2010). Bacillus subtilis ribonucleases J1 and J2 form a complex with altered enzyme behaviour. Molecular microbiology *75*, 489-498.

Matsumoto, Y., Marusawa, H., Kinoshita, K., Endo, Y., Kou, T., Morisawa, T., Azuma, T., Okazaki, I.M., Honjo, T., and Chiba, T. (2007). Helicobacter pylori infection triggers aberrant expression of activation-induced cytidine deaminase in gastric epithelium. Nature medicine *13*, 470-476.

McGee, D.J., Langford, M.L., Watson, E.L., Carter, J.E., Chen, Y.T., and Ottemann, K.M. (2005). Colonization and inflammation deficiencies in Mongolian gerbils infected by Helicobacter pylori chemotaxis mutants. Infection and immunity *73*, 1820-1827.

Megraud, F., and Lamouliatte, H. (2003). Review article: the treatment of refractory Helicobacter pylori infection. Aliment Pharmacol Ther *17*, 1333-1343.

Meighen, E.A. (1991). Molecular biology of bacterial bioluminescence. Microbiol Rev *55*, 123-142.

Meighen, E.A. (1993). Bacterial bioluminescence: organization, regulation, and application of the lux genes. FASEB journal : official publication of the Federation of American Societies for Experimental Biology *7*, 1016-1022.

Meighen, E.A., and Dunlap, P.V. (1993). Physiological, biochemical and genetic control of bacterial bioluminescence. Advances in microbial physiology *34*, 1-67.

Merrell, D.S., Thompson, L.J., Kim, C.C., Mitchell, H., Tompkins, L.S., Lee, A., and Falkow, S. (2003). Growth phase-dependent response of Helicobacter pylori to iron starvation. Infection and immunity *71*, 6510-6525.

Meyer-ter-Vehn, T., Covacci, A., Kist, M., and Pahl, H.L. (2000). Helicobacter pylori activates mitogen-activated protein kinase cascades and induces expression of the proto-oncogenes c-fos and c-jun. J Biol Chem *275*, 16064-16072.

Mimuro, H., Suzuki, T., Nagai, S., Rieder, G., Suzuki, M., Nagai, T., Fujita, Y., Nagamatsu, K., Ishijima, N., Koyasu, S.*, et al.* (2007). Helicobacter pylori dampens gut epithelial self-renewal by inhibiting apoptosis, a bacterial strategy to enhance colonization of the stomach. Cell host & microbe *2*, 250-263.

Mobley, H.L.T., Mendz, G.L., and Hazell, S.L. (2001). Overview. In Helicobacter pylori: Physiology and Genetics, H.L.T. Mobley, G.L. Mendz, and S.L. Hazell, eds. (Washington (DC)).

Mogk, A., Homuth, G., Scholz, C., Kim, L., Schmid, F.X., and Schumann, W. (1997). The GroE chaperonin machine is a major modulator of the CIRCE heat shock regulon of Bacillus subtilis. The EMBO journal *16*, 4579-4590.

Molloy, S. (2007). Bacterial virulence: The integrin connection. Nature Reviews Microbiology *5*, 908.

Morita, T., Maki, K., and Aiba, H. (2005). RNase E-based ribonucleoprotein complexes: mechanical basis of mRNA destabilization mediated by bacterial noncoding RNAs. Genes Dev *19*, 2176-2186.

Murata-Kamiya, N., Kikuchi, K., Hayashi, T., Higashi, H., and Hatakeyama, M. (2010). Helicobacter pylori exploits host membrane phosphatidylserine for delivery, localization, and pathophysiological action of the CagA oncoprotein. Cell host & microbe *7*, 399-411.

Naito, Y., and Yoshikawa, T. (2002). Molecular and cellular mechanisms involved in Helicobacter pylori-induced inflammation and oxidative stress. Free radical biology & medicine *33*, 323-336.

Narberhaus, F. (1999). Negative regulation of bacterial heat shock genes. Molecular microbiology *31*, 1-8.

Naumann, M., Wessler, S., Bartsch, C., Wieland, B., Covacci, A., Haas, R., and Meyer, T.F. (1999). Activation of activator protein 1 and stress response kinases in epithelial cells colonized by Helicobacter pylori encoding the cag pathogenicity island. J Biol Chem *274*, 31655-31662.

Niehus, E., Gressmann, H., Ye, F., Schlapbach, R., Dehio, M., Dehio, C., Stack, A., Meyer, T.F., Suerbaum, S., and Josenhans, C. (2004). Genome-wide analysis of transcriptional hierarchy and feedback regulation in the flagellar system of Helicobacter pylori. Molecular microbiology *52*, 947-961.

Niehus, E., Ye, F., Suerbaum, S., and Josenhans, C. (2002). Growth phase-dependent and differential transcriptional control of flagellar genes in Helicobacter pylori. Microbiology *148*, 3827-3837.

Ninio, S., and Roy, C.R. (2007). Effector proteins translocated by Legionella pneumophila: strength in numbers. Trends in microbiology *15*, 372-380.

Nomura, A., Stemmermann, G.N., Chyou, P.H., Perez-Perez, G.I., and Blaser, M.J. (1994). Helicobacter pylori infection and the risk for duodenal and gastric ulceration. Ann Intern Med *120*, 977-981.

Oh, J.D., Kling-Backhed, H., Giannakis, M., Xu, J., Fulton, R.S., Fulton, L.A., Cordum, H.S., Wang, C., Elliott, G., Edwards, J.*, et al.* (2006). The complete genome sequence of a chronic atrophic gastritis Helicobacter pylori strain: evolution during disease progression. Proceedings of the National Academy of Sciences of the United States of America *103*, 9999-10004.

Olbermann, P., Josenhans, C., Moodley, Y., Uhr, M., Stamer, C., Vauterin, M., Suerbaum, S., Achtman, M., and Linz, B. (2010). A global overview of the genetic and functional diversity in the Helicobacter pylori cag pathogenicity island. PLoS genetics *6*, e1001069.

Papenfort, K., and Vogel, J. (2010). Regulatory RNA in bacterial pathogens. Cell host & microbe *8*, 116-127.

Parsonnet, J., Hansen, S., Rodriguez, L., Gelb, A.B., Warnke, R.A., Jellum, E., Orentreich, N., Vogelman, J.H., and Friedman, G.D. (1994). Helicobacter pylori infection and gastric lymphoma. N Engl J Med *330*, 1267-1271.

Pattis, I., Weiss, E., Laugks, R., Haas, R., and Fischer, W. (2007). The Helicobacter pylori CagF protein is a type IV secretion chaperone-like molecule that binds close to the C-terminal secretion signal of the CagA effector protein. Microbiology *153*, 2896-2909.

Peek, R.M., Jr. (2005). Orchestration of aberrant epithelial signaling by Helicobacter pylori CagA. Sci STKE *2005*, pe14.

Peek, R.M., Jr., and Blaser, M.J. (2002). Helicobacter pylori and gastrointestinal tract adenocarcinomas. Nat Rev Cancer *2*, 28-37.

Pereira, L., and Hoover, T.R. (2005). Stable accumulation of sigma54 in Helicobacter pylori requires the novel protein HP0958. Journal of bacteriology *187*, 4463-4469.

Pereira, L.E., Brahmachary, P., and Hoover, T.R. (2006). Characterization of Helicobacter pylori sigma54 promoter-binding activity. FEMS microbiology letters *259*, 20-26.

Pereira, L.E., Tsang, J., Mrazek, J., and Hoover, T.R. (2011). The zinc-ribbon domain of Helicobacter pylori HP0958: requirement for RpoN accumulation and possible roles of homologs in other bacteria. Microbial informatics and experimentation *1*, 1-10.

Pernitzsch, S.R., and Sharma, C.M. (2012). Transcriptome Complexity and Riboregulation in the Human Pathogen Helicobacter pylori. Frontiers in cellular and infection microbiology *2*, 14.

Pflock, M., Dietz, P., Schar, J., and Beier, D. (2004). Genetic evidence for histidine kinase HP165 being an acid sensor of Helicobacter pylori. FEMS microbiology letters *234*, 51-61.

Pflock, M., Finsterer, N., Joseph, B., Mollenkopf, H., Meyer, T.F., and Beier, D. (2006a). Characterization of the ArsRS regulon of Helicobacter pylori, involved in acid adaptation. Journal of bacteriology *188*, 3449-3462.

Pflock, M., Kennard, S., Delany, I., Scarlato, V., and Beier, D. (2005). Acid-induced activation of the urease promoters is mediated directly by the ArsRS two-component system of Helicobacter pylori. Infection and immunity *73*, 6437-6445.

Pflock, M., Kennard, S., Finsterer, N., and Beier, D. (2006b). Acid-responsive gene regulation in the human pathogen Helicobacter pylori. Journal of biotechnology *126*, 52-60.

Pich, O.Q., Carpenter, B.M., Gilbreath, J.J., and Merrell, D.S. (2012). Detailed analysis of Helicobacter pylori Fur-regulated promoters reveals a Fur box core sequence and novel Fur-regulated genes. Molecular microbiology *84*, 921-941.

Prevost, K., Salvail, H., Desnoyers, G., Jacques, J.F., Phaneuf, E., and Masse, E. (2007). The small RNA RyhB activates the translation of shiA mRNA encoding a permease of shikimate, a compound involved in siderophore synthesis. Molecular microbiology *64*, 1260-1273.

Rader, B.A., Wreden, C., Hicks, K.G., Sweeney, E.G., Ottemann, K.M., and Guillemin, K. (2011). Helicobacter pylori perceives the quorum-sensing molecule AI-2 as a chemorepellent via the chemoreceptor TlpB. Microbiology *157*, 2445-2455.

Ramarao, N., Gray-Owen, S.D., Backert, S., and Meyer, T.F. (2000). Helicobacter pylori inhibits phagocytosis by professional phagocytes involving type IV secretion components. Molecular microbiology *37*, 1389-1404.

Rohde, M., Puls, J., Buhrdorf, R., Fischer, W., and Haas, R. (2003). A novel sheathed surface organelle of the Helicobacter pylori cag type IV secretion system. Molecular microbiology *49*, 219-234.

Romagnoli, S., Agriesti, F., and Scarlato, V. (2011). In vivo recognition of the fecA3 target promoter by Helicobacter pylori NikR. Journal of bacteriology *193*, 1131-1141.

Roncarati, D., Danielli, A., Spohn, G., Delany, I., and Scarlato, V. (2007). Transcriptional regulation of stress response and motility functions in Helicobacter pylori is mediated by HspR and HrcA. Journal of bacteriology *189*, 7234-7243.

Roux, C.M., DeMuth, J.P., and Dunman, P.M. (2011). Characterization of components of the Staphylococcus aureus mRNA degradosome holoenzyme-like complex. Journal of bacteriology *193*, 5520-5526.

Ryan, K.A., Karim, N., Worku, M., Penn, C.W., and O'Toole, P.W. (2005). Helicobacter pylori flagellar hook-filament transition is controlled by a FliK functional homolog encoded by the gene HP0906. Journal of bacteriology *187*, 5742-5750.

Sachs, G., Weeks, D.L., Melchers, K., and Scott, D.R. (2003). The gastric biology of Helicobacter pylori. Annu Rev Physiol *65*, 349-369.

Sambrook, J.E.F.F., and T. Maniatis (1989). Molecular cloning: a laboratory manual. In, C.S.H. Cold Spring Harbor Laboratory, NY, ed.

Scarlato, V., Delany, I., Spohn, G., and Beier, D. (2001). Regulation of transcription in Helicobacter pylori: simple systems or complex circuits? International journal of medical microbiology : IJMM *291*, 107-117.

Schroder, G., and Dehio, C. (2005). Virulence-associated type IV secretion systems of Bartonella. Trends in microbiology *13*, 336-342.

Schroder, G., Krause, S., Zechner, E.L., Traxler, B., Yeo, H.J., Lurz, R., Waksman, G., and Lanka, E. (2002). TraG-like proteins of DNA transfer systems and of the Helicobacter pylori type IV secretion system: inner membrane gate for exported substrates? Journal of bacteriology *184*, 2767-2779.

Schulz, A., and Schumann, W. (1996). hrcA, the first gene of the Bacillus subtilis dnaK operon encodes a negative regulator of class I heat shock genes. Journal of bacteriology *178*, 1088-1093.

Scott, D.R., Marcus, E.A., Weeks, D.L., and Sachs, G. (2002). Mechanisms of acid resistance due to the urease system of Helicobacter pylori. Gastroenterology *123*, 187-195.

Scott, D.R., Marcus, E.A., Wen, Y., Oh, J., and Sachs, G. (2007). Gene expression in vivo shows that Helicobacter pylori colonizes an acidic niche on the gastric surface. Proceedings of the National Academy of Sciences of the United States of America *104*, 7235-7240.

Selbach, M., Moese, S., Hurwitz, R., Hauck, C.R., Meyer, T.F., and Backert, S. (2003). The Helicobacter pylori CagA protein induces cortactin dephosphorylation and actin rearrangement by c-Src inactivation. The EMBO journal *22*, 515-528.

Selbach, M., Moese, S., Meyer, T.F., and Backert, S. (2002). Functional analysis of the Helicobacter pylori cag pathogenicity island reveals both VirD4-CagA-dependent and VirD4-CagA-independent mechanisms. Infection and immunity *70*, 665-671.

Servant, P., and Mazodier, P. (2001). Negative regulation of the heat shock response in Streptomyces. Archives of microbiology *176*, 237-242.

Sharma, C.M., Hoffmann, S., Darfeuille, F., Reignier, J., Findeiss, S., Sittka, A., Chabas, S., Reiche, K., Hackermuller, J., Reinhardt, R.*, et al.* (2010). The primary transcriptome of the major human pathogen Helicobacter pylori. Nature *464*, 250-255.

Smeets, L.C., and Kusters, J.G. (2002). Natural transformation in Helicobacter pylori: DNA transport in an unexpected way. Trends in microbiology *10*, 159-162; discussion 162.

Spohn, G., Beier, D., Rappuoli, R., and Scarlato, V. (1997). Transcriptional analysis of the divergent cagAB genes encoded by the pathogenicity island of Helicobacter pylori. Molecular microbiology *26*, 361-372.

Spohn, G., Danielli, A., Roncarati, D., Delany, I., Rappuoli, R., and Scarlato, V. (2004). Dual control of Helicobacter pylori heat shock gene transcription by HspR and HrcA. Journal of bacteriology *186*, 2956-2965.

Spohn, G., Delany, I., Rappuoli, R., and Scarlato, V. (2002). Characterization of the HspR-mediated stress response in Helicobacter pylori. Journal of bacteriology *184*, 2925-2930.

Spohn, G., and Scarlato, V. (1999a). The autoregulatory HspR repressor protein governs chaperone gene transcription in Helicobacter pylori. Molecular microbiology *34*, 663-674.

Spohn, G., and Scarlato, V. (1999b). Motility of Helicobacter pylori is coordinately regulated by the transcriptional activator FlgR, an NtrC homolog. Journal of bacteriology *181*, 593-599.

Storz, G., Vogel, J., and Wassarman, K.M. (2011). Regulation by small RNAs in bacteria: expanding frontiers. Mol Cell *43*, 880-891.

Suerbaum, S., Josenhans, C., and Labigne, A. (1993). Cloning and genetic characterization of the Helicobacter pylori and Helicobacter mustelae flaB flagellin genes and construction of H. pylori flaA- and flaB-negative mutants by electroporation-mediated allelic exchange. Journal of bacteriology *175*, 3278-3288.

Szczebara, F., Dhaenens, L., Armand, S., and Husson, M.O. (1999). Regulation of the transcription of genes encoding different virulence factors in Helicobacter pylori by free iron. FEMS microbiology letters *175*, 165-170.

Ta, L.H., Hansen, L.M., Sause, W.E., Shiva, O., Millstein, A., Ottemann, K.M., Castillo, A.R., and Solnick, J.V. (2012). Conserved Transcriptional Unit Organization of the Cag Pathogenicity Island among Helicobacter pylori Strains. Frontiers in cellular and infection microbiology *2*, 46.

Tanaka, J., Suzuki, T., Mimuro, H., and Sasakawa, C. (2003). Structural definition on the surface of Helicobacter pylori type IV secretion apparatus. Cellular microbiology *5*, 395-404.

Tegtmeyer, N., Hartig, R., Delahay, R.M., Rohde, M., Brandt, S., Conradi, J., Takahashi, S., Smolka, A.J., Sewald, N., and Backert, S. (2010). A small fibronectin-mimicking protein from bacteria induces cell spreading and focal adhesion formation. J Biol Chem *285*, 23515-23526.

Telford, J.L., Ghiara, P., Dell'Orco, M., Comanducci, M., Burroni, D., Bugnoli, M., Tecce, M.F., Censini, S., Covacci, A., Xiang, Z.*, et al.* (1994). Gene structure of the Helicobacter pylori cytotoxin and evidence of its key role in gastric disease. J Exp Med *179*, 1653-1658.

Thomason, M.K., and Storz, G. (2010). Bacterial antisense RNAs: how many are there, and what are they doing? Annual review of genetics *44*, 167-188.

Thompson, L.J., Merrell, D.S., Neilan, B.A., Mitchell, H., Lee, A., and Falkow, S. (2003). Gene expression profiling of Helicobacter pylori reveals a growth-phase-dependent switch in virulence gene expression. Infection and immunity *71*, 2643-2655.

Tomb, J.F., White, O., Kerlavage, A.R., Clayton, R.A., Sutton, G.G., Fleischmann, R.D., Ketchum, K.A., Klenk, H.P., Gill, S., Dougherty, B.A.*, et al.* (1997). The complete genome sequence of the gastric pathogen Helicobacter pylori. Nature *388*, 539-547.

Trieu-Cuot, P., Gerbaud, G., Lambert, T., and Courvalin, P. (1985). In vivo transfer of genetic information between gram-positive and gram-negative bacteria. The EMBO journal *4*, 3583-3587.

Trotochaud, A.E., and Wassarman, K.M. (2005). A highly conserved 6S RNA structure is required for regulation of transcription. Nat Struct Mol Biol *12*, 313-319.

Tsang, Y.H., Lamb, A., Romero-Gallo, J., Huang, B., Ito, K., Peek, R.M., Jr., Ito, Y., and Chen, L.F. (2010). Helicobacter pylori CagA targets gastric tumor suppressor RUNX3 for proteasome-mediated degradation. Oncogene *29*, 5643-5650.

Tsao, M.Y., Lin, T.L., Hsieh, P.F., and Wang, J.T. (2009). The 3'-to-5' exoribonuclease (encoded by HP1248) of Helicobacter pylori regulates motility and apoptosis-inducing genes. Journal of bacteriology *191*, 2691-2702.

Tsuda, M., Karita, M., Morshed, M.G., Okita, K., and Nakazawa, T. (1994). A urease-negative mutant of Helicobacter pylori constructed by allelic exchange mutagenesis lacks the ability to colonize the nude mouse stomach. Infection and immunity *62*, 3586-3589.

Valentin-Hansen, P., Eriksen, M., and Udesen, C. (2004). The bacterial Sm-like protein Hfq: a key player in RNA transactions. Molecular microbiology *51*, 1525-1533.

Valenzuela, M., Albar, J.P., Paradela, A., and Toledo, H. (2011). Helicobacter pylori exhibits a fur-dependent acid tolerance response. Helicobacter *16*, 189-199.

van der Meer, J.R., and Belkin, S. (2010). Where microbiology meets microengineering: design and applications of reporter bacteria. Nature reviews Microbiology *8*, 511-522.

van Vliet, A., Bereswill, S., and Kusters, J.G. (2001a). Ion metabolism and trasport. In Helicobacter pylori: Physiology and genetics, H.L. Mobley, G.L. Mendz, and S.L. Hazell, eds. (Washington DC: ASM Press).

van Vliet, A.H., Ernst, F.D., and Kusters, J.G. (2004). NikR-mediated regulation of Helicobacter pylori acid adaptation. Trends in microbiology *12*, 489-494.

van Vliet, A.H., Kuipers, E.J., Waidner, B., Davies, B.J., de Vries, N., Penn, C.W., Vandenbroucke-Grauls, C.M., Kist, M., Bereswill, S., and Kusters, J.G. (2001b). Nickel-responsive induction of urease expression in Helicobacter pylori is mediated at the transcriptional level. Infection and immunity *69*, 4891-4897.

van Vliet, A.H., Poppelaars, S.W., Davies, B.J., Stoof, J., Bereswill, S., Kist, M., Penn, C.W., Kuipers, E.J., and Kusters, J.G. (2002a). NikR mediates nickel-responsive transcriptional induction of urease expression in Helicobacter pylori. Infection and immunity *70*, 2846-2852.

van Vliet, A.H., Stoof, J., Poppelaars, S.W., Bereswill, S., Homuth, G., Kist, M., Kuipers, E.J., and Kusters, J.G. (2003). Differential regulation of amidase- and formamidase-mediated ammonia production by the Helicobacter pylori fur repressor. J Biol Chem *278*, 9052-9057.

van Vliet, A.H., Stoof, J., Vlasblom, R., Wainwright, S.A., Hughes, N.J., Kelly, D.J., Bereswill, S., Bijlsma, J.J., Hoogenboezem, T., Vandenbroucke-Grauls, C.M.*, et al.* (2002b). The role of the Ferric Uptake Regulator (Fur) in regulation of Helicobacter pylori iron uptake. Helicobacter *7*, 237-244.

Vannini, A., Agriesti, F., Mosca, F., Roncarati, D., Scarlato, V., and Danielli, A. (2012). A convenient and robust in vivo reporter system to monitor gene expression in the human pathogen Helicobacter pylori. Applied and environmental microbiology *78*, 6524-6533.

Viala, J., Chaput, C., Boneca, I.G., Cardona, A., Girardin, S.E., Moran, A.P., Athman, R., Memet, S., Huerre, M.R., Coyle, A.J.*, et al.* (2004). Nod1 responds to peptidoglycan delivered by the Helicobacter pylori cag pathogenicity island. Nature immunology *5*, 1166-1174.

Vogel, J., and Luisi, B.F. (2011). Hfq and its constellation of RNA. Nature reviews Microbiology *9*, 578-589.

Waidner, B., Melchers, K., Stahler, F.N., Kist, M., and Bereswill, S. (2005). The Helicobacter pylori CrdRS two-component regulation system (HP1364/HP1365) is required for copper-mediated induction of the copper resistance determinant CrdA. Journal of bacteriology *187*, 4683-4688.

Wallden, K., Rivera-Calzada, A., and Waksman, G. (2010). Type IV secretion systems: versatility and diversity in function. Cellular microbiology *12*, 1203-1212.

Wang, Y., and Taylor, D.E. (1990). Chloramphenicol resistance in Campylobacter coli: nucleotide sequence, expression, and cloning vector construction. Gene *94*, 23-28.

Wassarman, K.M. (2007). 6S RNA: a regulator of transcription. Molecular microbiology *65*, 1425-1431.

Wassarman, K.M., and Storz, G. (2000). 6S RNA regulates E. coli RNA polymerase activity. Cell *101*, 613-623.

Watanabe, T., Asano, N., Fichtner-Feigl, S., Gorelick, P.L., Tsuji, Y., Matsumoto, Y., Chiba, T., Fuss, I.J., Kitani, A., and Strober, W. (2010). NOD1 contributes to mouse host defense against Helicobacter pylori via induction of type I IFN and activation of the ISGF3 signaling pathway. The Journal of clinical investigation *120*, 1645-1662.

Waters, L.S., and Storz, G. (2009). Regulatory RNAs in bacteria. Cell *136*, 615-628.

Waters, V.L. (2001). Conjugation between bacterial and mammalian cells. Nature genetics *29*, 375-376.

Weeks, D.L., Gushansky, G., Scott, D.R., and Sachs, G. (2004). Mechanism of proton gating of a urea channel. J Biol Chem *279*, 9944-9950.

Wen, Y., Feng, J., Scott, D.R., Marcus, E.A., and Sachs, G. (2006). Involvement of the HP0165-HP0166 two-component system in expression of some acidic-pH-upregulated genes of Helicobacter pylori. Journal of bacteriology *188*, 1750-1761.

Wen, Y., Feng, J., Scott, D.R., Marcus, E.A., and Sachs, G. (2009). The pH-responsive regulon of HP0244 (FlgS), the cytoplasmic histidine kinase of Helicobacter pylori. Journal of bacteriology *191*, 449-460.

Wen, Y., Feng, J., Scott, D.R., Marcus, E.A., and Sachs, G. (2011). A cis-encoded antisense small RNA regulated by the HP0165-HP0166 two-component system controls expression of ureB in Helicobacter pylori. Journal of bacteriology *193*, 40-51.

Wen, Y., Marcus, E.A., Matrubutham, U., Gleeson, M.A., Scott, D.R., and Sachs, G. (2003). Acid-adaptive genes of Helicobacter pylori. Infection and immunity *71*, 5921-5939.

Wessler, S., and Backert, S. (2008). Molecular mechanisms of epithelial-barrier disruption by Helicobacter pylori. Trends in microbiology *16*, 397-405.

Williams, S.M., Chen, Y.T., Andermann, T.M., Carter, J.E., McGee, D.J., and Ottemann, K.M. (2007). Helicobacter pylori chemotaxis modulates inflammation and bacterium-gastric epithelium interactions in infected mice. Infection and immunity *75*, 3747-3757.

Winson, M.K., Swift, S., Fish, L., Throup, J.P., Jorgensen, F., Chhabra, S.R., Bycroft, B.W., Williams, P., and Stewart, G.S. (1998a). Construction and analysis of luxCDABE-based plasmid sensors for investigating N-acyl homoserine lactone-mediated quorum sensing. FEMS microbiology letters *163*, 185-192.

Winson, M.K., Swift, S., Hill, P.J., Sims, C.M., Griesmayr, G., Bycroft, B.W., Williams, P., and Stewart, G.S. (1998b). Engineering the luxCDABE genes from Photorhabdus luminescens to provide a bioluminescent reporter for constitutive and promoter probe plasmids and mini-Tn5 constructs. FEMS microbiology letters *163*, 193-202.

Xiang, Z., Censini, S., Bayeli, P.F., Telford, J.L., Figura, N., Rappuoli, R., and Covacci, A. (1995). Analysis of expression of CagA and VacA virulence factors in 43 strains of Helicobacter pylori reveals that clinical isolates can be divided into two major types and that CagA is not necessary for expression of the vacuolating cytotoxin. Infection and immunity *63*, 94-98.

Xu, H., and Hoover, T.R. (2001). Transcriptional regulation at a distance in bacteria. Current opinion in microbiology *4*, 138-144.

Yahr, T.L., and Wolfgang, M.C. (2006). Transcriptional regulation of the Pseudomonas aeruginosa type III secretion system. Molecular microbiology *62*, 631-640.

Ye, F., Brauer, T., Niehus, E., Drlica, K., Josenhans, C., and Suerbaum, S. (2007). Flagellar and global gene regulation in Helicobacter pylori modulated by changes in DNA supercoiling. International journal of medical microbiology : IJMM *297*, 65-81.

Zahrl, D., Wagner, M., Bischof, K., Bayer, M., Zavecz, B., Beranek, A., Ruckenstuhl, C., Zarfel, G.E., and Koraimann, G. (2005). Peptidoglycan degradation by specialized lytic transglycosylases associated with type III and type IV secretion systems. Microbiology *151*, 3455-3467.

Zambelli, B., Danielli, A., Romagnoli, S., Neyroz, P., Ciurli, S., and Scarlato, V. (2008). High-affinity Ni2+ binding selectively promotes binding of Helicobacter pylori NikR to its target urease promoter. Journal of molecular biology *383*, 1129-1143.